Suture(s) and Major Shear Zones in the Neoproterozoic Basement of Egypt

5

Zakaria Hamimi and Mohamed A. Abd El-Wahed

Contents

Abstract

The Arabian-Nubian Shield (ANS), the northern extension of the East African Orogen (EAO), consists of a number of amalgamated island-arc tectonic terranes, separated along suture zones, major shear zones and cryptic major high strain zones. The Allaqi-Heiani-Oneib-Sol Hamid-Yanbu Suture separates the Eastern Desert-Midyan terrane from the Gabgaba-Gebeit-Hijaz terrane. The latter terrane juxtaposes Haya-Jiddah terrane along the Nakasib-Bir Umq Suture which is the longest ophiolite-decorated shear zone allover the ANS. The Haya-Jiddah terrane is separated from the Nakfa-Asir terrane along Baraka-Al-Damm Fault Zone. The previously mentioned Hijaz-Jiddah-Asir borders the continental Afif terrane through the Hulaifa-Ad-Dafinah-Ruwah sinistral transpressional zone. Ad-Dawadimi and Ar-Rayan terranes occupy the eastern part of the Arabian Shield, being separated from the Afif terrane and from each others along the Halaban and Al-Amar Sutures. The smallest terrane in the ANS is the Ha'il terrane. This chapter reviews some of the major shear zones existed inside the Eastern Desert of Egypt (The Egyptian Nubian Shield; ENS). It addresses also the Allaqi-Heiani Suture which is regarded as the western segment of the enormous arc-arc Allaqi-Heiani-Oneib-Sol Hamid-Yanbu Suture Zone. The shear zones are dealt with through two main groups; syn-accretion- and post-accretion shear zones. The first group is manifested by the NNE-oriented Hamisana Shear Zone, whereas the second group is typified by the Najd-related NW-trending Shear Zones, such as Hodein-Karite-, Nugrus- and Atallah-Shear Zones, as well as by the relatively younger ENE- (to E-) trending shear zones and shear belts, such as

Z. Hamimi
Faculty of Science, Department of Geology, Benha University, Benha, 13518, Egypt
e-mail: zakariahamimi123@gmail.com; zakaria.hamimi@fsc.bu.edu.eg

M. A. Abd El-Wahed (✉)
Faculty of Science, Geology Department, Tanta University, Tanta, 31527, Egypt
e-mail: mohamed.abdelwahad@science.tanta.edu.eg

Z. Hamimi et al. (eds.), *The Geology of Egypt*, Regional Geology Reviews,
https://doi.org/10.1007/978-3-030-15265-9_5

Mubarak-Barramiya Shear Belt and Abu Dabbab Shear Zone. The shear zone-related mineralizations (particularly gold) is dealt in the last section.

5.1 Introduction

Sutures are sites delineating closure of ocean basins and back-arc basins, and therefore the obliteration of oceanic lithosphere by subduction and the consequent intracontinental welding of continental blocks. These sites provide the only record for the ancient sea-floor spreading and the subsequent continental collision. Sutures are widely distributed in the orogenic belts all over the globe (e.g. the Pan-African Sutures around North Africa, Arabia, West Congo, Damara and Zambesi, the Alpine Sutures, the Caledonides and Sveco-Norwegian Sutures, the Ural Sutures, the Cordilleran Sutures, the Northern and Southern Appalachian Sutures, the Grenville Sutures). Linear arrangement of ophiolitic belts and nappes is the solid evidence confirming the sutures. Likewise, shear zones are zones accommodating deformation and relative movement of crustal or lithospheric blocks. They are frequently planar zones of concentrated deformation help to accommodate imposed regional or local strain rates beyond the strength of the country rocks. These high strain zones are also widely distributed worldwide. However, the study of both sutures and shear zones in the Arabian-Nubian Shield (ANS) (Fig. 5.1), and probably in the entire East African Orogen (EAO) has given much more attention since the leading works of Abdelsalam and Stern (1996) who subdivided the deformational belts in the ANS (Fig. 5.1) into: (1) those associated arc-arc- and arc-continental-sutures; and (2) post-accretionary structures which include N-trending shortening zones and NW-trending strike-slip faults. According to these authors, the arc-arc sutures manifest collision between arc terranes at 800–700 Ma. The arc-continental sutures define the eastern and western boundaries of the ANS and are marked by N-trending deformational belts which accompanied collision of the ANS with E- and W-Gondwanalands at ~750–650 Ma. The

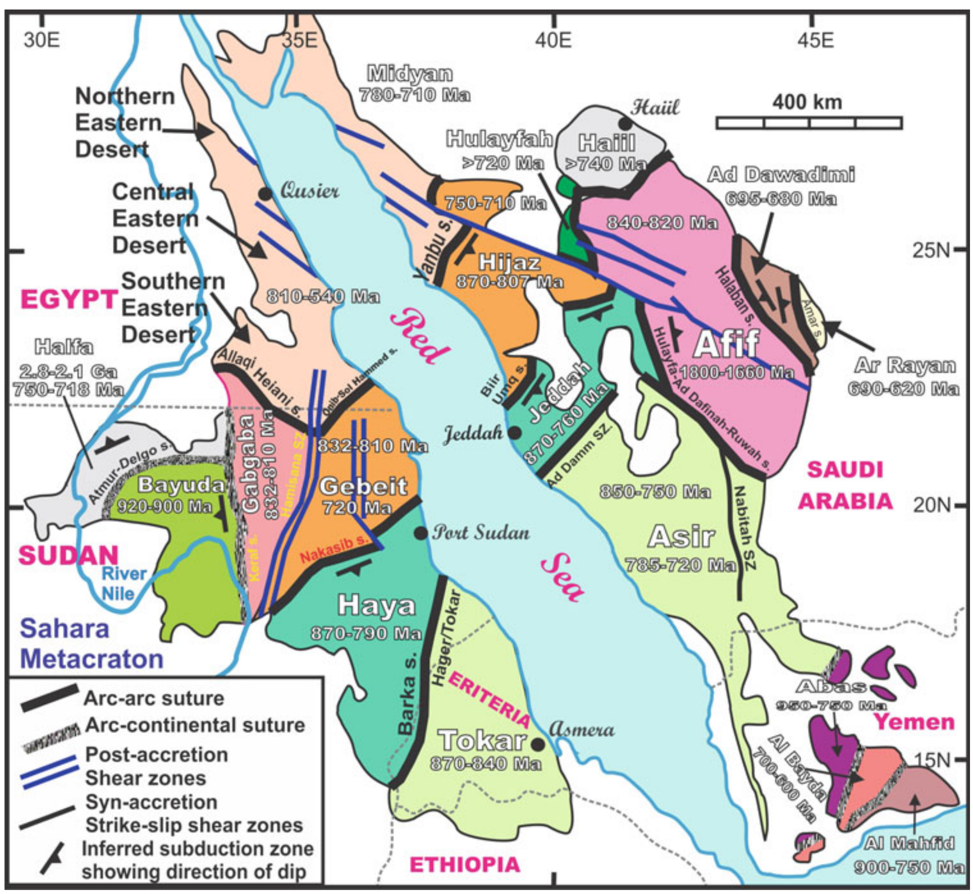

Fig. 5.1 Tectonic map of the Arabian–Nubian Shield showing the locations and extents of terranes, sutures and post-accretionary structures. Modified after Johnson and Woldehaimanot (2003), Hargrove et al. (2006a, b) and Abdelsalam (2010). Terrane ages from Stern et al. (1994), Stern et al. (1989), Kröner et al. (1992), Kröner et al. (1991), Pallister et al. (1988), Agar et al. (1992), Whitehouse et al. (2001), Hargrove et al. (2006a, b), Andresen et al. (2009), Küster et al. (2008)

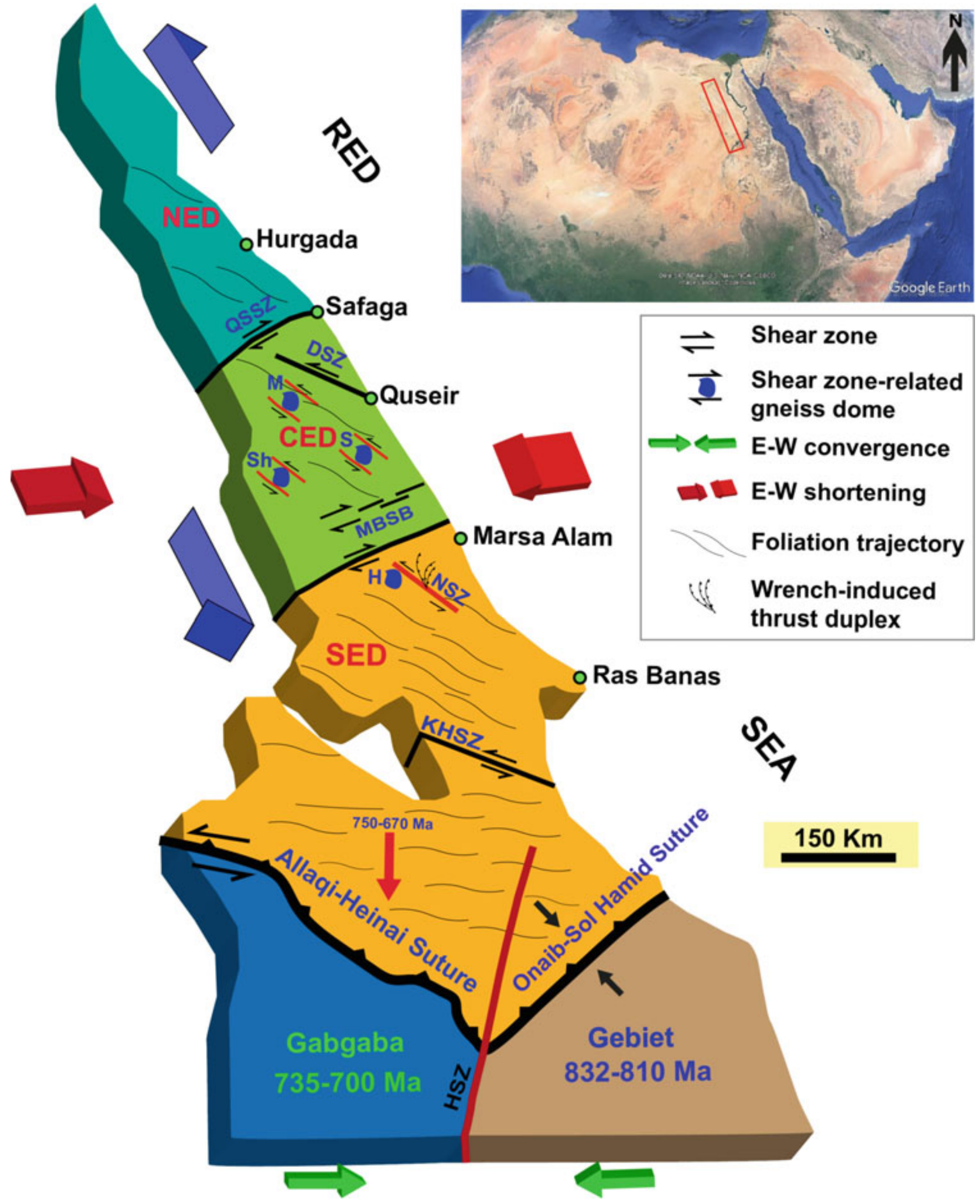

Fig. 5.2 The major shear zones in the Egyptian Nubian Shield

post-accretionary structures were developed between ~650 and 550 Ma due to continued shortening of the ANS.

The ENS outcrops mainly in the Eastern Desert and southern Sinai. The Eastern Desert is traditionally subdivided into Northern Eastern Desert (NED), Central Eastern Desert (CED) and Southern Eastern Desert (SED) (Fig. 5.2). In the ENS, major shear zones plays significant role in the structural shaping of the Neoproterozoic Pan-African belt. El-Gaby et al. (1988, 1990) considered Qena-Safaga Shear Zone as a conspicuous right-lateral shear zone juxtaposing remobilized older continental crust and infolded, locally metamorphosed, Dokhan Volcanics and molasse Hammamat sediments to the north, and ophiolites, island arc metavolcanics and metavolcanogenics to the south. The obvious shear trend in the ENS is the Najd-related NW- (to NNW-) trend. This trend is exemplified by Wadi Kharit-Wadi Hodein-, Nugrus- and Atallah-Shear Zones (Fig. 5.2). Other remarkable shearing trend is the NE (to ENE), such as Qena-Safaga- and Idfu-Mersa Alam-Shear Zones (Fig. 5.2). Whether the Najd-related NW- (to NNW-) and the NE (to ENE) trends are conjugate or not was and still is a matter of controversy.

5.2 Arc-Arc Sutures

In the northern ANS, the subduction stage in the northern ANS is dated as 850–650 Ma, with subduction terminated by arc-arc collisions and suturing between 760 and 690 Ma

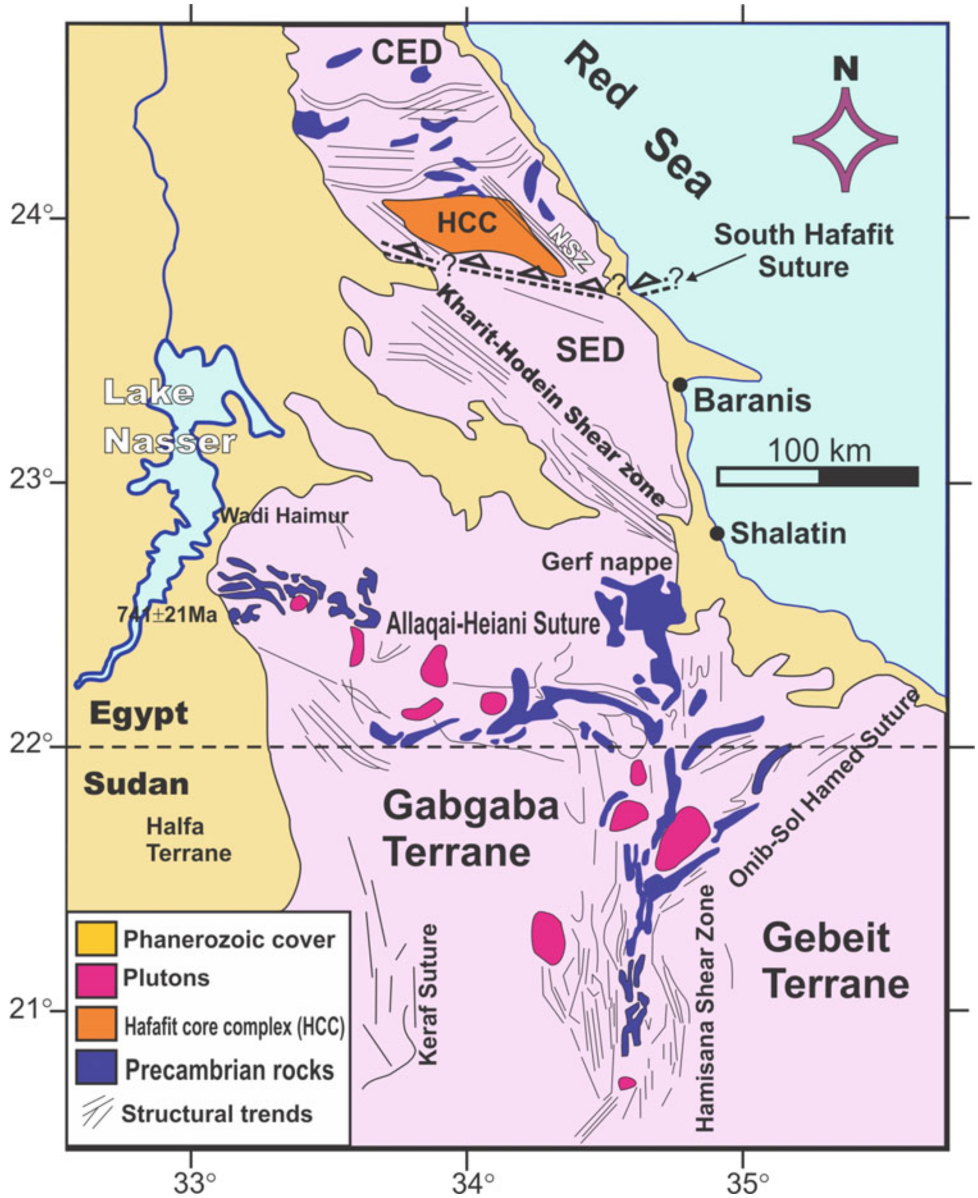

Fig. 5.3 Tectonic map of the Allaqi-Heiani-Gerf suture, South-Eastern Desert of Egypt (modified after Abdelsalam et al. 2003), showing location of ophiolites along the suture

(Stern 1994), but compressional deformation and subduction-related plutonism persisted until about 625 Ma (Johnson and Woldehaimanot 2003; Stern et al. 2010; Fritz et al. 2013). During deformation, lithologic volcanic, plutonic and sedimentary rocks belonging to this stage have been metamorphosed to greenschist facies. The ~715–765 Ma Shadli metavolcanics and equivalents of the SED are affiliated to the volcanic arc stage by many workers (e.g. Stern and Hedge 1985a, b; Stern et al. 1991). The arc-arc collisional zones are represented by ophiolite-decorated sutures that extend on both sides of the Red Sea. These zones include the Allaqi-Heiani-Onib-Sol Hamed-Yanbu Suture (AHOSHY) (Fig. 5.3), the Amur-Nakasib-B'ir Umq Suture (ANBU) (Stoeser and Camp 1985; Vail 1985; Shackleton 1986, 1994; Kröner et al. 1987; Stern et al. 1990; Johnson and Woldehaimanot 2003; Johnson et al. 2011). The AHOSHY is dated at 740–700 Ma, while the ANBU is dated at 780–750 Ma (Abdelsalam and Stern 1996; Ali et al. 2010; Johnson et al. 2011), and both zones are regarded as arc-arc sutures with NW-SE convergence directions, with some transpression resulting in strike-slip component.

5.2.1 Allaqi-Heiani Suture

The Allaqi-Heiani-Onib-Sol Hamed Zone (AHOSH) is the western continuation of the previously mentioned AHOSHY Suture (Fig. 5.3). The western segment of AHOSH is known

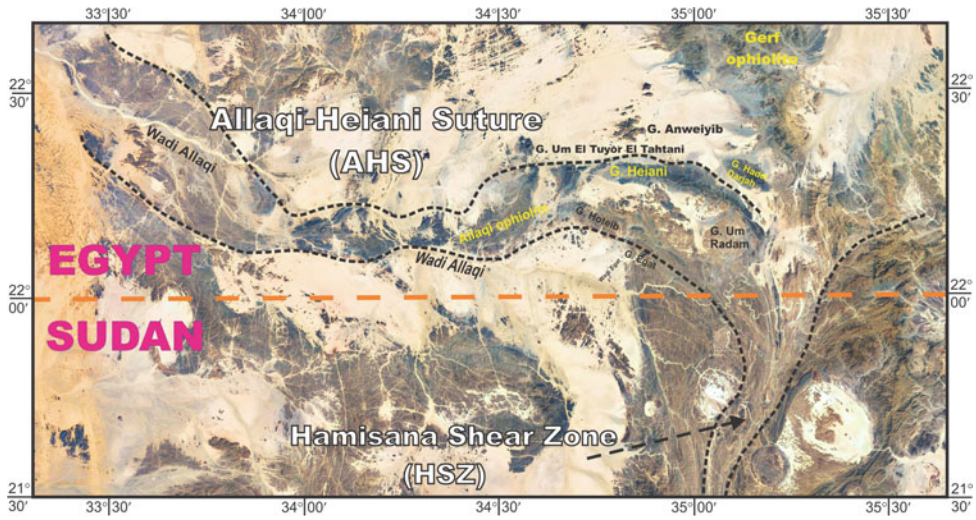

Fig. 5.4 The AHS extends over 200 km (average width 3 km) from Gabal Um Shilman and probably to Nasser Lake in the west to the NNE-trending Hamisana Shear Zone in the east

as Allaqi-Heiani Suture (AHS). Abdelsalam et al. (2003) believed that the Neoproterozoic AHS is the western extension of the AHOSHY that represents one of arc-arc sutures in the ANS. From the authors opinion, this suture is worthy to understand Neoproterozoic evolution of the ANS because: (1) It is the northernmost linear ophiolitic belt that defines an arc-arc suture in the ANS (Kröner et al. 1987; Stern 1994; Abdelsalam and Stern 1996); (2) It is the only suture in the ANS where a complete ophiolite is preserved at Gabal Gerf (Zimmer et al. 1995); (3) The suture extends in a general east-west direction and its western end is at a high angle to the proposed N-trending western margin of the ANS; and (4) Recent tectonic models have resulted in conflicting views about the continuity of the AHS, its structural style, and the overall tectonic transport direction involved. However, the AHS was described as a major shear zone for the first time by Taylor et al. (1993), Greiling et al. (1994) and EGSMA (1996). Abdelsalam et al. (2003) and others indicate that this zone is not a high strain zone, but an ophiolitic decorated shear zone (i.e. a suture zone). Kusky and Ramadan (2002) carried out integrated remote sensing and field work to distinguish exposed lithologic units, and to investigate overprinting relations between geologic structures along AHS in the vicinity of Gabal Um Shilman. These authors considered the AHS as an arc/arc collision suture zone (750–720 Ma) formed when the Gerf terrane (Eastern Desert or Aswan terrane) in the north overrode the Gabgaba terrane in the south, prior to the closure of the Mozambique Ocean (830–720 Ma).

The AHS extends over 200 km (average width ≈ 3–4 km) from Gabal Um Shilman probably to Nasser Lake (Figs. 5.3 and 5.4) in the west to the NNE-trending Hamisana Shear Zone in the east (Hamimi et al. 2019). It can be traced easily on the satellite imagery and aerial photomosaics (scale 1:50.000) covering Gabgaba-Elba Topographic Sheets (scale 1:250.000). The strike of this zone is remarkably variable from E-W, NW-SE and N-S. Such strike variation makes this suture to be perpendicular to the main Wadi Allaqi to the west (Fig. 5.4) and align the southern flank of the same wadi to the east, where it is apparently cut by the NE-oriented Hamisana Shear Zone (Greiling et al. 1994). The collision along the AHS is characterized by folding, and thrusting and the S- (to SE- or SW-) steeper imbrication of Gabal Gerf Nappe (Gabal Gerf Klippe) over the 830–720 Ma Gabgaba arc terrane (Abdelsalam and Stern 1996; Abdelsalam et al. 2003; Kusky and Ramadan 2002). Investigations of the ophiolitic rocks in the Gerf Nappe or klippe indicate that they are mainly massive almost intact ophiolite blocks and steeply dipping thrust slices (Fig. 5.5), with only minor mélange (Kusky and Ramadan 2002, Abdel-Karim et al. 2016) This is in complete harmony with opinion that the ophiolites having been transported only a short distance from its source (Abdelsalam and Stern 1996) and a long distance as suggested by Greiling et al. (2014). In this context, Abdelsalam et al. (2003) considered the AHS as an E-W to NW-SE trending fold/thrust belt forming three allochthons and one autochthonous block.

Abdelsalam and Stern (1996) proposed four Neoproterozoic deformations ($D_1 \rightarrow D_4$) for the development of the AHS. D_1 and D_2 are associated with early collisional stages between the Gerf terrane in the north, and Haya and Gabgaba terranes in the south, whereas D_3 and D_4 are associated with later stages of collision. Such conclusion is inconsistent with that given by El-Kazzaz and Taylor (2000) who used facing direction and folded thrust patterns to demonstrate north-verging and top-to-north transport direction. The AHS

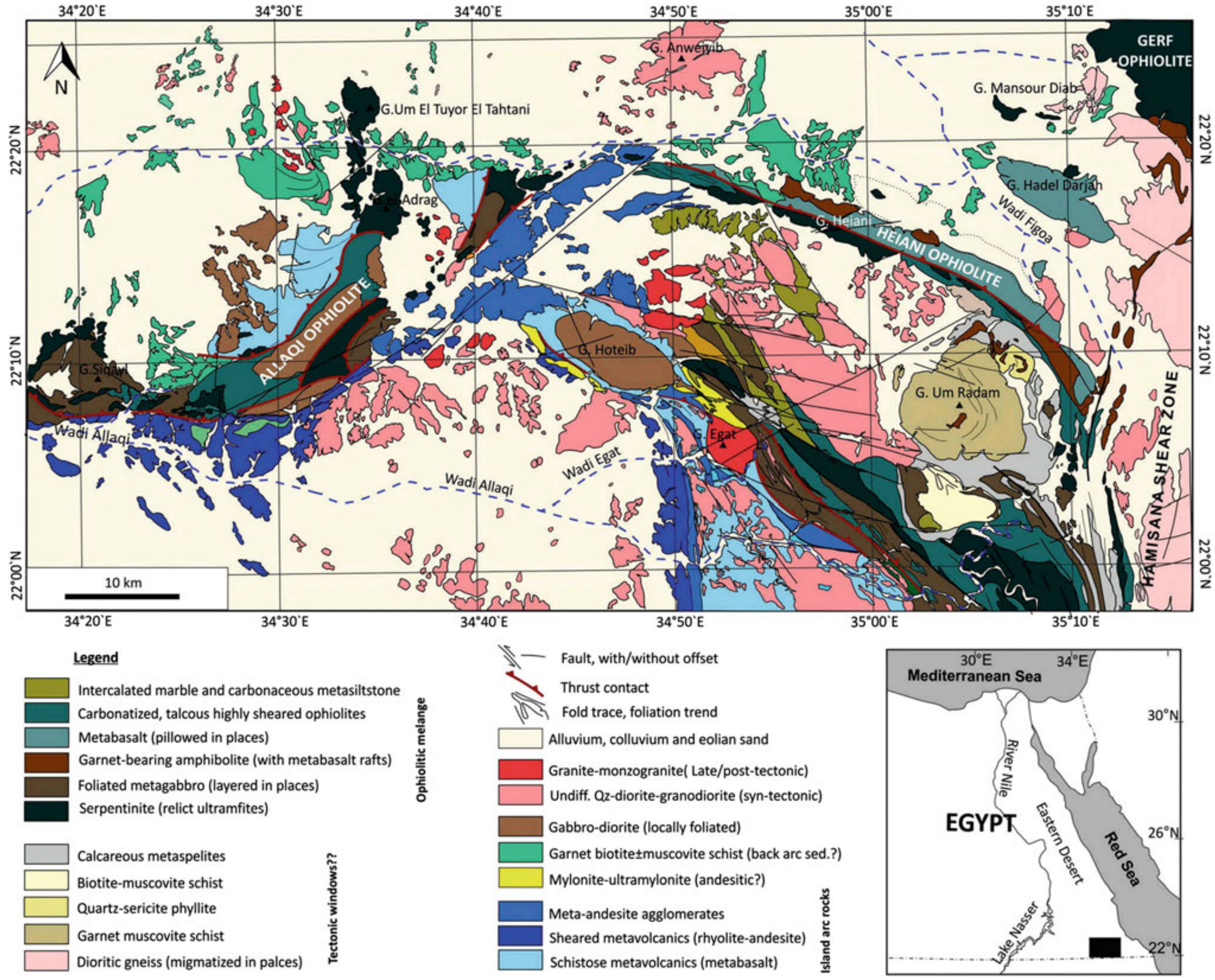

Fig. 5.5 Geologic map of the Allaqi-Heiani suture, related ophiolites, and structures (after Emam et al. 2015)

shows sinistral sense of shear indicated by shear band mylonitic foliation, mineral and mica fish, and S-C fabrics. Progressive shearing produced a complex history of folding with development of planar and non-planar refolded sheath folds. Abdeen and Abdelghaffar (2011) subdivided the Allaqi-Heiani belt into three structural domains. The western domain (I) is characterized by NNE dipping thrusts and SSW-vergent folds. The central domain (II) includes upright tight to isoclinal NNW–SSE oriented folds and transpressional faults. The eastern domain (III) shows NNW–SSE oriented open folds. Structural analysis indicates that the area has a polyphase deformation history involving at least two events. Event D_1 was a N–S to NNE–SSW regional shortening generating the SSW-verging folds and the NNE dipping thrusts. Event D_2 was an ENE–WSW shortening producing NNW–SSE oriented folds in the central and eastern parts of the Allaqi-Heiani belt and reactivating older thrusts with oblique-slip reverse fault movement.

5.2.2 South Hafafit Suture (?)

The South Hafafit Suture (SHS) (Fig. 5.3) was proposed by Greiling et al. (1994, 1996) who recognized SSW-wards thrusting immediately to the south of the Hafafit complex and proposed the existence of an offset segment of the AHS south of Hafafit. The proposed SHS juxtaposes Hafafit terrane to the north and Aswan terrane to the south, and restores for a lateral transport distance of at least 300 km to the SE to form the eastward continuation of the previously mentioned AHS. The Aswan terrane is considered to be the equivalent and westward continuation of the Hafafit terrane, and the terrane to the south of the South Hafafit suture is regarded to extend as far south as the Onib-Sol Hamed belt is an equivalent of the Gabgaba terrane (Fig. 5.3). However, such hypothesized restoration is not documented in the field either in the CED and SED of Egypt.

5.3 Shear Zones in the Egyptian Nubian Shield

5.3.1 Syn-accretion Shear Zones

In central and southern ANS, the collision between E- and W-Gondwana is expressed ultimately as typically N–S trending belts of intensely foliated and isoclinally upright folded rock cross-cutting and displacing the earlier arc-arc sutures (Johnson et al. 2011; Fritz et al. 2013). Typical example of these belts is the Hamisana Shear Zone (HSZ; Stern et al. 1989, 1990; Miller and Dixon 1992; Abdelsalam and Stern 1996; De Wall et al. 2001) and Oko Shear Zone (OSZ; Abdelsalam 1994). The major HSZ (Figs. 5.1, 5.2 and 5.6) covers an area of about 15,000 km^2 (300 × 50 km) in southeastern Egypt and northeastern Sudan (e.g. Stern et al. 1989; Miller and Dixon 1992; De Wall et al. 2001; Sakran et al. 2001; Takla et al. 2002). It consists of gneissic and schistose rocks (Fig. 5.6), and isoclinally folded slivers of ophiolite derived from the Allaqi-Heiani and Onib-Sol Hamed sutures. Because of its sinistral sense of shear, the HSZ causes remarkable dragging of the AHS and goes further north bounding the Gerf Nappe from the east, then continues to meet the Red Sea Coast. Abdelsalam and Stern (1996) proposed dextral sense of shear along the HSZ based on the dextral offsetting of the Yoshgah Suture (Stern et al. 1989, 1990). According to Stern et al. (1989), the HSZ deformation began after 660 Ma, with intense E–W shortening and N–S extension accompanied by greenschist to amphibolite facies metamorphism and development of upright isoclinal folds and vertical foliations. Deformation probably ceased by 550 Ma. Latest deformation effects are minor dextral NE-striking shears, especially at the northern end of the HSZ. The apparent dextral displacement between the Allaqi-Heiani and Onib-Sol Hamed sutures was disproved by Abdelsalam and Stern (1996) and De Wall et al. (2001) eliminating the main evidence for major shearing along the HSZ.

The geometric aspect and kinematic history of the HSZ have been the subject matter of controversy where it was

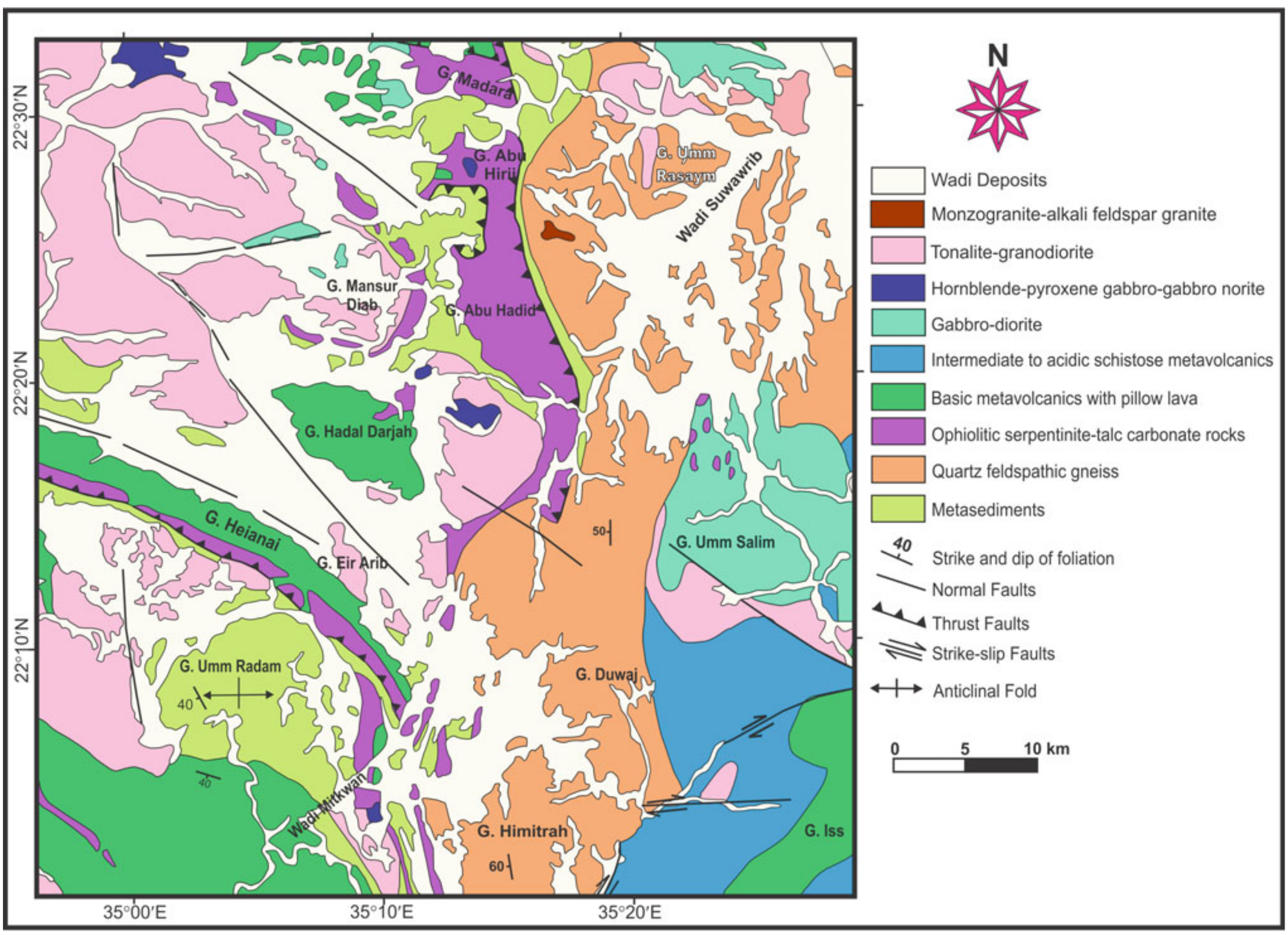

Fig. 5.6 Geologic map of the northern part of Hamisana Shear Zone (HSZ), southern Egypt, slightly modified after EGSMA (2002) and Ali-Bik et al. (2014)

regarded as (1) an arc-arc suture (e.g. Vail 1985, Shackleton 1986), (2) as a transcurrent or transpressive shear zone formed just after the arc accretion stage (e.g. Almond and Ahmed 1987; Kröner et al. 1987; Greiling et al. 1994; Smith et al. 1999; Ibrahim et al. 2016), or as (3) post accretion mainly dominated high strain zone with subordinate parallel or cross-cutting ductile shears (e.g. Stern et al. 1989,1990; Miller and Dixon 1992; Abdelsalam and Stern 1996; De Wall et al. 2001; Johnson and Woldehaimanot 2003). Miller and Dixon (1992) argued that transpression in itself is polyphase and this is consistent with the geometric relationship between the eastern extension of the AHS and the HSZ. De Wall et al. (2001) carried out integrated field and AMS studies, and demonstrated that deformation in the HSZ is dominated by pure shear under upper greenschist/ amphibolite grade metamorphic conditions, producing E–W shortening, but with a strong N–S-extensional component. The authors demonstrated that deformation was responsible for folding of regional-scale thrusts (including the base of Gerf and Onib ophiolitic nappes) and indicate that high strain deformation is younger than ophiolite emplacement and suturing of arc-arc terranes. The obtained data led these authors to conclude that the HSZ is dominated by late orogenic compressional deformation and cannot be related to either large-scale transpressional orogeny or major escape tectonics. Stern et al. (1990) proposed four deformation phases in the vicinity of the HSZ. The oldest phase (D_1) records emplacement of the ophiolitic rocks. This produced a complex imbrication of ophiolitic and metavolcanic sequences. D_2 folding around north-trending axes produced a regional cleavage (S_2), subhorizontal intersection lineation (L_2), and tight, upright to inclined folds (F_2). D_3 is coaxial with D_2 and refolds S_2, locally producing pencil structures and crenulations in the western Hamisana. The resultant pervasive northsouth fabric is truncated by narrow, NNE-trending D_3 dextral shear zones. These become more dominant in the extreme south as the HSZ turns southwest. Later kinks (D_4) and brittle faults have variable movement sense and account for limited regional strain. Thus, the principal ductile deformation in the HSZ is characterized by nearly coaxial folding about a north-south axis, indicating shortening normal to the zone, i.e. east-west.

5.3.2 Post-accretion Shear Zones

Hamimi et al. (2019) outlined three ANS-scale deformation events (D_1 to D_3). Among this scheme, the D_2 deformation was considered to be a post-accretion shortening phase, that produced transpressive structures, including NNW-SSE trending sinistral transcurrent shears (Fig. 5.7) (e.g. Nugrus, and Atalla Shear Zones), the dextral transcurrent shearing along NE-directed mega shears (e.g. Idfu-Mersa Alam and Qena Safaga Shear Zones), and the post-accretionary shear zone-related gneiss domes (Fig. 5.7) (e.g. Meatiq, Sibai, Shalul, and Hafafit gneiss domes) (Fritz et al. 1996, 2002, 2013; Loizenbauer et al. 2001; Abd El-Wahed 2008, 2014; Abdeen et al. 2014; Fowler and Osman 2009; Abd El-Wahed et al. 2016; Hamimi and Hagag 2017; Stern 2017; Hagag et al. 2018).

5.3.2.1 Najd-Related NW-Trending Shear Zones

It is widely accepted that there are significant effects of Najd Fault System (NFS) on the ANS and the CED of Egypt. Stern (1985) considered the NFS as the largest Proterozoic Shear System on Earth, representing the youngest major structural element in the Eastern Desert of Egypt. The NFS has a great importance due to its major extension, role in the exhumation of metamorphic core complexes and prominence in Gondwana cratonization. Moore (1979) studied primary and secondary faulting in the NFS of the Arabian Shield and defined the NFS as a major transcurrent (strike-slip) fault system of Proterozoic age in the Arabian Shield. He suggested a similarity of NFS to many of the world's major transcurrent fault systems, including the San Andreas (USA) and Alpine (New Zealand) faults in terms of its length (possible length of more than 2000 km). He added that the system is a braided complex of parallel and curved en echelon faults. For the NFS and especially close to the terminations of some major faults, a complex association of secondary structures including strike-slip-, oblique-slip-, thrust- and normal-faults, in addition to folds and dike swarms are usually present forming an intricate array. Therefore, the importance and complexity of NFS is augmented by this array of secondary structures that give an allusion to synchronous compressional, extensional and dilational conditions in various parts of the fault zone.

The NFS was identified originally as a NW-trending brittle–ductile shear zone with 300 km width and length over 1100 km extending across the northern part of the ANS (Brown and Jackson 1960; Delfour 1970). Stern (1985) and Johnson et al. (2011) defined the NFS as a huge shear zone system striking NW–SE and has more than 1000 km extension across the shield. So, how was it evolved or formed? Brown and Jackson (1960) earlier interpreted the NFS in the Arabian Shield as late Neoproterozoic and early Phanerozoic strike-slip faulting dislocation associated with the culmination of the Hijaz Orogenic Cycle (multiple episodes of sedimentation, volcanism and intrusive activity accompanied by deformation (Brown and Coleman 1972). Moore (1979) elucidates that the NFS formation is a result of simple shear that allowed the Nubian Shield and southern Arabian Shield to move several hundred kilometers sinistrally with respect to northern Arabia. Originally, the NFS and the other NW-trending strike-slip faults in the ANS are considered post-accretionary structures and were interpreted

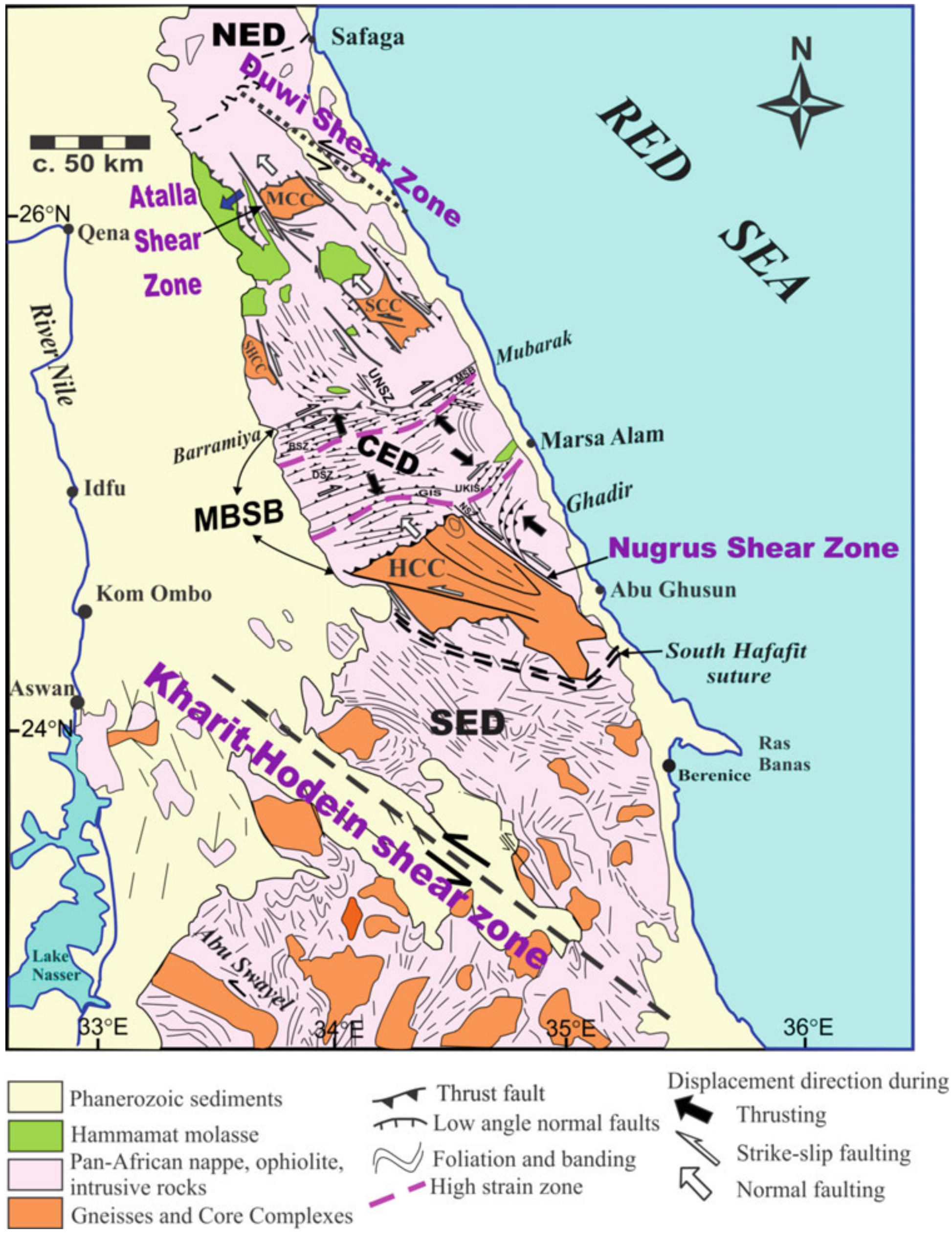

Fig. 5.7 Major structures in the Central Eastern Desert (CED). The Najd Fault Zone in the Eastern Desert is enclosed between Kharit-Hodein shear zone in the south and Duwi Shear Zone to the north. SED; South Eastern Desert, CED; Central Eastern Desert, NED; Northern Eastern Desert, NSZ, Nugrus shear zone, UNSZ, Um Nar shear zone, HCC; Hafafit Core Complex, SCC; Sibai Core Complex; MCC; Meatiq Core Complex; MBSB, Mubarak-Barramiya shear belt. This map is compiled from Greiling et al. (1994), Fritz et al. (1996), De Wall et al. (2001) and (Abd El-Wahed 2014)

to be the result of the squeezing of the ANS between E- and W-Gondwana (Berhe 1990; Stern 1994; Abdelsalam 1994; Abdelsalam and Stern 1996; Abdelsalam et al. 2003). The same mechanism is adopted also for N-trending shortening zones, such as the HSZ (Stern et al. 1989; De Wall et al. 2001) and supported also this mechanism for the formation of subordinate NE–SW trending ones.

The structures in the NFS were developed in response to a sinistral transpressive tectonic regime, with the axis of maximum compressional stress oriented at oblique angles to the NW-trending orogenic front (Abd El-Wahed 2014). The first requirement for any fault is the displacement. The displacement along the strike of the Najd shear zone was reported by Brown (1972) as 240 km cumulative displacement but field displacements can be demonstrated as only tens of kilometers for particular faults (Johnson et al. 2011). From the Arabian shield, the northwestern extensions are probably in the Eastern Desert of Egypt and to the southeast, the line of faulting coincides with structures in the south Yemen coast and in the bed of the Arabian Sea (Brown 1972). In southern Jordan rocks, the NFS is inferred to be present and disrupted by much younger Cenozoic slip on the Dead Sea Transform (El-Rabaa et al. 2001). In the Mozambique Belt in Kenya and Madagascar, similar NW-trending shear zones were identified (Raharimahefa and Kusky 2010). The influence of the NFS also continued to southeast into parts of India and the Lut block of Iran as s reported by Al-Husseini (2000) from Magnetic and gravity data.

Geochronologically, the absolute radiometric ages obtained from small intrusions denoted that the Najd-related shear zones were active from late Neoproterozoic into early Phanerozoic times, 580–530 Ma (Fleck et al. 1979). The late stages (630–535 Ma) of the Pan-African event witnessed the NFS development in the form of huge shear zone system striking NW–SE (Stern 1985; Johnson et al. 2011). Geophysically, subsurface aeromagnetic maps interpretation denoted a continuity of the NFS beneath the surface faults arrays concluding that NFS is broader at depth than the outcropping fault complex (Moore 1979). At depth and under amphibolite facies prevailing conditions, an early shear ductile activity of the NFS is prevailing which is turned into brittle shearing at the shallower levels (Johnson et al. 2011; Fritz et al. 2013). Hydrothermal activity, in turn was pervasive indicating abnormally high heat transfer in the time of faulting. The hydrothermal alteration is probably also a reflection of the mechanical importance of fluid pressure in the mechanism of faulting at this structural level (Phillips 1972).

Master faults of the NFS is constituted of parallel and en echelon major faults attaining more than 300 km in length. These faults or other major fractures are preferentially susceptible to weathering and form Wadi valleys shown clearly in aerial photographs and satellite images. Minor secondary structures are associated with the NFS and are simply classified according to their relation to the major structures into pre-date or independent of major faults, and those which are directly interrelated to master structures (Moore 1979).

Deformation analysis and field studies gave evidence that the ductile deformation was followed by brittle failure during the main faulting episodes. Strictly speaking, the NFS is dominated by northwest striking faults. On the other hand, the theoretical complements (Major northeast striking dextral faults) to the main system are rare (Moore 1979). It is worth mentioning to denote that the NFS is a coherent structure that can be explained by a single regional event (Moore 1979). The sinistral strike–slip shearing along the NFS was accompanied by transpressional and transtensional tectonic regimes (Fritz et al. 1996). Abu-Alam et al. (2014) assigned all of the structural events that occurred in the northern Arabian–Nubian Shield during the last 90 Myr of the Pan African orogeny as a part of the NFS, which start in a compressional tectonic setting, with strike-slip function that ultimately assisted escape tectonics.

Hassan et al. (2016) stated that the Najd-related Shear Zones are responsible for re-configuring the structure of the lithosphere, especially in active tectonic regions and also concluded that the timing of the Ajjaj Shear Zone (in the Arabian Shield) is younger than the exhumation history of the rest of the domes in Arabian Nubian Shield, perhaps correlating with differences in exhumation mechanism. In the Arabian part of the shield, the Ajjaj Shear Zone is one of strands of the NFS (Hassan et al. 2016) that is considered to be extended into the Eastern Desert of Egypt (Sultan et al. 1988). The CED and the northern parts of the SED are characterized mainly by the prevalence of a NW-trending tectonic fabric marking the NW–SE sinistral shear zone of the NFS (Fig. 5.7) (Fritz et al. 1996, 2002; Abd El-Wahed and Kamh 2010; Abd El-Wahed et al. 2016; Makroum 2017; Abd El-Wahed and Thabet 2017). Other comprehensive structural studies in the basement areas west of Quseir established time relationships between stages of Pan-African folding and thrusting and subsequent Najd wrench faulting (Abdeen et al. 1992; Fowler and El Kalioubi 2004; Greiling et al. 1994; Fritz et al. 1996; Abdeen and Greiling 2005). The CED deformation events (Loizenbauer et al. 2001; Makroum 2001; Fritz et al. 2002; Shalaby et al. 2005; Abd El-Wahed 2008, 2014; Abd El-Wahed and Abu Anbar 2009; Abdeen et al. 2008; Abd El-Wahed et al. 2016) might have started with an early phase preserved in amphibolite enclaves in the gneiss-cored domes. What is followed by thrust-related structures associated with oblique convergence of the arc and back-arc assemblage onto the Saharan Metacraton around 620–640 Ma (Loizenbauer et al. 2001). Subsequently, NW-trending sinistral shear zones of NFS were developed (Fritz et al. 2002; Abd El-Wahed 2007, 2008; Abd El-Wahed et al. 2016). This phase of deformation was associated with transpression and lateral extrusion and was followed by exhumation of core complexes in orogen parallel extension around 620–580 Ma (Fritz et al. 1996; Makroum 2001; Fritz et al. 2002; Bregar et al. 2002; Abd El-Wahed 2008; Abd El-Wahed et al. 2016; Makroum 2017; Abd El-Wahed and Thabet 2017).

In the CED, several lines of evidence indicate that the exhumation of the core complexes is related to the sinistral shearing along the NFS, which bound them from the SW and NE (Fig. 5.7). Not only core complexes of the CED, but also its Hammamat molasse sediments which are tectonically affected by the NFS (Abd El-Wahed 2010).

To sum up, the NFS consists of brittle–ductile shearing in a zone as much as 300 km wide and more than 1100 km long, extending across the northern part of the Arabian Shield. Its relation to the CED could be epitomized in the following three points:

- The role of sinistral shearing and transpression related to the NFS in the exhumation of the gneiss domes and in deformation styles,
- The tectonic history of the CED is recently explained through NW-trending sinistral shear zones of the NFS (Fritz et al. 1996, 2002, 2013; Bregar et al. 2002; Shalaby

et al. 2005; Abd El-Wahed 2008, 2010; Abd El-Wahed and Kamh 2010; Abd El-Wahed et al. 2016).

- The genetic relationship of the NFS deformation either with deposition and deformation of Hammamat sediments (Abd El-Wahed 2010) or with syntectonic granitoids emplacement (Fritz et al. 2013; Hamdy et al. 2017b).

Kharit-Hodein Shear Zone

Kharit-Wadi Hodein Shear Zone (KHSZ) (Fig. 5.8) is a distinctive high angle NW-oriented transcurrent shear zone extending for about 186 km in the SED of Egypt, and exhibiting sinistral sense of shear confirmed by various kinematic indicators such as veins, deflected markers, S-C structures, microscale foliations, porphyroclasts, mica fish and mineral fish (Hamimi et al. 2019). The KHSZ is suspected to have accommodated up to 300 km of sinistral displacement during late stages of transpression. Transpression has also been described as being confined to identifiable discrete shear zones (Greiling et al. 1994; Zoheir 2011; Hagag et al. 2018). Opinions differ about the tectonic affinity of this shear zone, where some workers (e.g. El Gaby et al. 1988; Stern et al. 1990) proved that it is a Najd-related shear system (analog of the 655–540 Ma NFS in the Egyptian Eastern Desert), others (e.g. Fritz et al. 1996; Fowler and El Kalioubi 2004) considered it as a youngest major structural element in the Egyptian Eastern Desert, or a transpressional corridor (Greiling et al. 1994; Nano et al. 2002). Ramadan and Kontny (2004) reported gold mineralization in listwaenite-type wallrock alteration at Gabal El-Anbat (Fig. 5.9) in the vicinity of this shear zone. Greiling et al. (1994) supposed that the KHSZ has connected the perhaps once continuous-previously mentioned Allaqi- and South Hafafit-Sutures (before being overprinted by the HSZ). Hamimi et al. (2016) reported a dextral sense of shear along the main Wadi Kharit overprinting the main sinistral shearing, which may demonstrate switching in tectonic regime from sinistral to dextral along the Najd Shear Corridor in the Egyptian Eastern Desert.

Nugrus Shear Zone

Nugrus Shear Zone (NSZ) represents one of the conspicuous Najd-related shears to the southwest of Mersa Alam Costal City, between Wadi Ghadir to the east and Hafafit Gneiss Complex to the west (Figs. 5.10, 5.11 and 5.12). The NSZ trends in a NW direction as a NE-steeply dipping high strain zone, with approximately 750 m maximum width. It separates hanging wall low-grade ophiolitic metaultramafic nappes and volcanogenic metasediments from Hafafit high grade gneisses in its footwall which is thought to be of high temperature–low pressure amphibolite facies (El-Ramly et al. 1984, 1993). The metamorphic conditions were estimated by Asran and Kabesh (2003) at 720–740 °C for Migif-Hafafit amphibolites and at 800–820 °C for associated migmatites, both under pressures of 6–7 kbar. The pressure

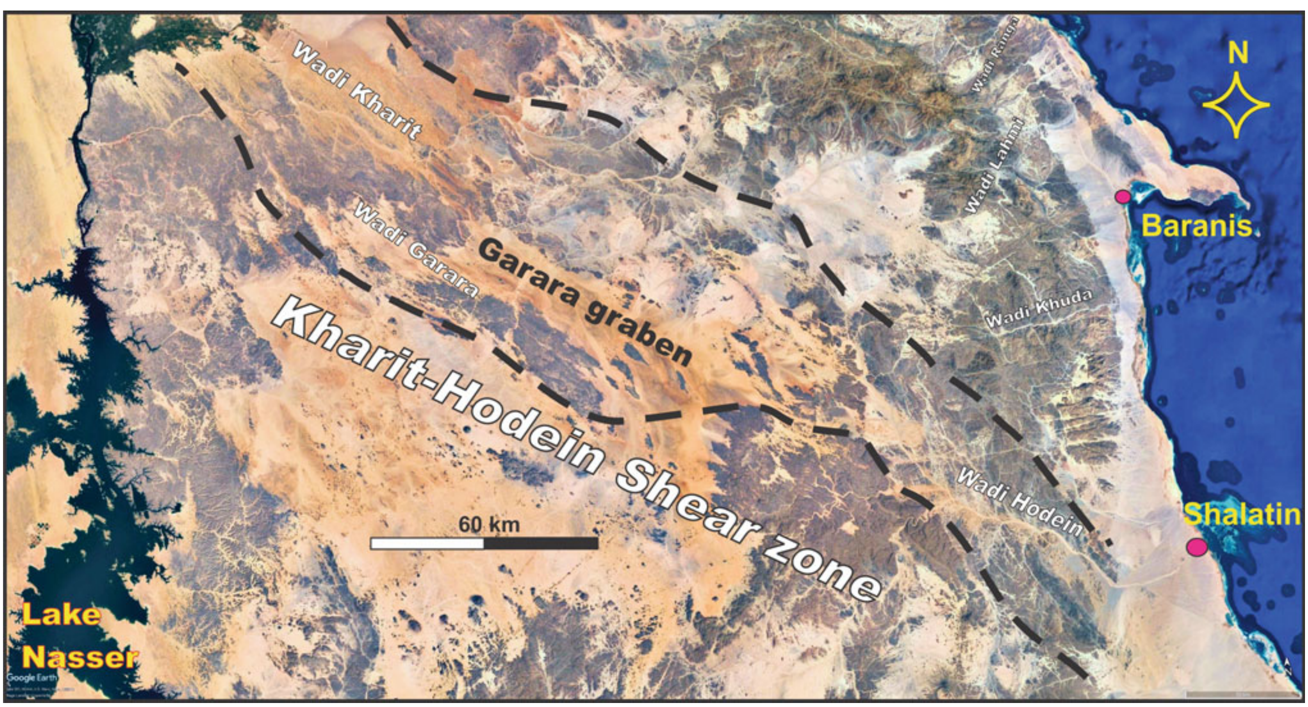

Fig. 5.8 Kharit-Wadi Hodein Shear Zone (KHSZ) is NW-oriented transcurrent shear zone extending for about 186 km in the SED of Egypt

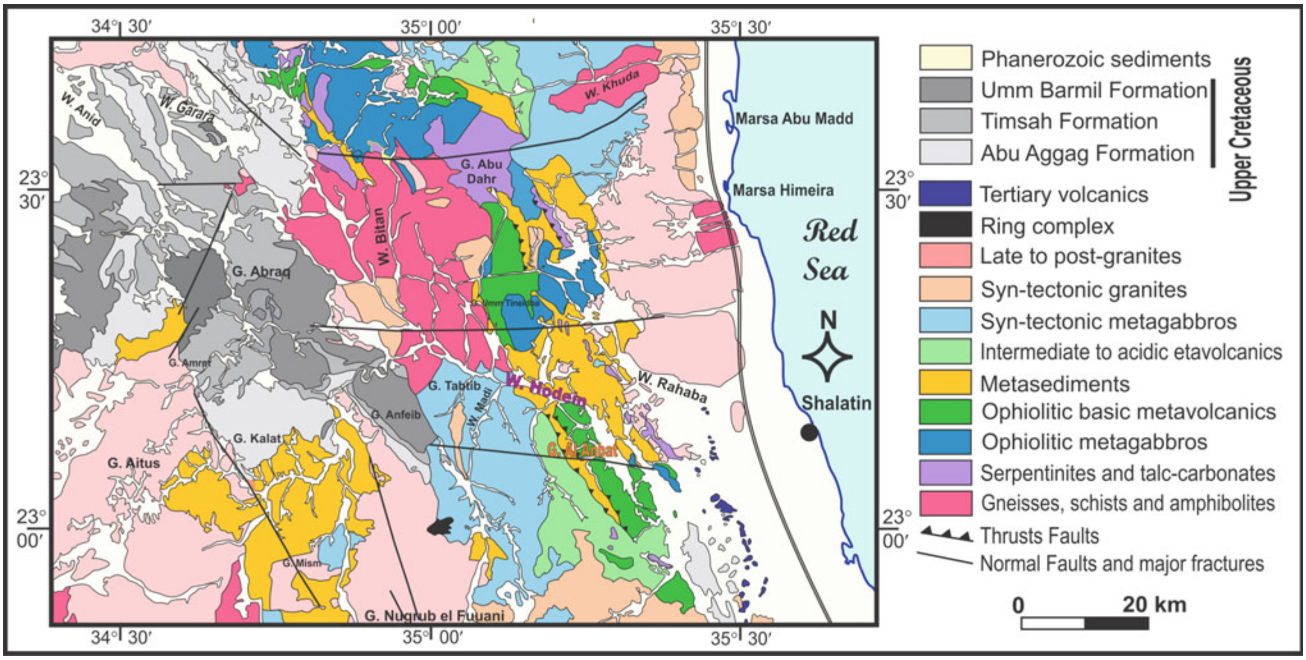

Fig. 5.9 Geological map of the eastern part of Kharit-Hodein Shear Zone (modified after Conoco 1987)

conditions were confirmed as 6–8 kbar by Abd El-Naby and Frisch (2006).

Emplacement of the low-grade meta-ultramafic nappes over the high-grade Hafafit gneisses taken place at c. 680 Ma (Greiling et al. 1988; Liégeois and Stern 2010). The NSZ was interpreted in terms of (a) thrust duplexes (Greiling et al. 1988; El-Ramly et al. 1993), (b) Najd-related Shear Zone with sinistral sense of shear (Fritz et al. 1996; Makroum 2003; Abd El-Wahed et al. 2016), and (c) as part of a northerly dipping Sha'it–Nugrus Shear Zone which is a post-arc collision low-angle normal ductile shear zone separating CED from SED (Fowler and Osman 2009). Various kinds of kinematic indicators reflect the sinistral sense of shearing along the NSZ, including mylonitic foliation, shear bands, S-C foliations and deformed objects with monoclinic symmetry. The sense of shearing is also confirmed at the microscopic scale by sigmoidal structure and mineral fish that are remarkably observed in the oriented thin sections. In the field, these structures overprint arc collision-related nappe structures ($\approx$680 Ma) and are therefore post-arc collision (Fowler and Osman 2009).

The timing of shearing of the NSZ is also debatable. Fowler and Osman (2009) argued that the timing of the NSZ shearing is a distinctly younger shearing event at around 600 Ma. This idea is supported by the conclusion of Greiling et al. (1994) that extensional collapse in the region began at about 600 Ma, and accelerated during the period 595–575 Ma. Greiling (1985) stated that NSZ age is bracketed between 680 Ma (the age of sheared trondhjemite) to 595 Ma (age of post-tectonic granite), relatively. On the other hand, Mohamed (1993) showed that the activity time on the NSZ was bracketed between the intrusion of the older granitoids and the younger granitoids. Rb/Sr whole rock ages of 610 $\pm$ 20 Ma and 594 $\pm$ 12 Ma for leucogranites intruded into the schists bordering the Sha'it-Nugrus Shear Zone was given by Moghazi et al. (2004).

The Hafafit-Nugrus area (Figs. 5.11 and 5.12) has attracted the attention of many authors through displaying an apparent contrast not only in metamorphic grade but also in the deformation intricateness which leads El Ramly et al. (1993) to disaggregate the area into two main groups disaffiliated mainly by a low angle Nugrus thrust tracing along the upper part of Wadi Sikait in a NW direction and intruded by the late granitoids. The Nugrus-Sikait belt was defined as structural contact represented by a regional NW-SE trending thrust belt dipping due NE direction and featured remarkably by ductile deformational fabrics including folding, mineral lineation and foliation (Fig. 5.13a, b) in the metamorphic exposure rocks. The NSZ is considered as a Najd-related ductile strike-slip shear (Fritz et al. 1996; Hassan 1998; Shalaby et al. 2005) considered the NSZ as a Najd-related ductile strike-slip shear. Shalaby et al. (2006) argued about the NSZ being a strike-slip shear zone as the NW trending, along strike, schistose shear foliations is ceased at the intersection of Wadi Nugrus with Wadi Sha'it. The NSZ is described as an example of a low-angle normal ductile shear (LANF) as its approximately E–W strike, low-angle N-dip and a normal shear sense.

Various interpretations were introduced for the NSZ formation. El-Gaby et al. (1988), El-Bayoumi and Greiling

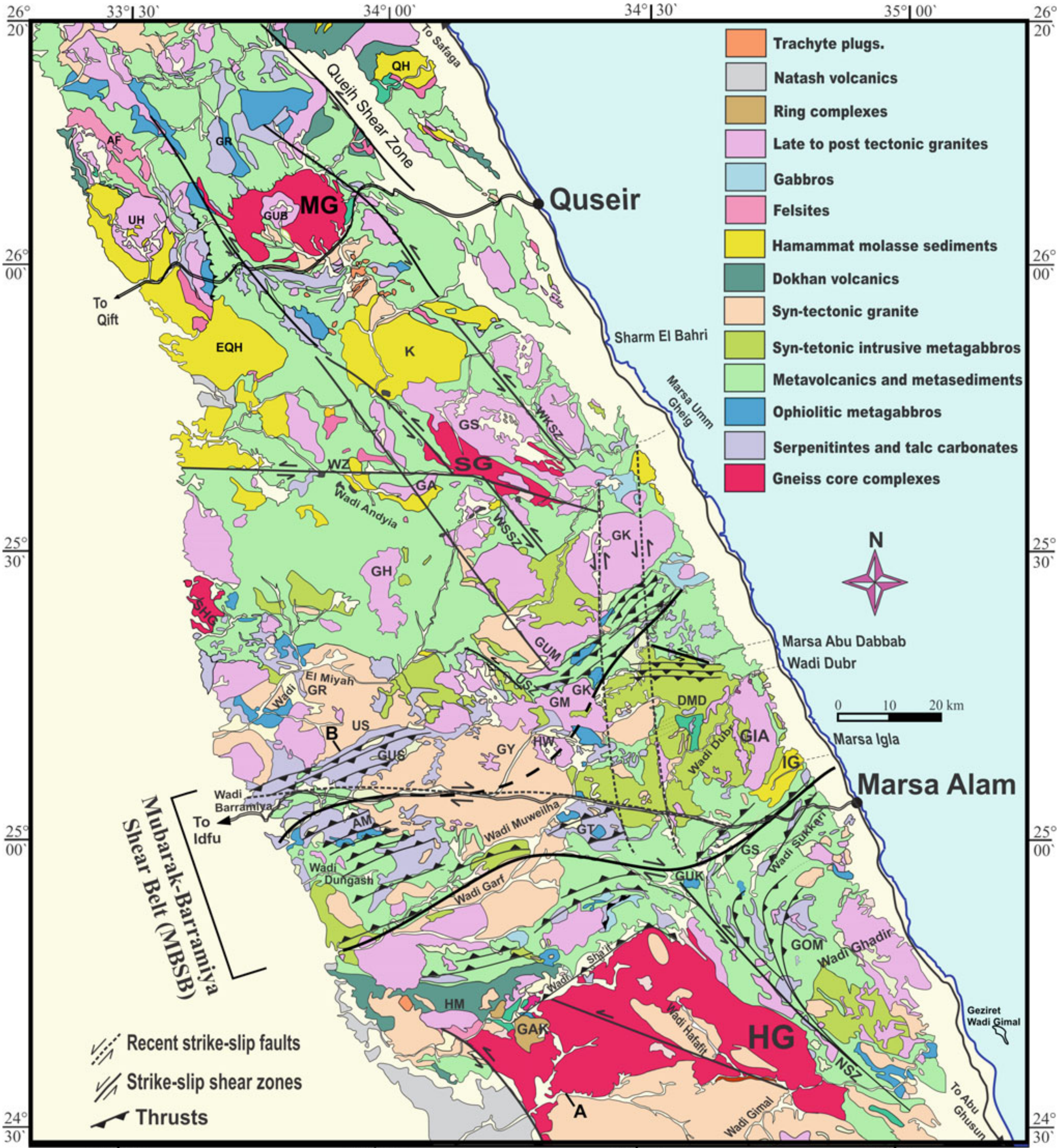

Fig. 5.10 Geological map of the southern part of the Central Eastern Desert of Egypt (modified after Conoco 1987). GAK; Gebel Abu Khruq, HG; Hafafit gneiss, GOM; Wadi Ghadir ophiolitic mèlange, HM; Hamash gold mine, NSZ; Wadi Nugrus shear zone, GS; Gebel Sukkari and Sukkari gold mine, GUK; Gebel Um Khariga, IG; Igla molasse basin, DMD; Dubr metagabbro-diorite complex, GIA; Gebel Igl Al-Ahmar, HW, Gebel Homrat Waggad, GY, Gebel El-Yatima, GUS; Gebel Umm Salim, US, Gebel Umm Saltit, GK; Gebel Abu Karanish, GM, Gebel Al Miyyat, USZ; Um Nar shear zone, GUM; Gebel El-Umra, GK; Gebel Kadabora, GA; GH; Gebel El-Hidilawi, GU; Gebel Umm Atawi, SHG; El Shalul gneiss, GR; Gebel El Rukham; SG; Sibai gneiss, GS; Gebel Sibai, WZ; Wadi Zeidon, WSSZ; Wadi Sitra shear zone, WKSZ; Wadi Kab Ahmed shear zone, K; Kareim molasse basin, MG; Meatiq gniess, AF: Gabal Atalla Felsites, QH, Quieh Hamammat sediments, EQH, El-Qash Hamammat sediments, UH; Um Had granite, GR; Gabal Rabshi, GUB; Gabal Um Ba'anib. The major structures are after Akaad et al. (1993), Fritz et al. (1996), Shalaby et al. (2005), Abd El-Wahed (2008) and Abd El-Wahed and Kamh (2010), Abd El-Wahed et al. 2016; Hamdy et al. (2017b) and Hamimi et al. (2019)

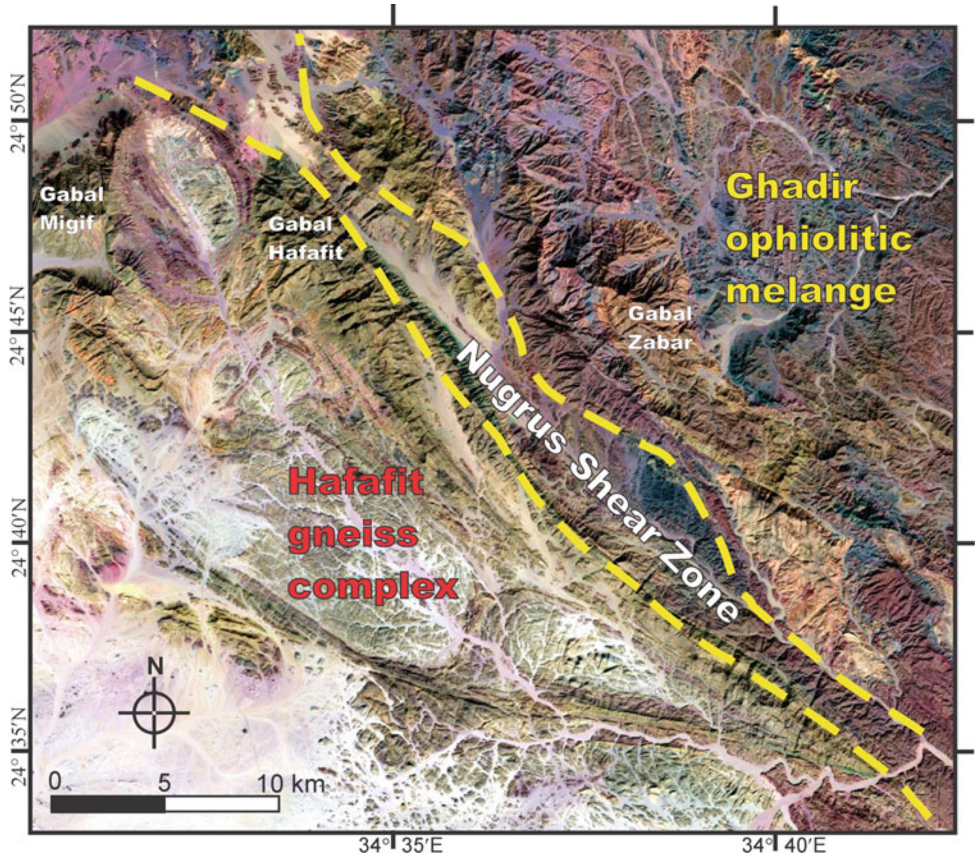

Fig. 5.11 Location of Nugrus Shear Zone

(1984), and El-Ramly et al. (1984) envisaged it as thrust accommodating westward or SW-ward ophiolitic material transport over the continental margin. In full awareness of that the NSZ shows top to-NW kinematic indicators, Greiling et al. (1994) and Greiling (1997) elucidated it as a roof thrust linked up NW-dipping thrust imbricates of gneissic rocks and allowing NW-ward displacement of low-grade CED metavolcanics over the latter gneisses. Let us remark that the gneisses are younger than the metavolcanics (Andresen et al. 2009).

A significant point of view was introduced by Fritz et al. (1996) and Unzog and Kurz (2000) who interpreted the NSZ as a sinistral strike-slip fault (along Wadi Nugrus) and also interpreted the remaining part of the CED and SED boundary as low-angle normal fault (along Wadi Sha'it). A dramatic hypothesis was claimed by Shalaby et al. (2006) denoting a continued extension of the sinistral strike-slip NSZ more northerly till the latitude of the Meatiq gneissic complex. The field evidence for this continuation are absent beyond the meeting point of Wadi Sha'it and Wadi Nugrus. Fowler and Osman, (2009) concluded that the NSZ was originally a gently N or NNW dipping shear structure with top-to-NW or NNW displacement. Such a fault has a normal sense of displacement supported by the juxtaposition of low-grade rocks in the hangingwall against high-grade footwall gneisses.

The metamorphic grade contrast along NSZ constitutes the main estimated displacement along it. The footwall of NSZ is Migif-Hafafit gneisses seemed to be of high temperature—low pressure amphibolite facies (El-Ramly et al. 1984, 1993). Numerically, the metamorphic conditions were estimated by Asran and Kabesh (2003) as 720–740 °C for Migif-Hafafit amphibolites and 800–820 °C for associated migmatites, both under pressures of 6–7 kbars. The pressure conditions were confirmed as 6–8 kbars by Abd El-Naby and Frisch (2006).

On the other hand, numerical estimations of the greenschist facies CED metamorphics show about 450 °C at 4 kbars pressure (Fritz et al. 2002). This gives a 3 ± 1 kbar pressure difference across the SNSZ corresponding to a loss of section measuring 10 ± 3.5 km. Assuming the 25° dip of the NSZ, an estimated displacement of 15–30 km is considered. Geochronologically, the data suggests that the emplacement of low-grade nappes above gneisses occurred at around 630 Ma (Andresen et al. 2009). The timing of the NSZ shearing is a distinctly younger shearing event at around 600 Ma (Fowler and Osman 2009). This corroborates the conclusion by Greiling et al. (1994) that extensional collapse in the region began at about 600 Ma, and

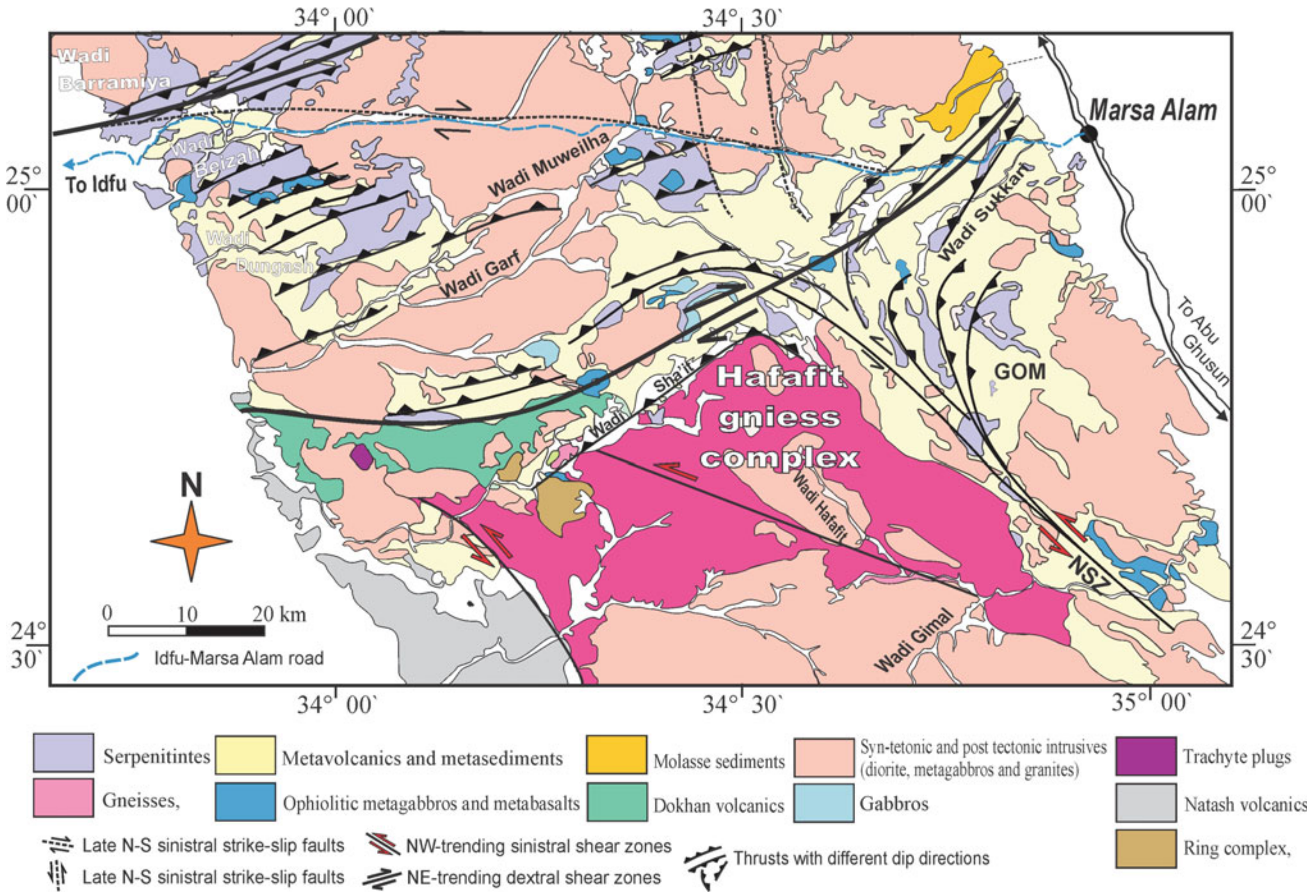

Fig. 5.12 Geological map of the southern part of the Central Eastern Desert of Egypt showing Nugrus Shear Zone and Hafafit gneiss complex (modified after Conoco 1987)

accelerated during the period 595–575 Ma. Greiling (1985) stated that NSZ age is bracketed between 680 Ma (the age of sheared trondhjemite) to 595 Ma (age of post-tectonic granite). Relatively, Mohamed (1993) mentioned the activity time on the NSZ was bracketed between the intrusion of the older granitoids and the younger granitoids. Rb/Sr whole rock ages of 610 ± 20 and 594 ± 12 Ma for leucogranites intruded into the schists bordering the SNSZ was given by Moghazi et al. (2004).

Atalla Shear Zones

Atalla Shear Zone (ASZ) (Fig. 5.14) is a NW-oriented steeply dipping high strain zone encompassing several map- to centimeter-scales kinematic indicators with monoclinic symmetries reflecting sinistral sense of shearing (Zoheir et al. 2018). The ASZ is marked by Atalla felsite mass (28.4 km long by 7.2 maximum width) (Akaad and Noweir 1977; Akaad 1996). Opinions differ about the tectonic setting of the Atalla felsite. Some authors (e.g. Noweir 1968) defined this unique lithologic unit as "a post Hammamat felsite", whereas others (e.g. Essawy and Abu Zeid 1972) considered the Atalla felsite and the associated siliceous metatuffs and acidic flows as rocks belonging to ummetamorphosed old volcanics of the Dokhan type. On the other hand, Akaad and Noweir (1977) and Akaad et al. (1979) considered the Atalla felsite as older than Um Had granite pluton, and this is proved in the field where the felsite extruded the mélange rocks (serpentinites, metasediments metavolcanics and acidic tuffs) and both of them are intruded by Um Had granite. Mélange in Wadi Atalla contains chaotically assembled smaller blocks of ophiolitic (but not arc) lithologies set in a foliated matrix of graphitic pelites and greywackes (Fig. 5.15). These blocks and matrix are encountered in many other areas in the CED and SED, such as Wadi Ghadir (El-Sharkawy and El-Bayoumi 1979; Elbayoumi and Greiling 1984), El-Barramiya Range (Gad and Kusky 2006), Wadi Mubarak (El-Bayoumi and Hassanein 1983; Farahat et al. 2004; Abdel-Karim et al. 2008), and Gabal El Rubshi (Amstutz et al. 1984; Habib 1987; El-Desoky et al. 2015). In this context, two belts of ophiolitic mélange were identified adjoining with both Meatiq and Hafafit complexes (Liégeois and Stern 2010). Both belts were interpreted in terms of an arc collision model as defining arc-arc sutures known as Wadi Atalla-Wadi

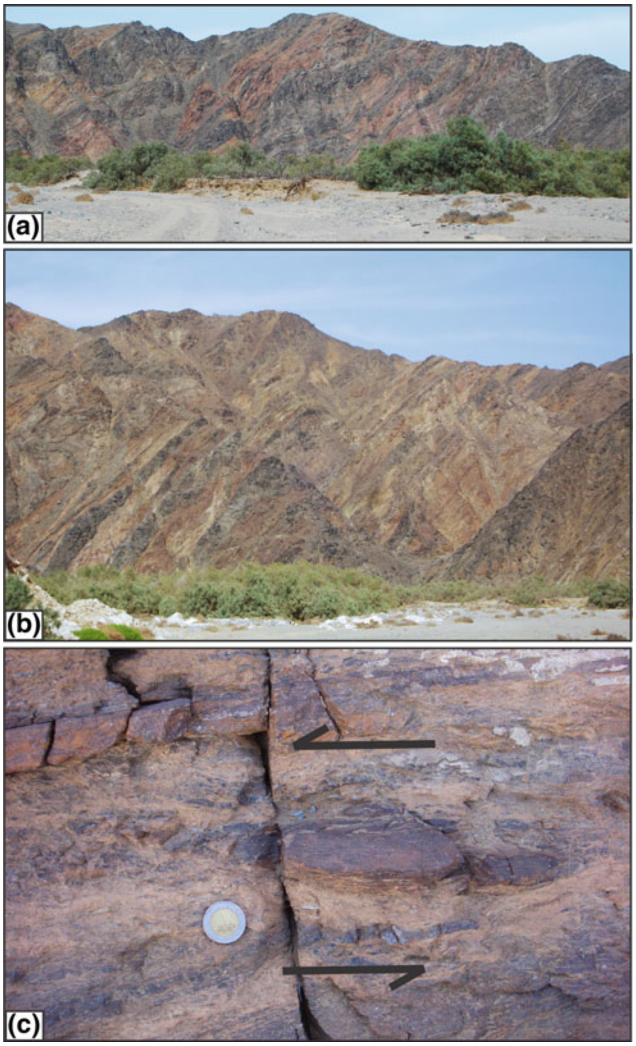

Fig. 5.13 **a**, **b** Banded gneisses within Nugrus Shear Zone, Wadi Nugrus, looking SE. **c** σ-type serpentinite porphyroclasts indicating sinistral sense of shear, northern part of Nugrus shear zone, looking NE

Hammuda- and Wadi Ghadir-Barramiya-sutures (e.g. Ragab 1993; Ragab et al. 1993). The so called Atalla-Wadi Hammud Suture was identified as a former forearc basin. Because of the effect of ASZ, both felsite and mélange are intensively sheared, cataclased and exhibiting stretching lineations and slickenlines particularly at their margins.

The NNW–SSE structural trend is related to marginal shear zones and steeply dipping mylonitic foliation. Strike-slip faults juxtapose the ophiolitic mélange nappe to the Dokhan Volcanics and Atalla felsites. Gold mineralization is related to milky and smoky quartz veins in NE-trending faults cutting a small monzogranite body, the Atalla intrusion. The mine area is underlain mainly by a NW–SE elongate belt of ophiolitic rocks, cut by felsic dyke swarms and the Atalla intrusion (Fig. 5.14). Fragments of metabasalt (Zoheir et al. 2018), serpentinite and metagabbro are embedded in a matrix of metasiltstone form large exposures west and north of the mine area. To the east, mafic and intermediate island arc metavolcanic/volcanogenic rocks include foliated metabasalt intercalated with andesite tuffs and breccias (Zoheir et al. 2018). Successions of purple metagreywacke, siltstone and conglomerate (Hammamat Sediments) unconformably overlie the arc metavolcanic rocks (Zoheir et al. 2018). These sediments are generally characterized by NW-SE bedding. Post-Hammamat felsite porphyries (Rb/Sr isochron age of 588 ± 12 Ma; Hassan 1998) form a NNW elongate body cutting the ophiolitic and island arc rocks. In the mine area, these rocks are intensely jointed, finegrained porphyritic rhyodacites. Monzo-syenogranite rocks occur as small intrusions orientated parallel to the NNW–SSE ASZ. The Atalla intrusion ($\sim$0.35 km^2) cuts ophiolitic serpentinites and the post-Hammamat felsite intrusion, and is composed of medium- to coarse-grained, pale pink monzogranite with abundant xenoliths of older rocks (Zoheir et al. 2018).

5.3.2.2 ENE- (to E-) Trending Shear Zones

The ENE- (to E-) trending Shear Zones are eye-catching high strain zones in the entire ANS. These megashear are typified by Fatima- and Ad-Damm-Shear Zones in the Arabian Shield, and Qena-Safaga-, Idfu-Mersa Alam-Shear Zones, along with Mubarak–Barramiya Shear Belt and Abu Dabbab seismotectonic Zone in northern Nubian Shield.

Idfu-Mersa Alam Shear Zone

Idfu-Mersa Alam Shear Zone (IMASZ) is an ENE-oriented dextral transcurrent megashear regarded by some authors (e.g. El Gaby et al. 1988) to represent the boundary between the CED and the SED. Greiling et al. (1994) considered the ENE-trending Idfu-Mersa Alam road a shear zone originated as extension collapse during a post collisional event. The effect of the IMASZ could be traced easily either in the field, or on the Landsat and ASTER imagery, for a distance over 110 km from the area to the west of Barramiya Gold Mine to Mersa Alam Coastal City. The IMASZ deforms the ophiolite-dominated supracrustal successions as well as the structures associated with the older Najd-related NW-trending shear fabrics. Sense of shearing along this shear zone is dextral and well observed at Sheikh Salem area where a huge leucocratic granitic intrusion is remarkably affected by right lateral shearing.

Mubarak–Barramiya Shear Belt

Mubarak-Barramiya Shear Belt (MBSB) is first named by Abd El-Wahed and Kamh (2010) for enormous NE- (to ENE-) trending high strain belt extends from Wadi Mubarak

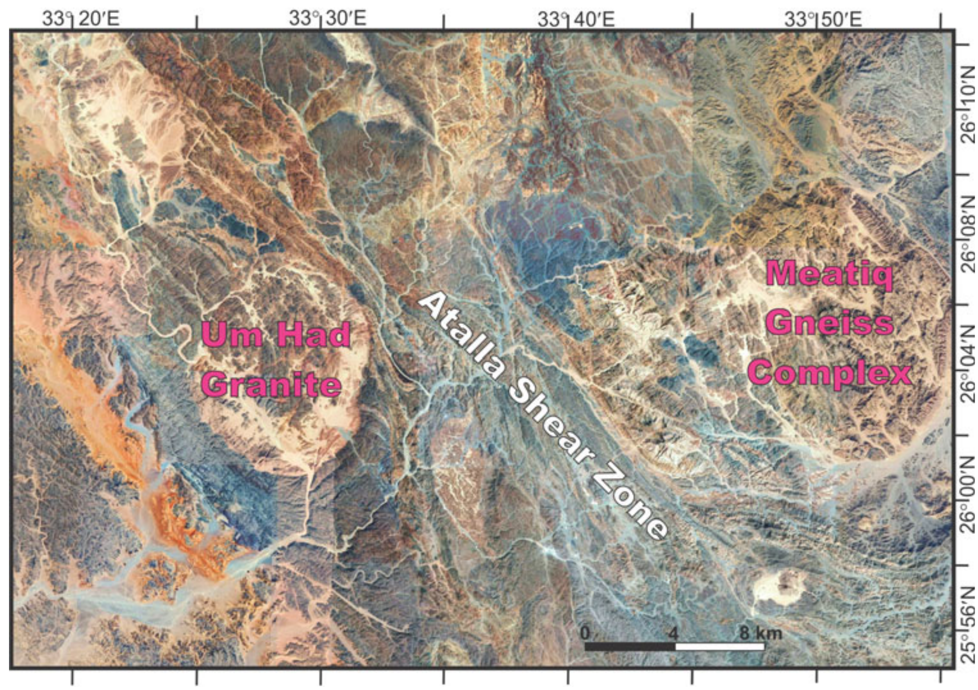

Fig. 5.14 Location of Atalla Shear Zone

on the Red Sea Coast to the area west of Barramiya. Abd El-Wahed and Kamh (2010) and Abd El-Wahed (2014) and reference therein considered this belt as being extending from Wadi Mubarak and Wadi Ghadir on the Red Sea to Wadi Barramiya and Wadi Sha'it to the west. Therefore, the previously mentioned IMASZ represents an elongated sector of the MBSB (Figs. 5.10, 5.16 and 5.17a). The NE-trending MBSB is marked by sheared ophiolites slices scattered in schistose mélange (El Bahariya 2012; 2018). This shear zone separates the low-grade volcanogenic metasediments and metavolcanics in the north from the medium-grade gneissic, migmatites of Hafafit dome. Various structures in this shear belt indicate highly oblique convergence leading to wrench-dominated transpression and development of a major flower structure between Wadi Mubarak and Hafafit dome (Fig. 5.17b) occupying the whole width of the CED (Abd El-Wahed and Kamh 2010).

Three major lithotectonic units were described in the MBSB (e.g. Shalaby et al. 2005; Abd El-Wahed and Kamh 2010; Abd El-Wahed 2014; Abd El-Wahed et al. 2016; Hamdy et al. 2018) namely (i) ophiolite slices and ophiolitic mélange (El Bahariya 2012, 2018), (ii) island arc metavolcanic and metasedimentary successions and (iii) syn- to post-orogenic gabbroic to granitic intrusions. The structural succession and tectonic evolution of the MBSB have been the subject matter of detailed investigations by many workers. Abd El-Wahed (2014) proposed the following sequence of tectonic events (1) Early NW–SE shortening (D_1) associated with accretion of island arcs and obduction of ophiolites over old continent. D_1 produced NNW-directed thrusts and ENE–WSW oriented folds in the CED. (2) an E–W-directed shortening deformation was superimposed due to oblique collision between the Arabian–Nubian Shield and the Nile Craton (D_2) this produced NW-trending upright folds, NE-dipping and SW-dipping thrusts and discreet NW–SE tending shear zones in the CED. NNW-directed thrusts belonging to D_1 were folded around NNW–SSE trending fold axes. Continuing E–W shortening rotated the folded thrust to steeply dipping orientations and initiation of major NW-trending sinistral shear zones and culminated in the initiation of major dextral strike–slip shear zones (D_3) as conjugate sets with the NW-trending sinistral shear zones at c. 640–540 Ma ago. The structures associated with the NW-sinistral shear zones are strongly superimposed by the NE-trending transpressional deformation of the MBSB.

Abu Dabbab Seismotectonic Zone

Abu Dabbab Zone (ADZ) is a Najd-related ENE-oriented high strain zone, located at about 30 km to north of the eastern segment of the previously mentioned IMASZ (Fig. 5.17a). The mouth of Wadi Abu Dabbab can be reached easily through the Marsa Alam-Quseir asphaltic road. ADZ represents one of five seismotectonic zones in Egypt (Hamimi and Hagag 2017), showing daily recorded microearthquakes with local magnitudes (ML < 2.0). In November 12, 1955 and July 2, 1984, two giant earthquakes were recorded with magnitudes 5.6 and 5.2, respectively (Fairhead and Girdler 1970; Badawy et al. 2008). The recorded seismic activity from Abu-Dabbab region by the Egyptian National Seismic Network (ENSN) ranges from 10

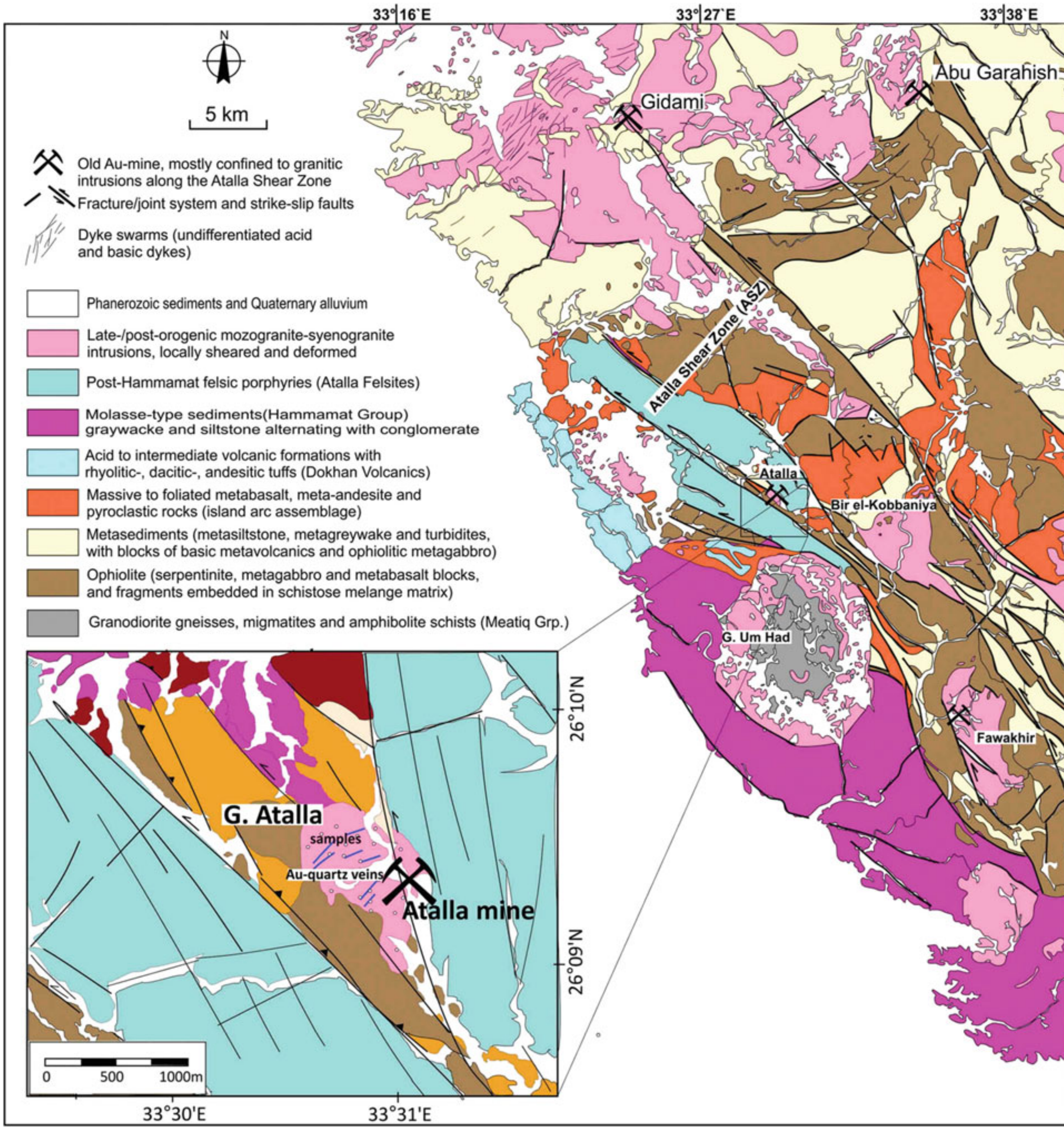

Fig. 5.15 Geological setting of the Atalla shear zone (ASZ) and associated granitic intrusions and gold mineralization (Zoheir et al. 2018)

to 15 events/day to more than 60 events/day, and sometimes attained 100 events/day during swarms (Badawy et al. 2008; Mohamed et al. 2013). Such enigmatic seismic record has attracted the attention of many workers (e.g. Fairhead and Girdler 1970; Daggett et al. 1986; Hassoup 1987; Kebeasy 1990; El-Hady 1993; Ibrahim and Yokoyama 1998; Badawy et al. 2008; Hosny et al. 2009, 2012; Azza et al. 2012; Mohamed et al. 2013) to decipher origin of the earthquakes. The magmatic origin of the seismicity and associated shallow and deep earthquakes is promoting most of the publications dealt with the tectonic setting and seismic activity of Abu Dabbab area (Hamimi et al. 2019). Sabet et al. (1976) suggested that the tectonic evolution of the area was associated with volcanic activity, whereas Daggett et al. (1986) attributed Abu Dabbab seismicity to the subsurface volcanic environment of a cooling pluton. Meanwhile, Hassoup (1987) interpreted this seismicity in the light of the subsurface structural heterogeneity. Hosny et al. (2009) proposed a structural model for the area based on seismic velocity tomography, and related the P and S-wave velocity

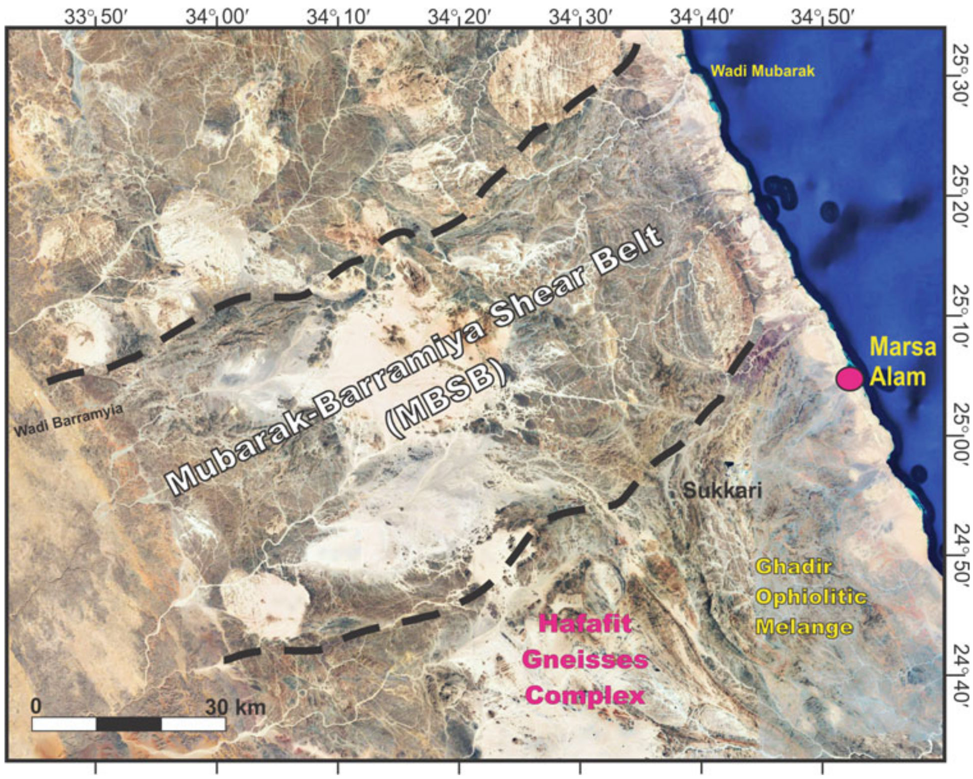

Fig. 5.16 Location of Mubarak-Barramiya Sher Belt (MBSB)

anomaly to magmatic intrusion. Recently, El Khrepy et al. (2015) reveal strong arguments for the tectonic origin of the seismicity of Abu Dabbab area despite of the prevalent magmatic origin. Hamimi and Hagag (2017) proposed a new tectonic model for Abu-Dabbab seismogenic zone based on integrated field-structural investigations, and EMR/seismic data. The obtained results led the authors to indicate a present-day faulting activity in the area and to determine the depth of the brittle-ductile transition zone underlies the Abu-Dabbab area. The transition zone is estimated to be existed at a relatively shallow depth (10–12 km) depending upon the following main criteria: (1) the absence of a large seismic main shock, (2) the periodically recorded swarm's hypocenters of focal depths not deeper than 16 km, (3) the high Vp/Vs ratio (from seismic tomography) until 12 km depth, (4) the occurring of tensile earthquakes of high compensated linear-vector dipole (CLVD) ratios, and (5) the high heat flow rates (about 92 mW/m^2 ± 10, which is more than twice the average value of Egyptian Eastern Desert; 47 mW/m^2). The authors came to the conclusion that there is a mechanical decoupling between the shallow and deep crustal-levels of Abu-Dabbab Neoproterozoic basement succession, where the maximum principal stress axis (σ1) rotates from a sub-horizontal position at the uppermost crustal-levels practicing transpressional deformation to a near vertical attitude in the deeper levels, where the transtensional deformation predominated.

5.3.3 Shear Zone-Related Gneiss Domes

The gneiss domes (Fig. 5.10) in the Eastern Desert terrane (e.g., Meatiq, Sibai, El-Shalul and Hafafit) have been interpreted as metamorphic core complexes exhumed in extensional settings. The origin and mode of deformation and exhumation of these gneissic domes and their relation to the Najd Fault System have been the subjects of many publications (e.g. Fritz et al. 1996, 2002, 2013; Loizenbauer et al. 2001; Bregar et al. 2002; Shalaby et al. 2005; Fowler et al. 2007; Abd El-Wahed 2008, 2014; Andresen et al. 2010; Fowler and Osman 2009; Abd El-Wahed and Abu Anbar 2009; Abu Alam and Stüwe 2009; Abd El-Wahed and Kamh 2010; Shalaby 2010; Johnson et al. 2011; Abu Alam et al. 2014; Abd El-Wahed et al. 2016; Makroum 2017; Stern 2017; Hassan et al. 2016). Gneiss domes in Egypt are mostly bordered by NW-striking sinistral shear zones and low angle normal-faults (Fritz et al. 1996). Geochronology suggests that extension and exhumation of gneiss domes commenced around 620–606 Ma (Fritz et al. 2002; Andresen et al. 2009), contemporaneously with the metamorphism itself (Andresen et al. 2009), all the lithologies being juvenile Neoproterozoic rocks (Liégeois and Stern 2010; Stern et al. 2010).

Some points support the role of the Najd shear zones in the evolution and exhumation of core complexes in the Eastern Desert: (i) The large scale, oblique transpressive shear zones of the Najd Fault System in the Eastern Desert and Sinai was developed during the second

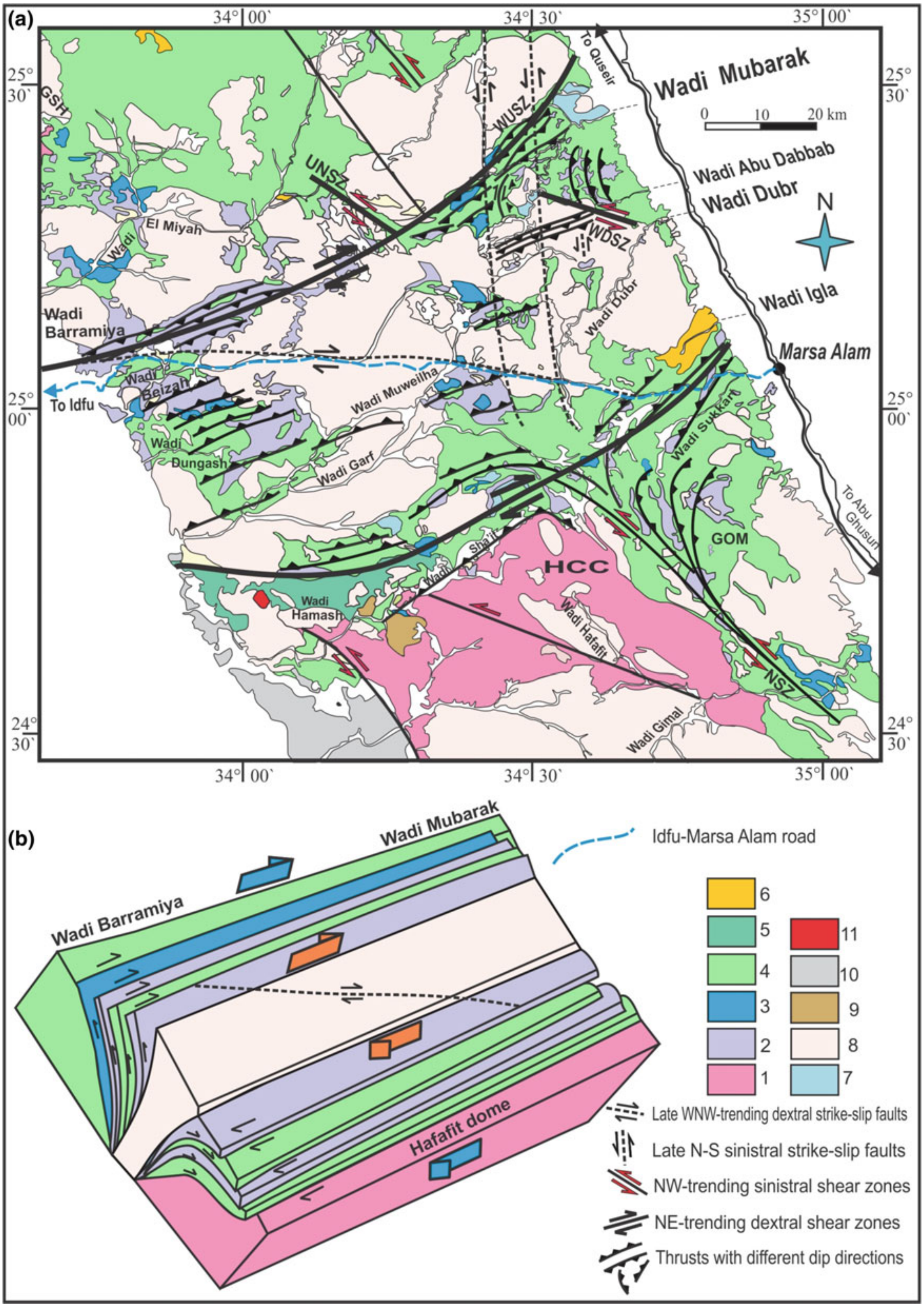

Fig. 5.17 **a** Geological map of the southern part of the Central Eastern Desert of Egypt (after Abd El-Wahed and Kamh 2010, modified from Conoco 1987). 1; gneisses, 2; serpenitintes, 3; ophiolitic metagabbros and metabasalts, 4; metavolcanics and metasediments, 5; Dokhan volcanics, 6; molasse sediments, 7; gabbros, 8; syn-tetonic and post tectonic intrusives (diorite, metagabbros and granites), 9; ring complex, 10; Natash volcanics and 11; trachyte plugs, **b** block diagram showing flower structure constituting Mubarak-Baramiya shear belt. HCC; Hafafit core complex, GOM; Wadi Ghadir ophiolitic mèlange, NSZ; Wadi Nugrus shear zone, UNSZ; Um Nar shear zone, WDSZ; Wadi Abu Dabbab shear zone, WUSZ; Wadi El-Umra shear zone

tectonometamorphic event (D_2) occurred between 680 and 640 Ma (Johnson et al. 2011). During D_2 the ANS collided with the Sahara Metacraton (Liégeois et al. 2013) and moved towards the paleo-Tethys ocean (Stern 1994), (ii) the gneiss domes is bounded by transtensional marginal shears linked by low angle normal faults (Fritz et al. 1996, 2002, 2013), (iii) The oblique setting of the gneiss domes to the main NW-trending shear zones (Abd El-Wahed and Kamh 2010; Abu Alam et al. 2014), (iv) Exhumation history of the core complexes is accompanied by crustal thickening, development of molasse sedimentary basins (e.g. Kareim Basin to the north of Sibai core complex; Abd El-Wahed 2010), (v) There is a relationship between change of the Najd shear kinematics from transpressive to transtension through time and emplacement of transpressive and transtension related granitoids (655 and 645 Ma respectively, Bregar et al. 2002; Abu Enen et al. 2016).

The main constituents of the infrastructural sequence in the Eastern Desert are gneisses and amphibolites which are found in core complexes (e.g., Meatiq, Sibai, El-Shalul and Hafafit). The Meatiq Core Complex is located ~40–60 km west of Quseir, north of the Quseir-Qift road, forming the most prominent gneisscored dome in the Central Eastern Desert of Egypt. The core of the dome consists of coarse-grained, foliated granitic gneisses (Um Ba'anib gneiss; c. 640 Ma; Andresen et al. 2009, the whole gneissic sequence being late Neoproterozoic lithologies; Liégeois and Stern 2010) structurally overlain by metasedimentary succession of quartz-rich schists which are locally intercalated with metapelitic rocks (Fig. 5.18). The Um Ba'anib gneiss is granitic to granodioritic gneiss which is mylonitized close to high strain shear zones. These orthogneisses at their NE side, contain strongly folded migmatized amphibolite xenoliths of several tens of meters in size (Neumayr et al. 1996, 1998; Hamdy et al. 2017a). On the other hand, the metapelitic rocks at the western flank of the MCC are intercalated with weakly foliated, gabbroic and amphibolitic bodies of several hundred meters in size (Loizenbauer et al. 2001). These bodies were interpreted as klippen or outliers of the eugeoclinal allochthon (Loizenbauer et al. 2001; Fritz et al. 2002; Hamdy et al. 2017a). The MCC lies within a NW–SE oriented corridor bordered by two sub-parallel left-lateral NW–SE oriented strike-slip shear zones (Wallbrecher et al. 1993; Fritz et al. 1996; Loizenbauer et al. 2001; Hamdy et al. 2017a). These shear zones separate the medium- to high grade granitic gneisses in the core of the dome from the low grade metamorphosed rocks and consist of steeply dipping biotite, muscovite schists, garnet-mica schists and quartzofeldspathic-schists/gneisses, and mica-rich mylonites. The main segment of the shear zone is principally composed of steeply E- and W-dipping porphyroclastic and ribbon mylonites carrying plunging lineations (Hamdy et al. 2017a). A well-developed mylonitic fabric formed under amphibolite grade conditions dominates the Abu Fannani mylonitic schist where slightly deformed granitic gneiss lenses occur (Hamdy et al. 2017a). Both the granitic gneisses and mylonitic schists are characterized by well-developed stretching lineation that together with shear sense indicators, indicate top-to-NW displacement (Sturchio et al. 1983; Fritz et al. 1996; Loizenbauer et al. 2001). During oblique island arc convergence, deformation in MCC partitioned into NW-SE sinistral strike-slip shear zones marking the eastern and western borders of the core complex and constraining orogen-parallel extension including NE-SW normal faults (Fig. 5.19). Top-to-NNW ductile shearing in the Meatiq Core Complex resulted from the transpression combined with lateral extrusion dynamics (Hamdy et al. 2017a). Oblique extrusion of the deep crust during oblique convergence together with magma generation and extensional structures supports a transpression–extrusion kinematics model (Robin and Cruden 1994; Teyssier and Tikoff 1999) for evolution and exhumation of Meatiq Core Complex (Fritz et al. 1996, 2002) that occurred after 630 Ma (Andresen et al. 2009). NW-SE directed orogen parallel extension leads to formation of strike-slip shear zone bordering the MCC, emplacement of the Abu Ziran granite (606 ± 1 Ma; Andresen et al. 2009), formation of the low angle normal ductile shear zones and final exhumation of MCC. This followed by intrusion of the post-tectonic granites (598–590 Ma; Andresen et al. 2009; Hamdy et al. 2017a).

Hafafit is one of the famous core complexes in the Nubian Shield and represents one of the important suture zones occupying the southern part of the Central Eastern Desert of Egypt. It represents the largest antiformal structures in the Nubian Shield and considered as one of the prodigious structures in the Eastern Desert. El Ramly et al. (1993) studied the tectonic evolution of Wadi Hafafit area and environs and called it Wadi Hafafit culmination (WHC). The Hafafit gneiss complex (Figs. 5.10, 5.11, 5.12, 5.16 and 5.20) attracted the attention of many authors. Not only its controversial formation mechanism, but also the closeness of the area from Ghadir ophiolitic mélange and Nugrus-Sikait belt (very rich in various economic mineralization such as U, Th, Nb, Ta, Zn, Be, Sn, Cu, Ga and REEs) makes this area as one of the most significant areas in the Egyptian Eastern Desert. A major feature is that all lithologies are Neoproterozoic juvenile rocks (Liégeois and Stern 2010; Stern et al. 2010). Petrographically, it has a wide range in composition from orthogneiss to paragneiss (Shalaby 2010). Hafafit gneiss complex comprises five granitoid-cored domes constituted of medium grade gneisses, detached from the overlying low grade metamorphic rocks by low angle thrust zones (Fig. 5.20). The main composition of the overlying unit (Nugrus unit) is low grade mica schists and metavolcanics associated with serpentinites and metagabbros

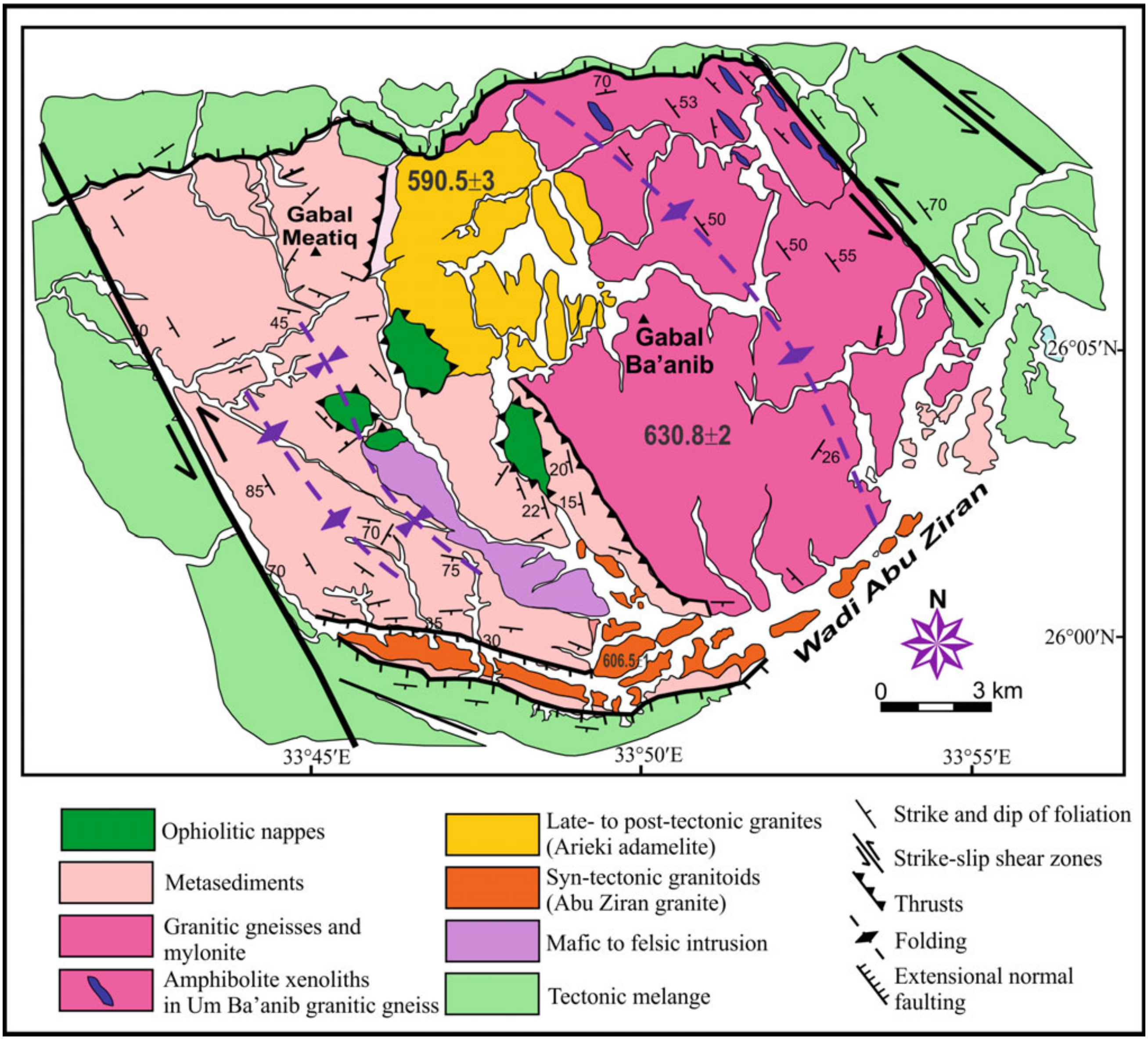

Fig. 5.18 Geological map of Meatiq Core Complex (MCC) (modified after Fritz et al. 2002) and Hamdy et al. (2017b)

outcropping in the eastern and northern part of the Hafafit gneiss complex. On the other hand, the underlying unit (Hafafit unit) is represented mainly by the Hafafit domes and consists of (from core to rim): granitic gneiss of tonalitic and trondhjemitic composition, metagabbro and banded amphibolite, altered ultramafic rocks, biotite- and hornblende-gneiss and psammitic gneiss at the rim of the domal structure (Fig. 5.21a–c). Both units have well developed folds (Fig. 5.22) and have been intruded by leucogranites, especially along thrust zones (Gharib 2012). Strictly speaking and from structural point of view, the entire structural history for core complexes formation is still not fully understood and the formation process is controversial and still a matter of debate.

The most common and generic mechanism for Hafafit gneiss complex exhumation is believed to be regional-scale extension and crustal thinning, where higher grade rocks are brought up in the footwalls of gently dipping shear zone systems oblique to the regional extension direction (often termed 'low-angle detachments') forming so called core complexes (Lister et al. 1984; Tirel et al. 2008; Huet et al. 2010). Meyer et al. (2014) stated that core complexes can also be locally exhumed along major vertical strike-slip shear zones in areas of crustal shortening without regional-scale crustal thinning using an example from the Najd shear-zone system in Saudi Arabia (Abdelsalam and Stern 1996). Although recent studies have dealt in a considerable detail with the gneissic domes of CED; their origin

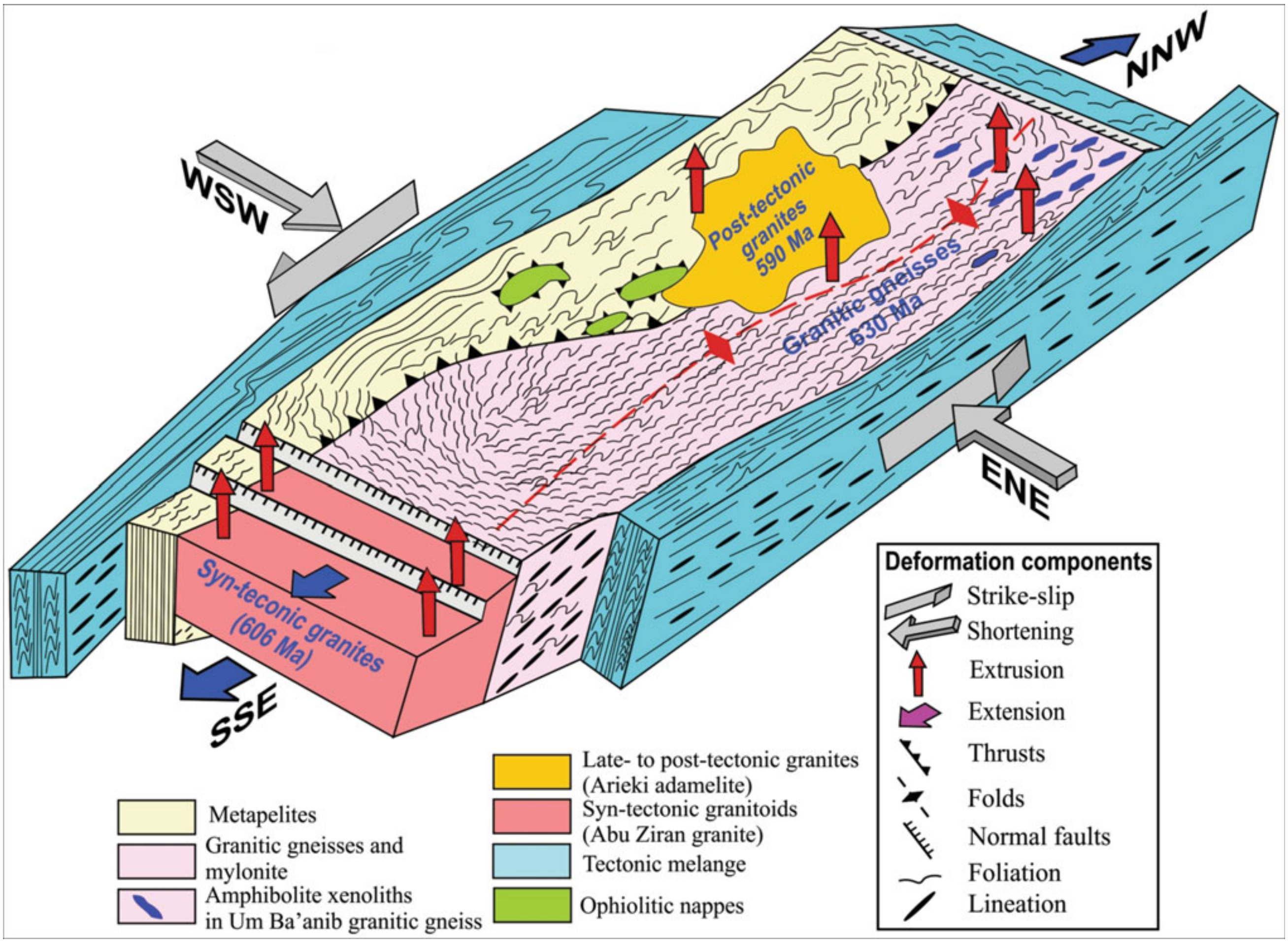

Fig. 5.19 Cartoon explaining evolution of the Meatiq gneiss complex during orogen parallel extension in the Central Eastern Desert (After Hamdy et al. 2017b)

remains controversial. Intrinsically, four scenarios are posited. The first scenario considered a parallel crustal extension origin, the second argues for emplacement within antiformal stacks, the third conceptualize a young emplacement within a core of a sheath fold origin and the final scenario envisages that the emplacement is due to overlap of regional folds and extension parallel to the fold axes (Shalaby 2010). The involvement of a significant extension within NW-trending zones bounded by sinistral strike-slip shears of the Najd Fault System is adopted by Stern (1985) that was accompanied by NW- and SE-dipping normal faults that created intramontane molasse basins (Wallbrecher et al. 1993; Fritz et al. 1996, 2002; Neumayr et al. 1998; Fritz and Messner 1999; Loizenbauer et al. 2001; Bregar et al. 2002; Abd El-Wahed 2007, 2008).

Strike-slip shear zones of Najd Fault System and the accompanied subsidiary shear arrays postdate emplacement of the dome (Shalaby 2010). The gneisses contiguously underlie the Pan-African nappe assemblages through discrete low-angle left-lateral thrust-dominated shear zones from the East. Ceaseless and continued nappe assemblages accretion on the gneisses augments the density disparity and contrast between the overlying denser intensified nappe and the underlying lighter quartz-rich gneisses, resulting in squeezing the gneissic components in oblique convergence regime. Subsequently, the gneisses are thought to have up-domed vertically through the rock units of the nappe.

The Sibai gneissic complex (Figs. 5.23 and 5.24) occur within the core of Gabal-El Sibai that located in Umm Ghieg area. Nearly, 90% of the Sibai core complex is consist of Neoproterozoic granitoid rocks of calcalkaline to alkaline chemical affinity (Kamal El Din 1993; Khudeir et al. 1995; Bregar et al. 2002). The gneisses of Sibai have been considered as pre-Neoproterozoic continental crust by El Gaby et al. (1984) and Khudeir et al. (1992, 1995), but are actually all late Neoproterozoic in age as the other core gneisses in the Eastern Desert (Johnson et al. 2011 and references therein). Sibai gneissic complex consist of two major lithological associations. The first unit include arc metavolcanics, metavolcanogenics, ophiolitic masses and mélange

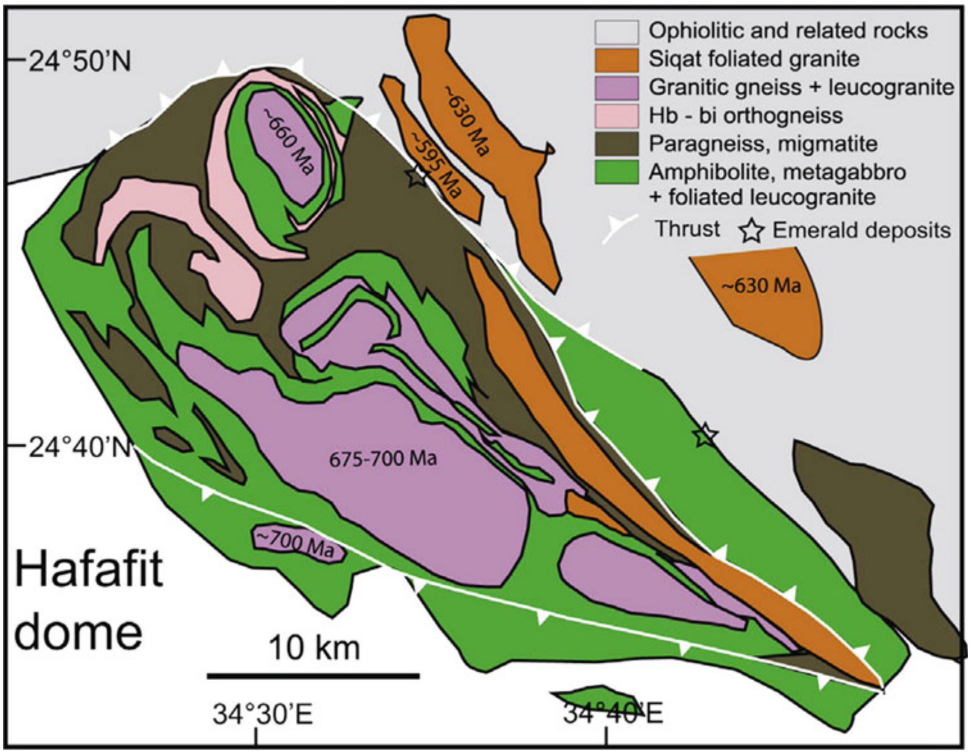

Fig. 5.20 Simplified geological map for the Hafafit gneiss complex (after Stern 2017). Also shown are approximate U-Pb zircon ages for Hafafit from Lundmark et al. (2012) and Kröner et al. (1994). Approximate emerald deposit localities are from Grundmann and Morteani (2008)

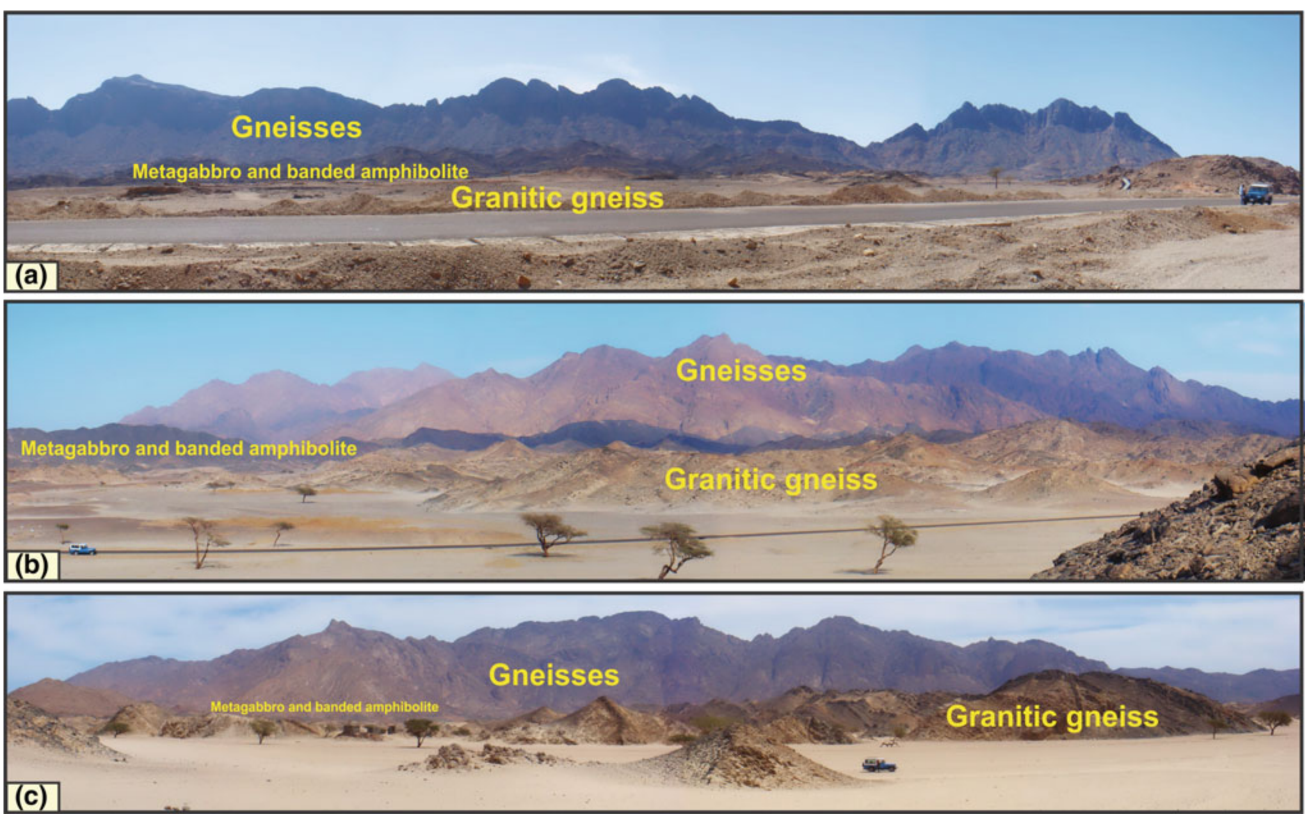

Fig. 5.21 Panoramic views showing hafafit domes consisting of granitic gneiss of tonalitic and trondhjemitic composition, metagabbro and banded amphibolite, altered ultramafic rocks, biotite- and hornblende-gneiss and psammitic gneiss at the rim of the domal structure

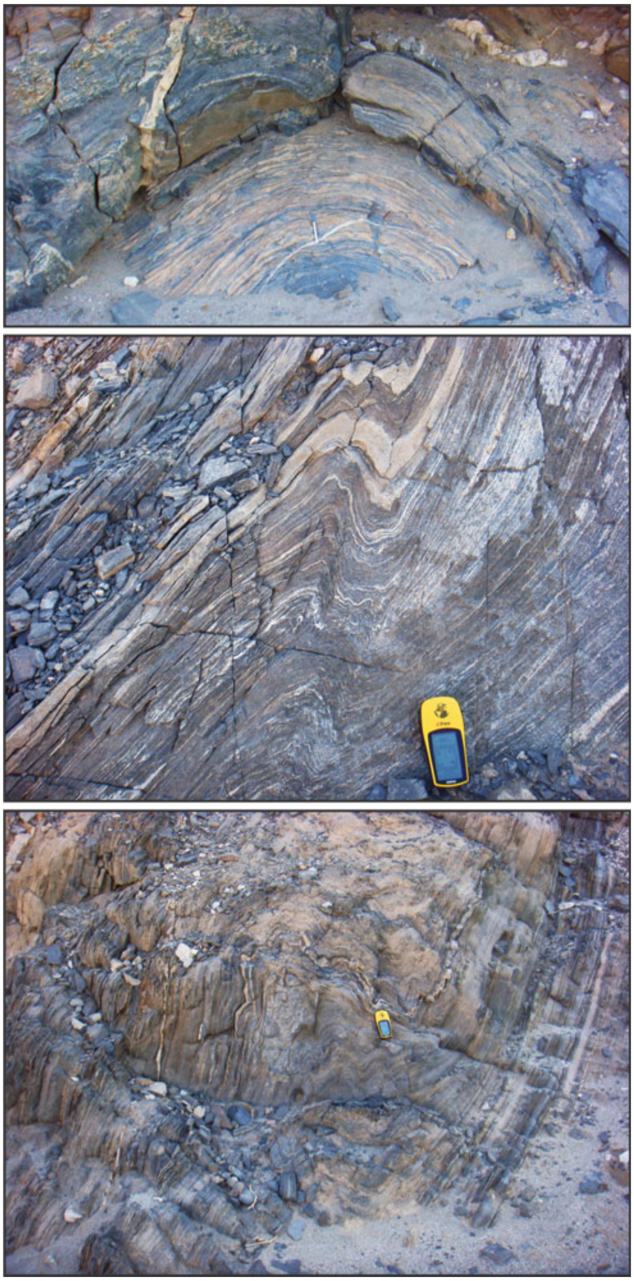

Fig. 5.22 Different types of folds from Hafafit dome

(ophiolitic association) that known by pan-African nappes. Some rocks of these associations metamorphosed to greenschist facies and some reaching amphibolites Facies. While the other unit that form the gneissic domes or Sibai core complex consist of a gneissic association of amphibolite, gneissic diorite, tonalite, granodiorite, schists and granite, As well as minor mafic intrusions. Pan-African nappe separated from the Sibai gneissic complex by strike slip shear zones (Fowler et al. 2007).

Bregar et al. (2002) and Abd El-Wahed (2008) divided the Sibai Core Complex into four groups of variably deformed granitoids related to different tectonic events and magmatic depending on petrography, geochemical composition, structural setting and age: Group (I), syntectonic granitoids (El-Shush gneissic tonalites), Group (II) Central Gneisses or first extension stage granitoids (El-Shush gneissic granodiorites), Group (III), exhumation-related granites or orogen parallel-extension or second extension stage granitoids (Abu Markhat syenogranites, Umm Shaddad syenogranites, Al Miyah granodiroite-monzogranite, Al-Andiya syenogranites and El-Sibai alkali granites), Group (IV), late tectonic granitoids (Umm Luseifa porphyritic granodiorites).

The Sibai Core Complex and their enveloping Pan-African nappe have been evolved through four main phases, namely, Oceanic stage (900–740 Ma), compressional arc-accretion and lithospheric thickening (740–660 Ma), gravitational collapse and core complex formation (660–645 Ma), transtension and core complex exhumation (645–560 Ma) (Abd El-Wahed 2008).

Two stage models have been suggested by Bregar et al. (2002) for the evolution of the Sibai Core Complex. (a) Formation of the sinistral wrench corridor associated with NE–SE directed extension and synkinematic intrusion of group (II) granitoids (central block). (b) Ongoing northwest–southeast directed extension triggered the intrusion of group (III) granitoids and the formation of detachment shear zones. Continuous activity of strike-slip and normal shear zones leads to the exhumation of the core complex and the formation of the Kareim molasse basin in the northwest.

Gabal El Shalul (Figs. 5.25 and 5.26) represents one of the westernmost deformed plutons (El Shalul granitoid) in the Central Eastern Desert forming a NW–SE-trending antiform (Fig. 5.26). The core of the variably deformed granitoid is dominated by monzogranite, whereas granitic gneisses are more common structurally upwards and away from the core (Ali et al. 2012). Enclaves of monzogranite in the deformed granites show the granite to be the younger of the two (Hamimi et al. 1994). The dominant structural feature within the gneiss dome is a NW–SE-trending mineral lineation. Isoclinal folds with hinge-lines trending NW–SE are also observed. A high-strain zone separates the El Shalul granitoid from the structurally overlying ophiolitic mélange, composed of tectonic blocks of meta-ultramafite, pyroxenite and metagabbro (Ali et al. 2012). The mélange is overlain tectonostratigraphically by basic to intermediate volcanic rocks, including pillowed basalts and andesites. The ophiolitic mélange and volcanic rocks are succeeded by volcanogenic metasediments, including deformed flat pebble conglomerates interbedded with grey phyllite, mudstone and graded greywackes (Ali et al. 2012). Hamimi et al. (1994) interpreted the high-strain zone (El Shalul Shear Zone) separating the eugeoclinal rocks (= ophiolite mélange + island arc sequence) from the underlying orthogneisses to

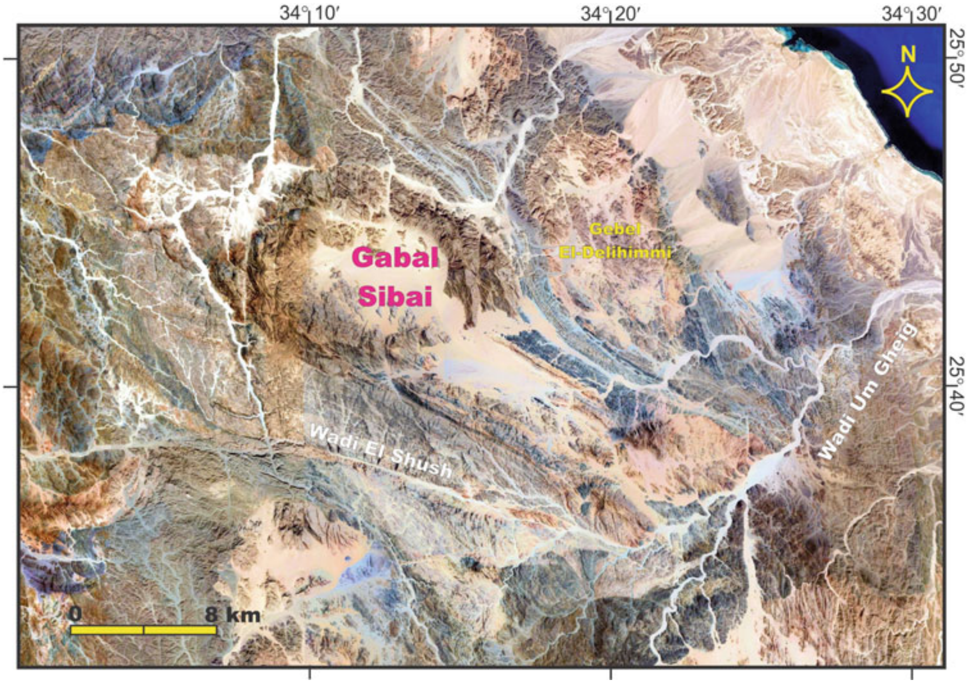

Fig. 5.23 Geological map of the El Sibai study area showing the main gneissic and ophiolitic association units. Planar structural data and macroscopic fold axial traces are also shown. DA = Delihimmi Antiform; HA = Higlig Antiform; KASZ = Kab Ahmed shear zone; ESSZ = El Shush shear zone. Faults are strike-slip. A–A0 and B–B0 are cross-sections presented in (b). Wadis: WA = Wadi Al Hamra; WG = Wadi Um Gheig; WL = Wadi Um Luseifa; WT = Wadi Talat Salah; WM = Wadi Abu Markhat; WH = Wadi Higlig; WD = Wadi El Dabbah; WS = Wadi El Shush; WR = Wadi Sitra; WW = Wadi Wizr; WB = Wadi Sharm El Bahari; WI = Wadi Abu Garadi; WK = Wadi Kareim

have developed during NW to WNW thrusting of the former (Ali et al. 2012). The El Shalul shear zone is c. 10 m wide and characterized by a mix of foliated metasediments and lenses of mylonitic granite, and it post-dates folding and cleavage development on the structurally overlying eugeoclinal rocks (Ali et al. 2012).

5.4 Shear Zone-Related Mineralizations

Most significant gold deposits throughout the world are controlled by major and subsidiary shear zones (e.g., Bonnemaison and Marcoux 1990; Hodgson 1989; Roberts 1987). Syn-deformational ore deposition played an important role in many Au deposits according to field and laboratory evidence, which indicates that flow of Au-bearing fluids was synchronous with regional-scale deformation events. Gold-related deformation events linked to ore genesis were distinct from high-level, brittle deformation that is typical of many epithermal deposits. Many Au deposits, with brittle–ductile features, most likely formed during tectonic events that were accompanied by significant fluid flow. Interactive deformation-fluid processes involved brittle–ductile folding, faulting, shearing, and gouge development that were focused along illite–clay and dissolution zones caused by hydrothermal alteration (Peters 2004). Alteration along these deformation zones resulted in increased porosity and enhancement of fluid flow, which resulted in decarbonated, significant dissolution, collapse, and volume and mass reduction. On the other hand, intrusion-related systems of the TGB exhibit intermediate structural styles of mineralization that provide a useful bridge in understanding the diversity of mechanically controlled structural styles in otherwise mostly unrelated gold deposit types (Stephens et al. 2004).

The Eastern Desert was a gold-mining province in ancient Egypt since the pre-dynastic times (Zoheir et al. 2018). Despite the several thousand years mining history, the large number of gold deposits (Fig. 5.27), and considerable recent research, the age of Au mineralization in the Eastern Desert is poorly known. The area is considered to be highly prospective for undiscovered gold deposits that occur as shear zone-hosted, disseminated sulfide mineralization or as quartzcarbonate veins along major structures in ophiolitic and island arc metasediments. Gold mineralization is closely associated with the granitic rocks that can be grouped into three categories i.e. syn-late tectonic calc-alkaline granites, calc-alkaline to mildly alkaline granites of the transitional stage and post-tectonic alkaline granites (Botros 2015). Tectonically, gold mineralization is linked with the

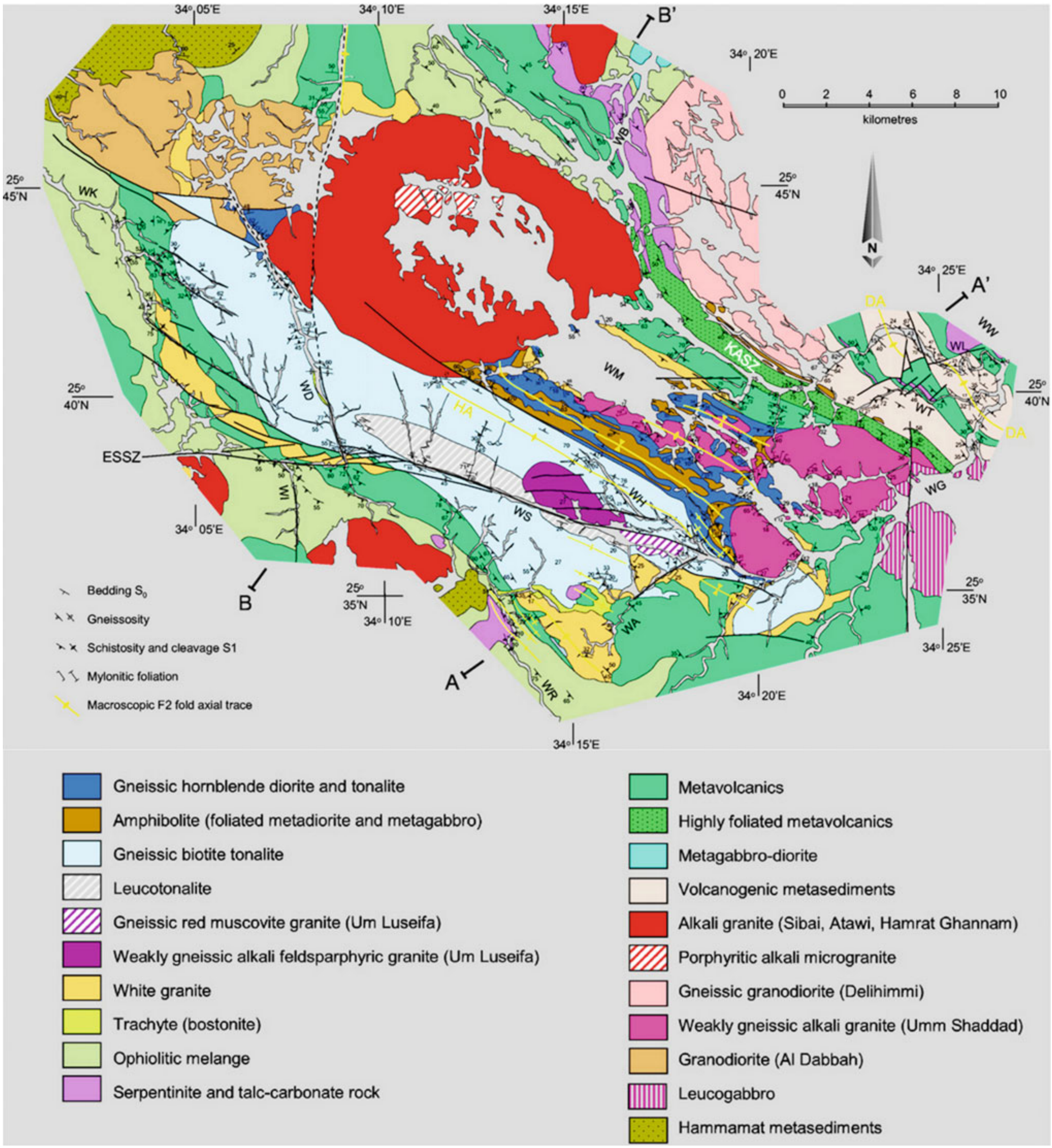

Fig. 5.24 Geological map of the Gabel El Shalul area (after Ali et al. 2012)

deformational tectonothermal events that were active during the evolution of the ANS. During the primitive stages of the island-arc formation, pre-orogenic gold mineralization was formed by hot brines accompanying submarine volcanic activity (Botros 2015).

Wrench-dominated transpression, a characteristic feature of obliquely convergent mobile belts, has been suggested to explain the complex deformation kinematics in the Eastern Desert of Egypt (e.g., Wallbrecher et al. 1993; Greiling et al. 1994; Loizenbauer et al. 2001; Makroum 2001; Fritz et al.

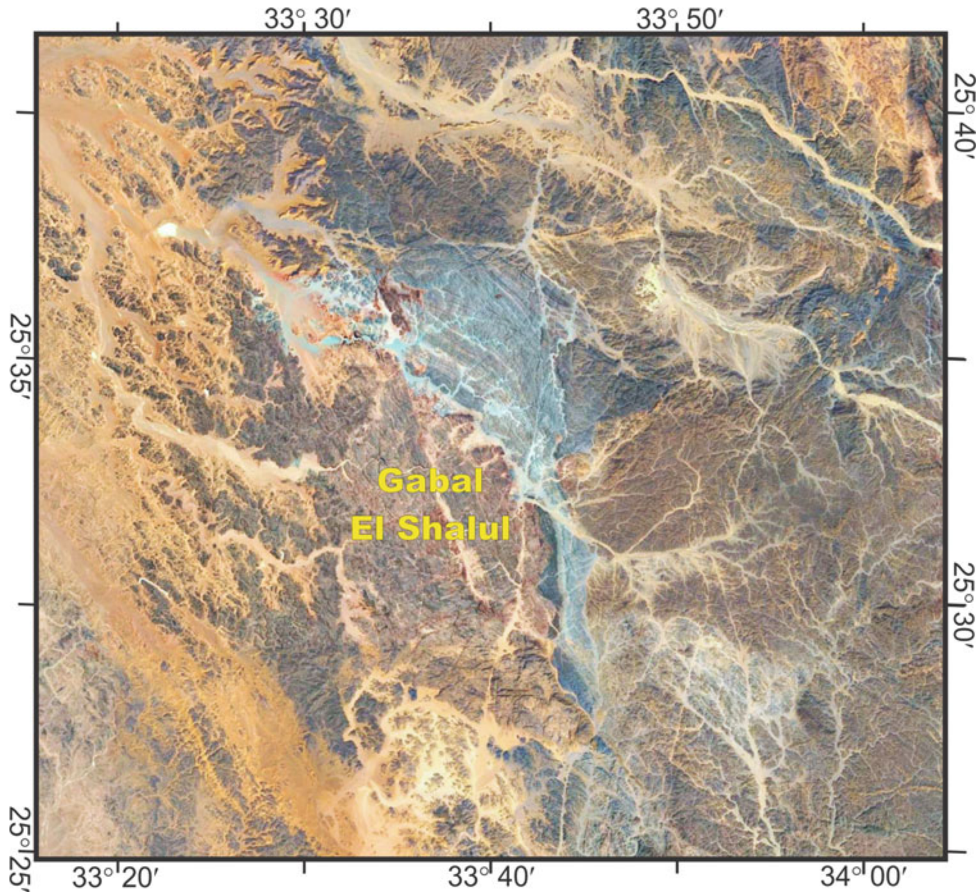

Fig. 5.25 Location of El-Shalul gneiss complex

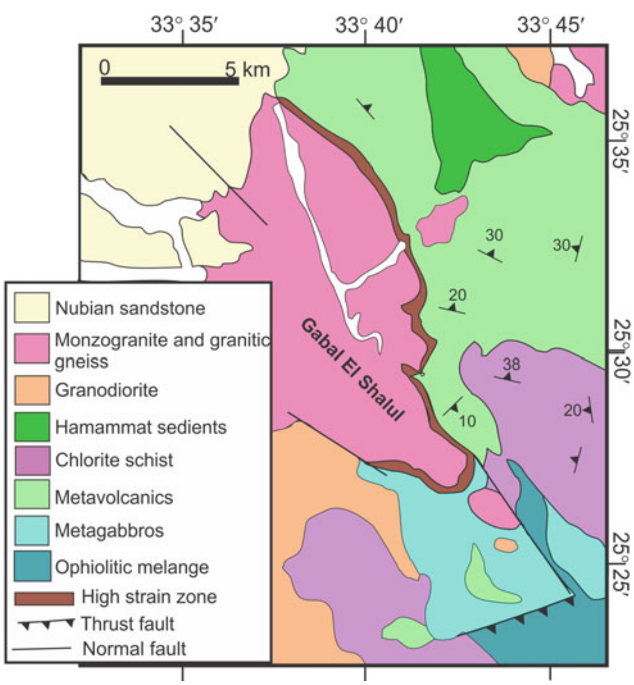

Fig. 5.26 Geological map of the Gabel El Shalul area (after Ali et al. 2012)

1996, 2002; Shalaby et al. 2005; Abd El-Wahed 2008; Abdeen et al. 2008; Abd El-Wahed and Kamh 2010; Abd El-Wahed et al. 2016) and to explain the geometry and kinematics of gold-bearing quartz veins (Hassaan et al. 2009; Zoheir 2008, 2011; Zoheir and Lehmann 2011; Abd El-Wahed 2014; Zoheir et al. 2017, 2018). Gold mineralization occurs mainly in fault-fill quartz veins, and appears to be confined to zones of strike-slip fault/shear structures cutting ophiolites and molasse-type sediments (Fig. 5.10). At least 70% of the auriferous quartz veins in this area is associated with late-orogenic, I-type granitic intrusions (e.g. Murr 1999; Zoheir et al. 2011; Harraz 1999, 2000; Helmy et al. 2004; Zoheir and Moritz 2014; Helmy and Zoheir 2015; Zoheir et al. 2017, 2018). These intrusions are commonly small in size and their emplacement was most likely subsequent to northeast-southwest transpressional regime rather than in an extensional tectonic environment (Fowler 2001).

Botros (2015) classified the gold mines in the CED as follows: (i) Veins hosted in volcanogenic metasediments and/or the syn-orogenic granites surrounding them (e.g. Sukari, Dungash, Kurdeman), (ii) Veins localized at the

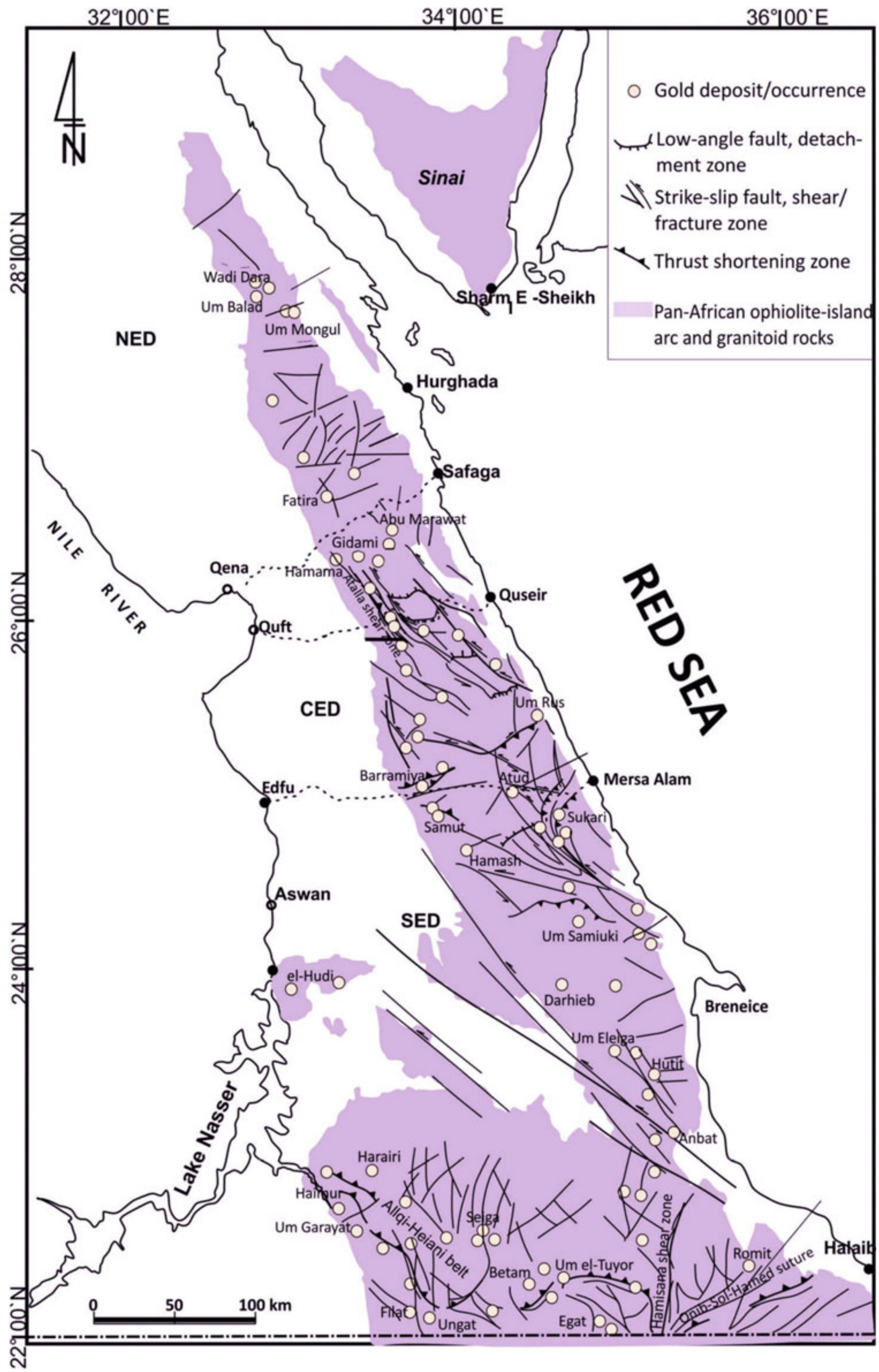

Fig. 5.27 Distribution of gold occurrences in the Eastern Desert of Egypt in relation to the main lithological units and major faults/shear zones (after Zoheir et al. 2018). Gold mines and occurrences names and locations are verified by Basem Zoheir, through field work and Global Positioning System (GPS) readings based on Bing Maps

contacts between younger gabbros and younger granites (e.g. Atud gold mines, Harraz and Hamdy 2015; Abdel-nasser and Kumral 2016), (iii) Quartz veins traversing calc-alkaline to mildly alkaline younger granites (e.g. Hangalia gold mine), (iv) Gold hosted in altered ophiolitic serpentinites along thrust faults (e.g. Barramiya gold mines). Gold mineralization in the Barramiya, Dungash, Sukari and Kurdeman gold mines are mainly controlled by the regional, NNW- and NE-trending zones of transpression. The Hangalia gold deposit (Khalil and Helba 2000) and the Hamash Au–Cu deposit (Hilmy and Osman 1989; Helmy and Kaindl 1999) occur within post tectonic granites of Egypt. Gold mineralization at Um Rus is in quartz veins along NE-SW trending fractures in granitoid-gabbroic rocks (Harraz and El-Dahhar 1993).

In the Atalla mine area, gold-bearing sulfide-quartz veins cutting mainly through the Atalla monzogranite intrusion in the Eastern Desert of Egypt are controlled by subparallel NE-trending brittle shear zones. These veins are associated with pervasive sericite-altered, silicified and ferruginated rocks (Zoheir et al. 2017, 2018). The new geochronological data demonstrate that the post-intrusion Au-mineralization that formed during the ~600 Ma period, controlled by wrench tectonics along Najd-related structures in the region (620–585 Ma) (Zoheir et al. 2017, 2018).

The Fawakhir–El Sid district is part of a regional NNW-trending shear corridor (15 km wide) that hosts several other historic gold mines associated with left-lateral wrench structures and related granite intrusions. Vein-style gold mineralization is hosted within and at the margin of an I-type and magnetite-series monzogranite, the Fawakhir granite intrusion (Zoheir et al. 2015), and a Pan-African (~740 Ma) ophiolite sequence (El Bahariya 2018).

At the Barramiya gold mine, the mineralized zone is composed of mylonitized graphite schist, talc–carbonate rocks containing bodies of listwaenite and quartz veins and veinlets (Zoheir and Lehmann 2011; Harraz et al. 2012; Botros 2015). The Au-bearing main lode is flanked by listwaenite on one side and talc–carbonate on the other side. The mineralized and folded quartz and quartz–carbonate veins are associated with ENE-WSW dextral shear zones (Abd El-Wahed et al. 2016), whereas some barren and unfolded milky quartz veins are accommodated in steeply dipping NW–SE extensional fractures (Zoheir and Lehmann 2011; Abd El-Wahed et al. 2016). The Barramiya shear belt consists of two conjugate sets of shear zones, namely a NW-SE-trending sinistral and NESW-trending dextral (Abd El-Wahed 2014; Abd El-Wahed et al. 2016).

In the Dungash mine area, Dungash mélange composed of remnants of imbricate ophiolitic slices tectonically intermixed with island arc metavolcanic/volcanogenics and metasedimentary rocks. The transpressive character of deformation in the Dungash mine area is shown by the coexistence of strike-slip and dip-slip shear zones. The gold deposits at Dungash mine area occur in an EW-trending quartz vein along post-metamorphic brittle–ductile shear zones in metavolcanic and metasedimentary host rocks (Helba et al. 2001; Abd El-Wahed and Abu Anbar 2009; Zoheir and Weihed 2014; Abd El-Wahed 2014). The sigmoidal geometry of a zone of quartz pods along the Dungash shear zone defines E–W dextral shear system between foliated metavolcanic and volcanogenic metasediments (Abd El-Wahed et al. 2016).

The Hamash gold mine area is mainly occupied by metamudstones, phyllites, chlorite–quartz–epidote schists and actinolite–epidote schists. Serpentinite and talc–carbonate rocks are enclosed in metasediments (Hilmy and Osman 1989; Helmy and Kaindl 1999). The gold mineralization in Hamashmine initiated during D_2 dextral shearing and continued until D_3 which an extensional phase related to intrusion of post tectonic granites (Abd El-Wahed et al. 2016).

The highest Au contents in Sukari gold mine (e.g. Main Zone and Hapi Zone) are principally SSE-dipping back-thrusts branching from the major Sukari Thrust. Gold mineralization at Quartz Ridge, V-Shear and North Sukari are largely controlled by NE-trending strike-slip shear zones and transpressional imbricate thrust zones in the East Sukari Thrust belt. From the structural point of view, Quartz Ridge, North Sukari and V Shear are most suitable sites for gold exploration in Sukari mine area (Abd El-Wahed et al. 2016).

Gold-bearing quartz veins are widespread in south Eastern Desert of Egypt, commonly showing spatial and temporal association with shear zones (e.g., Kusky and Ramadan 2002; Zoheir 2008, 2011). Au-quartz lodes in the Wadi El Beida–Wadi Khashab area are associated with NNW-trending shear zones in pervasively silicified, ferruginated volcanic/volcanogenic rocks, or along steeply dipping thrust segments bounding allochthonous ophiolitic blocks. Development of the mineralized shear zones is attributed to a wrench-dominated transpression (Zoheir 2012a, b). Structural analysis of the shear fabrics along the ore zones in El-Anbat mine area indicate that geometry of the mineralized quartz veins and alteration patterns are controlled by the regional, NNW-trending zone of transpression, known as the Wadi Kharit–Wadi Hodein shear system, which is related to the 655–540 Ma, Najd strike–slip fault system in the Eastern Desert of Egypt (Zoheir 2011).

Finally, many of the mineralized quartz veins and alteration patterns in the Central Eastern Desert and the Southern Eastern Desert are controlled by the regional, NW to NNW-trending zones of transpressional strike slip shear zone associated with Najd Fault System.

5.5 Discussion

Progress in understanding the tectonic setting, deformation history and structural architecture of the ENS, the northwestern continuation of the ANS, is attributed to intensive field-structural mapping since the establishment of the Egyptian Geological Survey (1896), wealth of remote

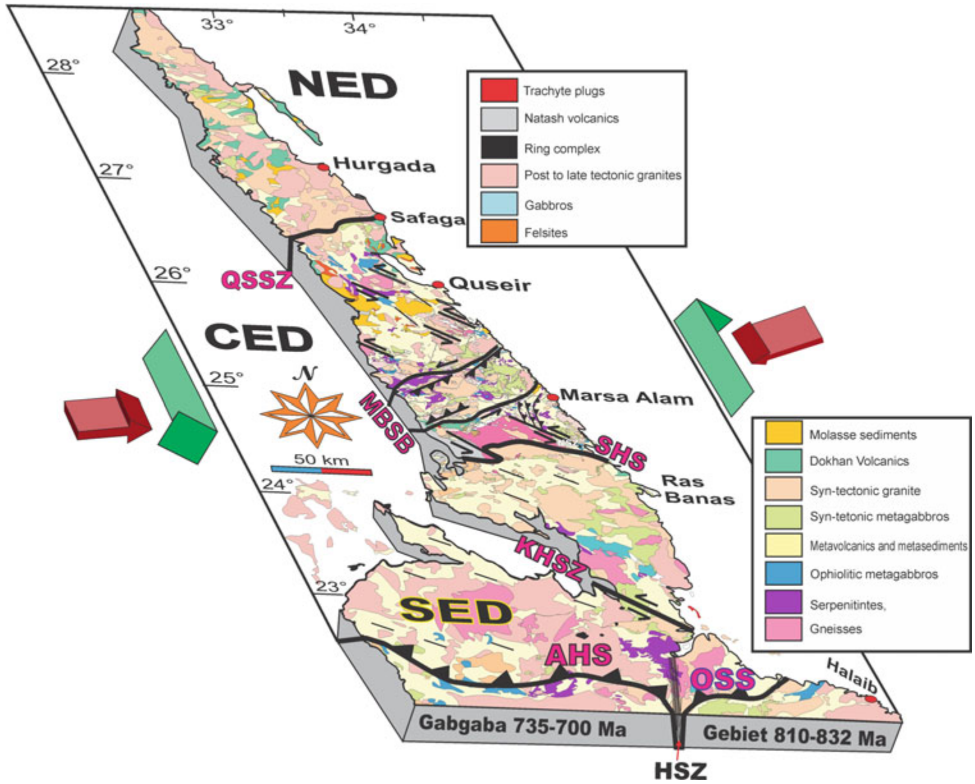

Fig. 5.28 Major shear zones and sutures in the Egyptian Nubian Shield

sensing data and a growing geochronological database. Recently, application of anisotropy of magnetic susceptibility (AMS) technique and quantitative strain analysis play also a crucial role in unraveling strain in rocks, especially in the absence of potential strain markers (De Wall et al. 2001; Abdeen et al. 2014; Greiling et al. 2014; Hagag et al. 2018). The predominantly Neoproterozoic basement complex outcropping in the ENS is traversed by map-scale semi ductile-semi brittle shear zones of variable orientations, dimensions and ages. These shear zones are consistent and in complete harmony with those encountered elsewhere in the entire ANS in terms of their extensions, widths, and degree and sense of shearing. Among these high strain zones, Qena-Safaga- and Idfu-Mersa Alam-Zones split the Eastern Desert of Egypt into three main provinces; NED, CED and SED (Fig. 5.28). Such traditional subdivision is based mainly on the lithologic variations recorded in the three provinces, where voluminous granitoids, Dokhan Volcanis and post-amalgamation Hammamat volcanosedimentary Sequence are dominated in the NED, and infracrustal units (gneisses, migmatites, gneissose granites and remobilized equivalents) and ophiolite- and island arc-dominated supracrustal units occupy both the CED and the SED with variable proportions. In the CED and SED, low angle shear zones separate hanging walls low grade ophiolite- and island arc-dominated supracrustal lithologies from high grade infracrustal rocks in their footwalls. Such detachment surfaces are marked by zones of intensive mylonitization and cataclasis, and are best represented in Beitan, Hafafit, Meatiq and Shalul areas (Fig. 5.28). Because of the absence of gneisses and ophiolites, it is not easy to deal with these two tiers in the NED or in Sinai.

However, based on our own field investigations and studies, along with reviewing previous literature, it can be stated with reasonable confidence that AHS is the only confirmed suture zone in the extreme SED. This suture forms a segment of the greater AHOSHY that separates the Eastern Desert-Midyan terrane to the north from the Gabgaba-Gebeit-Hijaz terrane to the south. Elongation of ophiolitic nappes in the vicinity of Wadi Allaqi is rather evidence demonstrating suturing in this zone.

In the ENS, shear zones could be subdivided into two main categories; syn-accretion- and post-accretion-shear zones. From our opinion, the syn-accretion shear zones are typified by the HSZ that juxtaposes Gabgaba and Gebeit terranes located just to the south of the AHS (Fig. 5.28). As mentioned before, the HSZ was considered as an arc-arc suture, a transcurrent, or a transpressive shear zone formed just after the arc accretion stage. The HSZ deformation began after 660 Ma, with intense E–W shortening and N–S extension accompanied by greenschist to amphibolite facies metamorphism and development of upright isoclinal folds and vertical foliations. Whether the sense of shearing along the HSZ is sinistral or dextral was and still is a matter of much debate. Abdelsalam and Stern (1996) proposed dextral sense of shearing depending on the dextral offsetting of the Yoshgah Suture (Stern et al. 1989, 1990). The post-accretion shear zones are manifested by the NW- and ENE- (to E-) oriented high strain zones. Both shearing trends are affiliated to the D_2 deformation in the proposed ANS-scale deformation scheme of Hamimi et al. (2019). The NW trend is evidently Najd-related exhibiting sinistral sense of movement. This trend is exemplified by KHSZ, NSZ and ASZ. The ENE- (to E-) trend shows dextral sense of shearing and is obviously younger than the former trend. Such conclusion indicates that both trends are not conjugate pairs as mentioned in some previous publications.

Also, the major shear zones bounding the gneiss domes have been interpreted as sinistral strike-slip shear zones combined with extensional shears that formed during exhumation of domes (e.g., Fritz et al. 1996, 2002; Abd El-Wahed 2008, 2014) or as remnants of NW-directed thrusts (Andresen et al. 2010). Nowadays, sinistral shearing along the NW-trending shear zones of the Najd Fault System is genetically linked with deposition of sediments, exhumation of gneiss domains, and emplacement of syn-tectonic granitoids (e.g. Fritz et al. 1996, 2002, 2013; Bregar et al. 2002; Shalaby et al. 2005; Abd El-Wahed 2008, 2010; Abd El-Wahed and Kamh 2010; Abdeen et al. 2014; Abd El-Wahed et al. 2016: Makroum 2017).

In general, the syn-orogenic gold mineralization in the Eastern Desert of Egypt is connected with oblique transpression associated with conjugate NW-sinistral strike slip shear zones related to the Najd fault system and hosted by volcanogenic metasediments and altered ophiolitic serpentinites. The NW-sinistral and NE-dextral shear zones (620–540 Ma) and extensional NW-trending fractures play a great role in the development of gold bearing quartz veins in the CED and SED.

References

Abd El-Naby H, Frisch W (2006) Geochemical constraints from the Hafafit Metamorphic Complex (HMC): evidence of Neoproterozoic back-arc basin development in the central Eastern Desert of Egypt. J Afr Earth Sci 45:173–186

Abd El-Wahed MA (2007) Pan-African strike-slip tectonics of Wadi El-Dabbah area, north Sibai Core Complex, Central Eastern Desert, Egypt. Ann Egypt Geol Surv 29:1–36

Abd El-Wahed MA (2008) Thrusting and transpressional shearing in the Pan-African nappe southwest El-Sibai core complex, Central Eastern Desert, Egypt. J Afr Earth Sci 50:16–36

Abd El-Wahed MA (2010) The role of the Najd Fault System in the tectonic evolution of the Hammamat molasse sediments, Eastern Desert, Egypt. Arab J Geosci 3:1–26

Abd El-Wahed MA (2014) Oppositely dipping thrusts and transpressional imbricate zone in the Central Eastern Desert of Egypt. J Afr Earth Sci 100(2014):42–59

Abd El-Wahed MA, Abu Anbar MM (2009) Syn-oblique convergent and extensional deformation and metamorphism in the Neoproterozoic rocks along Wadi Fatira shear zone, Northern Eastern Desert, Egypt. Arab J Geosci 2:29–52

Abd El-Wahed MA, Kamh SZ (2010) Pan-African dextral transpressive duplex and flower structure in the Central Eastern Desert of Egypt. Gondwana Res 18:315–336

Abd El-Wahed MA, Thabet IA (2017) Strain geometry, microstructure and metamorphism in the dextral transpressional Mubarak Shear Belt, Central Eastern Desert, Egypt. Geotectonics 51(4):438–462

Abd El-Wahed MA, Harraz HZ, El-Behairy MH (2016) Transpressional imbricate thrust zones controlling gold mineralization in the Central Eastern Desert of Egypt. Ore Geol Rev 78:424–446

Abdeen MM, Abdelghaffar AA (2011) Syn- and post-accretionary structures in the Neoproterozoic Central Allaqi-Heiani suture zone, Southeastern Egypt. Precambr Res 185:95–108

Abdeen MM, Greiling RO (2005) A quantitative structural study of late Pan-African compressional deformation in the Central Eastern Desert (Egypt) during Gondwana assembly. Gondwana Res 8 (4):457–471

Abdeen MM, Dardir AA, Greiling RO (1992) Geological and structural evolution of the Wadi Queih Area (N Quseir), Pan-African Basement of the Eastern Desert of Egypt. Zbl Geol Palfiontol Teil I:2653–2659

Abdeen MM, Sadek MF, Greiling RO (2008) Thrusting and multiple folding in the Neoproterozoic Pan-African basement of Wadi Hodein area, south Eastern Desert, Egypt. J Afr Earth Sci 52:21–29

Abdeen MM, Greiling RO, Sadek MF, Hamad SS (2014) Magnetic fabrics and Pan-African structural evolution in the Najd Fault corridor in the Eastern Desert of Egypt. J Afr Earth Sci 99:93–108

Abdel-Karim AM, Azzaz SA, Moharem AF, El-Alfy H (2008) Petrological and geochemical studies on the ophiolite and island arc association of Wadi Hammaryia, Egypt. Arab J Sci Eng 33 (1C):117–138

Abdel-Karim A-AM, Ali S, Helmy HM, El-Shafei SA (2016) A fore-arc setting of the Gerf ophiolite, Eastern Desert, Egypt: Evidence from mineral chemistry and geochemistry of ultramafites. Lithos 263:52–65

Abdelnasser A, Kumral M (2016) Mineral chemistry and geochemical behavior of hydrothermal alterations associated with mafic intrusive-related Au deposits at the Atud area, Central Eastern Desert, Egypt. Ore Geol Rev 77:1–24. https://doi.org/10.1016/j.oregeorev.2016.01.011

Abdelsalam MG (1994) The Oko Shear Zone: post-accretionary deformation in the Arabian-Nubian Shield. J Geol Soc Lond 151:767–776

Abdelsalam MG (2010) Quantifying 3D post-accretionary tectonic strain in the Arabian-Nubian Shield: Superimposition of the Oko Shear Zone on the Nakasib Suture, Red Sea Hills, Sudan. J Afr Earth Sci 56(4–5):167–178

Abdelsalam MG, Stern RJ (1996) Sutures and shear zones in the Arabian-Nubian Shield. J Afr Earth Sci 23:289–310

Abdelsalam MG, Abdeen MM, Dowaidar HM, Stern RJ, Abddelghaffar AA (2003) Structural evolution of the Neoproterozoic western Allaqi-Heiani structure, southeastern Egypt. Precambr Res 124:87–104

Abu-Alam TS, Hassan M, Stüwe K, Meyer S, Passchier C (2014) Multistage tectonism during Gondwana collision: Baladiyah Complex, Saudi Arabia. J Petrol 55:1941–1964

Abu-Alam TS, Stüwe K (2009) Exhumation during oblique transpression: The Feiran-Solaf region, Egypt. J Metamorph Geol 27:439–459

Abu El-Enen MM, Abu-Alam TS, Whitehouse MJ, Ali K, Okrusch M (2016) P-T path and timing of crustal thickening during amalgamation of East and West Gondwana: a case study from the Hafafit

Metamorphic Complex, Eastern Desert of Egypt. Lithos 263:213–238

Agar RA, Stacey JS, Whitehouse MJ (1992) Evolution of the southern Afif terrane—a geochronologic study. Saudi Arabian Deputy Ministry for Mineral Resource Open File Report DGMR-OF-10-15, 41 pp

Akaad MK (1996) Rock succession of the basement: an autobiography and assessment. In: The Egyptian Geological Survey, Centennial Conference, Paper No. 71, p 87

Akaad MK, Noweir AM (1977) The post Hammamat felsites and their age relation with the younger granites of Egypt. Proc Acad Sci 30:163–168

Akaad MK, Noweir AM, Kotb H (1979) Geology and petrochemistry of the granite association of the Arabian Desert Orogenic Belt of Egypt between 25°35′ and 26°30′. Delta J Sci 3:107–151

Akaad MK, El Ela AM Abu, El Kamshoshy HI (1993) Geology of the region West of Marsa Alam, Eastern Desert, Egypt. Ann Egypt Geol Survey 19:1–18

Al-Husseini M (2000) Origin of the Arabian plate structures: Amar collision and Najd rift. Geo Arabia 5:527–542

Ali KA, Azer MK, Gahlan HA, Wilde SA, Samuel MD, Stern RJ (2010) Age constraints on the formation and emplacement of Neoproterozoic ophiolites along the Allaqi-Heiani Suture, South Eastern Desert of Egypt. Gondwana Res 18:583–595

Ali KA, Andresen A, Stern RJ, Manton WI, Omar SA, Maurice AE (2012) U-Pb zircon and Sr-Nd-Hf isotopic evidence for a juvenile origin of the c 634 Ma El-Shalul Granite, Central Eastern Desert, Egypt. Geol Mag 149:783–797

Ali-Bik MW, Sadek MF, Ghabrial DS (2014) Late Neoproterozoic metamorphic assemblages along the Pan-African Hamisana Shear Zone, Southeastern Egypt: Metamorphism, geochemistry and petrogenesis. J Afr Earth Sci 99:24–38

Almond DC, Ahmed F (1987) Ductile shear zones in the northern Red Sea Hills of Sudan and their implications for crustal collision. In: Bowden P, Kinnaird JA (eds) African geology reviews. Geol J 22:175–184

Amstutz GC, El-Gaby S, Ahmed AA, Habib ME, Khudeir AA (1984) Back-arc ophiolite association, central Eastern Desert, Egypt. Bull Fac Sci Assiut Univ 13:95–136

Andresen A, Abu El-Rus MA, Myhre PI, Boghdady GY, Corfu F (2009) U-Pb TIMS age constraints on the evolution of the Neoproterozoic Meatiq Gneiss Dome, Eastern Desert, Egypt. Int J Earth Sci (Geol Rundsch) 98:481–497

Andresen A, Augland LE, Boghdady GY, Lundmark AM, El Nady OM, Hassan MA, El Rus MA (2010) Structural constraints on the evolution of the Meatiq gneiss dome (Egypt), east-African orogen. J Afr Earth Sci 57:413–422

Asran AM, Kabesh M (2003) Evolution and geochemical studies on a stromatic migmatite-amphibolite association in Hafafit area CED Egypt. Egypt J Geol 47:1–24

Azza M, Hosny A, Gharib A (2012) Rupture process of Shallow Earthquakes of Abou-Dabbab Area, South East of Egypt. Egypt J Appl Geophys 11(1):85–100

Badawy A, El-Hady S, Abdel-Fattah AK (2008) Microearthquakes and neotectonics of Abu-Dabbab, Eastern Desert of Egypt. Seismol Res Lett 79(1):55–67

Berhe SM (1990) Ophiolites in northeast and east Africa: implications for Proterozoic crustal growth. J Geol Soc Lond 147:41–57

Bonnemaison M, Marcoux E (1990) Auriferous mineralization in some shear zones. A three stage model of metallogenesis. Miner Deposita 25:96–104

Botros NS (2015) The role of the granite emplacement and structural setting on the genesis of gold mineralization in Egypt. Ore Geol Rev 70:173–187

Bregar M, Bauernhofer A, Pelz K, Kloetzli U, Fritz H, Neumayr P (2002) A late Neoproterozoic magmatic core complex in the Eastern Desert of Egypt; emplacement of granitoids in a wrench-tectonic setting. Precambr Res 118:59–82

Brown GB (1972) Tectonic map of the Arabian Peninsula. Saudi Arabian Directorate General of Mineral Resources Map AP-2, Scale 1:4,000,000

Brown GF, Jackson RO (1960) The Arabian Shield. In: XIX international geological congress, Pt 9, pp 69–77

Cononco (1987) Egyptian General Petroleum Corporation-Conoco Coral, 1987. Geological map of Egypt, Scale 1:500,000, Cairo

Daggett PH, Morgan P, Boulos FK, Hennin SF, El-Sherif AA, El Sayed AA, Basta NZ, Melek YS (1986) Seismicity and active tectonics of the Egyptian Red Sea margin and the northern Red Sea. Tectonophysics 125:313–324

De Wall H, Greiling RO, Sadek MF (2001) Post-collisional shortening in the late Pan-African Hamisana high strain zone, SE Egypt: field and magnetic fabric evidence. Precambr Res 107:179–194

Delfour J (1970) Le Group de J'balah, une nouvelle unite de Bouclier Arabe. BRGM Bull 2:19–32

EGSMA (1996) Egyptian Geological Survey and Mining Authority, Geological map of Wadi Jabjahah Quadrangle, Egypt, Scale 1:250.000

EGSMA (2002) Geological Map of Marsa Shaab Quadrangle, Egypt at Scale 1:250,000. Egyptian Geological Survey and Mining Authority, Cairo, Egypt

Emam A, Zoheir B, Johnson P (2015) ASTER-based mapping of ophiolitic rocks: examples from the Allaqi–Heiani suture, SE Egypt. Int Geol Rev 1–15. https://doi.org/10.1080/00206814.2015.1094382

El Bahariya G (2012) Classification and origin of the Neoproterozoic ophiolitic mélanges in the Central Eastern Desert of Egypt. Tectonophysics 568–569:357–370

El Bahariya G (2018) Classification of the Neoproterozoic ophiolites of the Central Eastern Desert, Egypt based on field geological characteristics and mode of occurrence. Arab J Geosci 11(12). https://doi.org/10.1007/s12517-018-3677-1

El-Bayoumi RM, Greiling R (1984) Tectonic evolution of a Pan-African plate margin in southeastern Egypt—a suture zone overprinted by low angle thrusting? In: Klerkx J, Michot J (eds) African geology. Tervuren, pp 47–56

El-Desoky HM, Khalil AE, Salem AKA (2015) Ultramafic rocks in Gabal El-Rubshi, Central Eastern Desert, Egypt: petrography, mineral chemistry, and geochemistry constraints. Arab J Geosci 8(5):2607–2631. https://doi.org/10.1007/s12517-014-1407-x

El-Gaby S, List FK, Tehrani R (1988) Geology, evolution and metallogenesis of the Pan-African Belt in Egypt. In: El-Gaby S, Greiling RO (eds) The Pan-African Belt of Northeast Africa and Adjacent Areas. Vieweg & Sohn, Weisbaden, pp 17–68

El-Gaby S, El Nady O, Khudeir A (1984) Tectonic evolution of the basement complex in the central Eastern Desert of Egypt. Geol Rundsch 73:1019–1036

El-Gaby S, List FK, Tehrani R (1990) The basement complex of the Eastern Desert and Sinai. In: Said R (ed) The geology of Egypt. Balkema, Rotterdam, pp 175–184

El-Hady ShM (1993) Geothermal evolution of the Red Sea margin and its relation to earthquake activity. MSc thesis, Cairo University, Cairo, Egypt

El-Kazzaz YA, Taylor WE (2000) Tectonic evolution of the Allaqi Shear Zone and implications for the Pan-African terrain amalgamation in the South Eastern Desert of Egypt. J Afr Earth Sci 33(2):177–197

El Khrepy S, Koulakov I, Al-Arifi N (2015) Crustal structure in the area of the cannon earthquakes of Abu Dabbab (Northern Red Sea, Egypt), from seismic tomography inversion. Bull Seismo Soc Am 105(4):13. http://dx.doi.org/10.1785/0120140333

El-Rabaa SM, Al-Shumaimri MS, Al-Mishwat AT (2001) Fate of the Najd fault system in northwestern Saudi Arabia and southwestern Jordan. Gondwana Res 4:164–165

El-Ramly MF, Greiling R, Kröner A, Rashwan AA (1984) On the tectonic evolution of the Wadi Hafafit area and environs, Eastern Desert of Egypt. Bull Fac Earth Sci 6:114–126

El-Ramly MF, Greiling RO, Rashwan AA, Ramsy AH (1993) Explanatory note to accompany the geological and structural maps of Wadi Hafafit area, Eastern Desert of Egypt. Ann Geol Surv Egypt 9:1–53

El-Ramly MF, Hussein AAA (1983) The ring complexes of the Eastern Desert of Egypt. J Afr Earth Sci 3(1/2):77–82

El-Sharkawy MA, El-Bayoumi RM (1979) The ophiolites of Wadi Ghadir area Eastern Desert, Egypt. Ann Geol Survey Egypt 9:125–135

Essawy MA, Abu Zeid KM (1972) Atalla felsite intrusion and its neighbouring rhylitic flows and tuffs, Eastern Desert, Egypt. Ann Geol Surv Egypt 2:271–280

Fairhead JD, Girdler RW (1970) The seismicity of the Red Sea, Gulf of Aden and Afar triangle. Philos Trans R Soc A 267:49–74

Farahat ES, El Mahalawi MM, Hoinkes G, Abdel Aal AY (2004) Continental back-arc basin origin of some ophiolites from the Eastern Desert of Egypt. Mineral Petrol 82:81–104

Fleck RJ, Greenwood WR, Hadley DG, Anderson RE, Schmidt DL (1979) Rubidium-Strontium geochronology and plate-tectonic evolution of the southern part of the Arabian Shield. US Geological Survey Saudi Arabian Mission Report 245, p 105

Fowler AR, El-Kalioubi B (2004) Gravitational collapse origin of shear zones, foliations and linear structures in the Neoproterozoic cover nappes, Eastern Desert, Egypt. J Afr Earth Sci 38:23–40

Fowler TJ, Osman AF (2001) Gneiss-cored interference dome associated with two phases of late Pan-African thrusting in the Central Eastern Desert, Egypt. Precambr Res 108:17–43

Fowler AR, Osman AF (2009) The Sha'it-Nugrus shear zone separating Central and South Eastern Deserts, Egypt: a post-arc collision low-angle normal ductile shear zone. J Afr Earth Sci 53:16–32

Fowler A, Khamees H, Dowidar H (2007) El Sibai gneissic complex, Central Eastern Desert, Egypt: folded nappes and syn-kinematic gneissic granitoid sheets-not a core complex. J Afr Earth Sci 49 (4):119–135

Fritz H, Messner M (1999) Intramontane basin formation during oblique convergence in the Eastern Desert of Egypt: magmatically versus tectonically induced subsidence. Tectonophysics 315:145–162

Fritz H, Abdelsalam M, Ali KA, Bingen B, Collins AS, Fowler AR, Ghebreab W, Hauzenberger CA, Johnson PR, Kusky TM, Mace P, Muhongo S, Stern RG, Viola G (2013) Orogen styles in the East African Orogen: a review of the Neoproterozoic to Cambrian tectonic evolution. J Afr Earth Sci 86:65–106

Fritz H, Dalmeyer DR, Wallbrecher E, Loizenbauer J, Hoinkes G, Neumayr P, Khudeir AA (2002) Neoproterozoic tectonothermal evolution of the Central Eastern Desert, Egypt: a slow velocity tectonic process of core complex exhumation. J Afr Earth Sci 34:543–576

Fritz H, Wallbrecher E, Khudeir AA, Abu El Ela F, Dallmeyer DR (1996) Formation of Neoproterozoic core complexes during oblique convergence (Eastern Desert, Egypt). J Afr Earth Sci 23:311–329

Gad S, Kusky TM (2006) Lithological mapping in the Eastern Desert of Egypt, the Barramiya area using Landsat thematic mapper (TM). J Afr Earth Sci 44:196–202

Gharib ME (2012) Origin and evolution history of magmatic garnet-bearing pegmatites and associated granitoids, Abu Had area, south Eastern Desert, Egypt: inference from petrology and geochemistry. J Amer sci 8(10):536–554

Greiling RO (1985) Thrust tectonics in Pan-African rocks of SE Egypt. Terra Cognita 5

Greiling RO (1997) Thrust tectonics in crystalline domains: the origin of a gneiss dome. Proc Ind Acad Sci (Earth Planet Sci) 106:209–220

Greiling RO, Kröner A, El-Ramly MF, Rashwan AA (1988) Structural relationship between the southern and central parts of the Eastern desert of Egypt: details of a fold and thrust belt. In: El-Gaby S, Greiling RO (eds) The Pan-African Belt of Northeast Africa and adjacent areas. Vieweg & Sohn, Weisbaden, Germany, pp 121–146

Greiling RO, De Wall H, Sadek MF, Dietl C (2014) Late Pan-African granite emplacement during regional deformation, evidence from magnetic fabric and structural studies in the Hammamat-Atalla area, Central Eastern Desert of Egypt. J Afr Earth Sci 99:109–121

Greiling RO, Abdeen MM, Dardir AA, El Akhal H, El Ramly MF, Kamal El Din GM, Osman AF, Rashwan AA, Rice AH, Sadek MF (1994) A structural synthesis of the Proteorozoic Arabian-Nubian Shield in Egypt. Geol Rundsch 83:484–501

Greiling RO, de Wall H, Warr LN, Naim GM, Hussein AA, Sadek MF, Abdeen MM, El Kady MF, Makhlouf A (1996) Basement structure in Eastern Egypt: quantitative perspectives for the second century. Proc Geol Surv Egypt Cenn Conf 289–302

Grundmann G, Morteani G (2008) Multi-stage emerald formation during Pan-African regional metamorphism: The Zabara, Sikait, Umm Kabo deposits, South Eastern desert of Egypt. J Afr Earth Sci 50(2–4):168–187. https://doi.org/10.1016/j.jafrearsci.2007.09.009

Habib ME (1987) Arc ophiolites in the Pan-African basement between Meatiq and Abu Furad, Eastern Desert, Egypt. Bull Fac Sci Assiut Univ 16:241–283

Hagag W, Moustafa R, Hamimi Z (2018) Neoproterozoic evolution and Najd-related transpressive shear deformations along Nugrus Shear Zone, South Eastern Desert, Egypt (Implications from field-structural data and AMS-technique). Geotectonics 52(1):114–133

Hargrove US, Stern RJ, Kimura JI, Manton WI, Johnson PR (2006a) How juvenile is the Arabian-Nubian Shield? Evidence from Nd isotopes and pre-Neoproterozoic inherited zircon in the Bi'r Umq suture zone, Saudi Arabia. Earth Planet Sci Lett 252:308–326

Hargrove US, Stern RJ, Griffin WR, Johnson PR, Abdelsalam MG (2006b) From island arc to craton: timescales of crustal formation along the Neoproterozoic Bi'r Umq Suture zone, Kingdom of Saudi Arabia. Saudi Geological Survey Technical Report SGS-TR-2006-6, 69 pp

Hamdy M Abd, El-Wahed MA, Thabet E (2017a) Origin of dyke swarms in Wadi El Redi area, south Eastern Desert Egypt. Arab J Geosci 10(18):414

Hamdy MM, Abd El-Wahed MA, Gamal El Dien H, Morishita T (2017b) Garnet hornblendite in the Meatiq core Complex, Central Eastern Desert of Egypt: Implications for crustal thickening preceding the ~600 Ma extensional regime in the Arabian-Nubian Shield. Precambr Res 298:593–614

Hamdy M, Gamal El-Dien H, Abd El-Wahed MA, Morishita T (2018) Garnierite-bearing serpentinite from the Central Eastern Desert of Egypt: a signature of paleo-weathering in the Arabian Nubian Shield? J Afr Earth Sci 146:95–117

Hamimi Z, Ghazaly MK, Mohamed EA, Younis AM (2016) Structural history of Wadi Kharit transpressional Shear Zone, Eastern Desert tectonic terrane, Northern Nubian Shield. Ann Meeting of the Egyptian Geological Society (Abstract)

Hamimi Z, Hagag W (2017) A new tectonic model for Abu-Dabbab seismogenic zone (Eastern Desert, Egypt): evidence from field-structural, EMR and seismic data. Arab J Geosci 10:11. https://doi.org/10.1007/s12517-016-2786-y

Hamimi Z, Abd El-Wahed MA, Gahlan HA, Kamh SZ (2019) Tectonics of the Eastern Desert of Egypt: key to understanding the Neoproterozoic evolution of the Arabian-Nubian Shield (East African Orogen). In: Bendaoud A, Hamimi Z, Hamoudi M, Djemai S, Zoheir B (eds) Geology of the Arab world—an overview, Springer Geology, pp 1–81. https://doi.org/10.1007/978-3-319-96794-3_1

Hamimi Z, El Amawy MA, Wetait M (1994) Geology and structural evolution of El Shalul Dome and environs, Central Eastern Desert, Egypt. Egypt J Geol 38–2:575–959

Harraz HZ (1999) Wall rock alteration, Atud gold mine, Eastern Desert, Egypt: processes and P-T-XCO2 conditions of metasomatism: J Afr Earth Sci 28(3):527–551. https://doi.org/10.1016/s0899-5362(99)00031-7harraz

Harraz HZ (2000) A genetic model for a mesothermal Au deposit: evidence from fluid inclusions and stable isotopic studies at El Sid gold mine, Eastern Desert, Egypt. J Afr Earth Sci 30:267–282. https://doi.org/10.1016/s0899-5362(00)00019-1

Harraz HZ, El-Dahhar MA (1993) Nature and composition of gold-forming fluids at Umm Rus area, Eastern Desert, Egypt: evidence from fluid inclusions in vein materials. J Afr Earth Sci 16:341–353

Harraz HZ, Hamdy MM (2015) Zonation of primary haloes of Atud auriferous quartz vein deposit, Central Eastern Desert of Egypt: A potential exploration model targeting for hidden mesothermal gold deposits. J Afr Earth Sc 101:1–18. https://doi.org/10.1016/j.jafrearsci.2014.09.001

Harraz HZ, Hamdy MM, El-Mamoney MH (2012) Multi-element association analysis of stream sediment geochemistry data for predicting gold deposits in Barramiya gold mine, Eastern Desert, Egypt. J Afr Earth Sci 68:1–14

Hassaan MM, Ramadan TM, Abu El Leil I, Sakr SM (2009) Lithochemical surveys for ore metals in arid region, Central Eastern Desert, Egypt: using Landsat ETM+ imagery. Aust J Basic Appl Sci 3:512–528

Hassan M, Stüwe K, Abu-Alam TS, Klötzli U, Tiepolo M (2016) Time constraints on deformation of the Ajjaj branch of one of the largest Proterozoic shear zones on Earth: The Najd Fault System. Gondwana Res 34:346–362

Hassan AM (1998) Geochemistry, Rb-Sr geochronology and petrogenesis of the Late Pan-African Atalla Felsite, central Eastern Desert, Egypt. In: Geology of the Arab world, 4th international conference, Cairo University. Cairo University Press, Giza, pp 89–90

Hassoup A (1987) Microearthquakes and magnitude studies on earthquake activity at Abu Dabbab region, Eastern Desert Egypt. MSc thesis, Fac. Sci., Cairo Univ., pp 1–169

Helba HA, Khalil KI, Abdou NM (2001) Alteration patterns related to hydrothermal gold mineralization in meta-andesites at Dungash area, Eastern Desert Egypt. Resour Geol 51:19–30

Helmy HM, Kaindl R (1999) Mineralogy and fluid inclusion studies of the Au–Cu quartz veins in the Hamash area, South-Eastern Desert, Egypt. Mineral Petrol 65:69–86

Helmy H, Zoheir B (2014) Metal and fluid sources in a potential world-class gold deposit: El-Sid mine, Egypt. Int J Earth Sci 104 (3):645–661. https://doi.org/10.1007/s00531-014-1094-6

Helmy H, Kaindl R, Fritz H, Loizenbauer J (2004) The Sukari Gold Mine, Eastern Desert, Egypt: structural setting, mineralogy and fluid inclusion study. Mineral Deposita 39:495–511

Hilmy ME, Osman A (1989) Remobilization of gold from a chalcopyrite–pyrite mineralization Hamash gold mine, Southeastern Desert, Egypt. Mineral Deposita 24:244–249

Hodgson CJ (1989) The structure of shear-related, vein-type gold deposits: a review. Ore Geol Rev 4:635–678

Hosny A, El Hady SM, Mohamed AA, Panza GF, Tealeb A, El Rahman MA (2009) Magma intrusion in the upper crust of Abu Dabbab area, south east of Egypt, from Vp and Vp/Vs tomography. Rend Fis Acc Lincei 20:1–19. http://dx.doi.org/ https://doi.org/10.1007/s12210-009-0001-8

Hosny A, El-Hady SM, Guidarelli M, Panza GF (2012) Source moment tensors of the earthquake Swarm in Abu-Dabbab area, South-East Egypt. Rend Fis Acc Lincei 23:149–163

Huet B, Le Pourhiet L, Labrousse L, Burov E, Jolivet L (2010) Post-orogenic extension and metamorphic core complexes in a heterogeneous crust: the role of crustal layering inherited from collision, Application to the Cyclades (Aegean domain). Geophys J Int 184:611–625

Ibrahim ME, Yokoyama I (1998) Probable origin of the Abu Dabbab earthquakes swarms in the Eastern Desert of Egypt. Bull IISEE 32

Ibrahim WS, Watanabe K, Yonezu K (2016) Structural and litho-tectonic controls on Neoproterozoic base metal sulfide and gold mineralization in North Hamisana shear zone, South Eastern Desert, Egypt: the integrated field, structural, Landsat 7 ETM+ and ASTER data approach. Ore Geol Rev 79:62–77

Johnson PR, Andresen A, Collins AS, Fowler AR, Fritz H, Ghebreab W, Kusky T, Stern RJ (2011) Late Cryogenian-Ediacaran history of the Arabian-Nubian Shield: a review of depositional, plutonic, structural, and tectonic events in the closing stages of the northern East African Orogen. J Afr Earth Sci 61:167–232

Johnson PR, Woldehaimanot B (2003) Development of the Arabian-Nubian Shield: perspectives on accretion and deformation in the northern East African Orogen and the assembly of Gondwana. Geol Soc Lond Spec Publ 206:289–325

Kamal El Din GM (1993) Geochemistry and tectonic significance of the Pan-African El Sibai Window, Central Eastern Desert, Egypt. Unpublished PhD thesis, Forschungzentrum Julich GmbH, 19, p 154

Kebeasy RM (1990) Seismicity. In: Said R (ed) Geology of Egypt. Balkema, Rotterdam, pp 51–59

Khalil KI, Helba A (2000) Gold mineralization and its alteration zones at the Hangalia Gold Mine area, Eastern Desert, Egypt. Egypt Mineral 12:65–92.

Khudeir AA, El-Gaby S, Greiling RO, Kamal El Din GW (1992) Geochemistry and tectonic significance of polymetamorphosed amphibolites in the Gebel Sibai window, Central Eastern Desert, Egypt. Geology of the Arab world conference. Cairo University, Egypt, pp 461–476

Khudeir AA, Kamal El-Gaby S, El Din GM, Asran AMH, Greiling RO (1995) The pre-Pan-African deformed granite cycle of the Gabal El-Sibai swell, Eastern Desert, Egypt. J Afr Earth Sci 21:395–406

Kröner A, Greiling RO, Reischmann T, Hussein IM, Stern RJ, Durr St, Kruger J, Zimmer M (1987) Pan-African crustal evolution in northeast Africa. In: Kröner A (eds) Proterozoic lithospheric evolution. American Geophysical Union, Geodynamic Series 17, pp 235–257

Kröner A, Krüger J, Rashwan AA (1994) Age and tectonic setting of granitoid gneisses in the Eastern Desert of Egypt and south-west Sinai. Geol Rundsch 83:502–513

Kröner A, Linnebacher P, Stern RJ, Reischmann T, Manton WI, Hussein IM (1991) Evolution of Pan-African island arc assemblages in the southern Red Sea Hills, Sudan and in southwestern Arabia as exemplified by geochemistry and geochronology. Precambr Res 53:99–118

Kröner A, Todt W, Hussein IM, Mansour M, Rashwan AA (1992) Dating of late Proterozoic ophiolites in Egypt and the Sudan using the single grain zircon evaporation technique. Precambr Res 59:15–32

Kusky TM, Ramadan TM (2002) Structural controls on Neoproterozoic mineralization in the South Eastern Desert, Egypt: an integrated field, Landsat TM, and SIRC/ X SAR approach. J Afr Earth Sci 35:107–121

Küster D, Liégeois J-P, Matukov D, Sergeev S, Lucassen F (2008) Zircon geochronology and Sr, Nd, Pb isotope geochemistry of granitoids from Bayuda Desert and Sabaloka (Sudan): Evidence for a Bayudian event (920–900 Ma) preceding the Pan-African orogenic cycle (860–590 Ma) at the eastern boundary of the Saharan Metacraton. Precambr Res 164(1–2):16–39

Liégeois J-P, Abdelsalam MG, Ennih N, Ouabadi A (2013) Metacraton: nature, genesis and behavior. Gondwana Res 23(1):220–237

Liégeois JP, Stern RJ (2010) Sr–Nd isotopes and geochemistry of granite-gneiss complexes from the Meatiq and Hafafit domes, Eastern Desert, Egypt: no evidence for pre-Neoproterozoic crust. J Afr Earth Sci 57:31–40

Lister GS, Banga G, Feenstra A (1984) Metamorphic core complexes of Cordilleran type in the Cyclades, Aegean Sea, Greece. Geology 12:221–225

Loizenbauer J, Wallbrecher E, Fritz H, Neymayr P, Khudeir AA, Kloetzli U (2001) Structural geology, single zircon ages and fluid inclusion studies of the Meatiq metamorphic core complex: implications for Neoproterozoic tectonics in the Eastern Desert of Egypt. Precambr Res 110:357–383

Lundmark AM, Andresen A, Hassan MA, Augland LE, Abu El-Ru MA, Boghdady GY (2012) Repeated magmatic pulses in the East African Orogen of Central Eastern Desert, Egypt: an old idea supported by new evidence. Gondwana Res 22:227–237

Makroum FM (2001) Pan-African tectonic evolution of the Wadi El Mayit Area and its environs, Central Eastern Desert, Egypt. In: The second international conference on the geology of Africa, Assiut University, Egypt, 2, pp 219–233

Makroum FM (2003) Lattice preferred orientation (LPO) study of the orogen-parallel Wadi Nugrus and Wadi Um Nar shears, Eastern Desert-Egypt, using EBSD-technique. In: The third international conference on the geology of Africa 1, pp 213–232

Makroum F (2017) Structural interpretation of the Wadi Hafafit culmination: a Pan African gneissic dome in the central Eastern Desert, Egypt. Lithosphere (in press)

Meyer SE, Passchier C, Abu-Alam T, Stüwe K (2014) A strike-slip core complex from the Najd fault system, Arabian shield. Terra Nova 26(5):387–394. https://doi.org/10.1111/ter.12111

Miller MM, Dixon TH (1992) Late Proterozoic evolution of the north part of the Hamisana zone, northeast Sudan: constraints on Pan-African accretionary tectonics. J Geol Soc Lond 149:743–750

Moghazi AM, Hassanen MA, Mohammed FH, Ali S (2004) Late Neoproterozoic strongly peraluminous leucogranites, South Eastern Desert, Egypt—petrogenesis and geodynamic significance. Mineral Petrol 81:19–41

Mohamed AS, Hosny A, Abou-Aly N, Saleh M, Rayan A (2013) Preliminary crustal deformation model deduced from GPS and earthquakes' data at Abu-Dabbab area, Eastern Desert, Egypt. NRIAG J Astronomy and Geophysics 2(1):-67–76

Mohamed FH (1993) Rare metal-bearing and barren granites, Eastern Desert of Egypt: geochemical characterization and metallogenetic aspects. J Afr Earth Sci 17:525–539

Moore JM (1979) Tectonics of the Najd transcurrent fault system, Saudi Arabia. J Geol Soc Lond 136:441–454

Murr, A., 1999, Genesis of gold mineralization of Fatria, Gidami, Atalla and Hangaliya, Eastern Desert of Egypt. Münchner Geological Hefte A 27:202 (in German)

Nano L, Kontny A, Sadek MF, Greiling RO (2002) Structural evolution of metavolcanics in the surrounding of the gold mineralization at El Beida, South Eastern Desert, Egypt. Ann Geol Surv Egypt 25:11–22

Neumayr P, Hoinkes G, Puhl J, Mogessie A, Khudeir AA (1998) The Meatiq dome (Eastern Desert, Egypt) a Precambrian metamorphic core complex: petrological and geological evidence. J Metamorph Geol 16:259–279

Neumayr P, Mogessie P, Hoinkes G, Puhl J (1996) Geological setting of the Meatiq metamorphic core complex in the Eastern Desert of Egypt based on amphibolite geochemistry. J Afr Earth Sci 23 (3):331–345

Noweir AM (1968) Geology of the Hammamat-Um Seleimat District, Eastern Desert, Egypt. PhD Thesis, Assiut Univ, Egypt

Pallister JS, Stacey JS, Fischer LB, Premo WR (1988) Precambrian ophiolites of Arabia; geologic setting, U-Pb geochronology, Pb-isotope characteristics, and implications for continental accretion. Precambr Res 38:1–54

Peters SG (2004) Syn-deformational features of Carlin-type Au deposits. J Struct Geol 26(6–7):1007–1023

Phillips WJ (1972) Hydraulic fracturing and mineralization. Geol Soc Lond 128:337–361

Ragab A (1993) A geodynamic model for the distribution of the oceanic plate slivers within a Pan-African orogenic belt, Eastern Desert, Egypt. J Geodyn 17(1–2):21–26. https://doi.org/10.1016/0264-3707(93)90014-w

Ragab Al, El-Gharabawi RI, El-Ally Z (1993) Pan-African tectonostratigraphic assemblages of Gabal Meatiq-Wadi AtaUa area, Eastern Desert, Egypt: evidence for arc-arc suturing. MERC Ain Shams University. Earth Sci Ser 7:131–145

Raharimahefa T, Kusky TM (2010) Structural and remote sending analysis of the Betsimisaraka Suture in northeastern Madagascar. Gondwana Res 15:14–27

Ramadan TM, Kontny A (2004) Mineralogical and structural characterization of alteration zones detected by orbital remote sensing at Shalatin District area, SE Desert, Egypt. J Afr Earth Sci 40: 89–99

Roberts RG (1987) Archean lode gold deposits. Geosci Can 14:1–19

Robin PYF, Cruden AR (1994) Strain and vorticity patterns in ideal transpression zones. J Struct, Geol

Sabet AH, Tsogoev V, Sarin LP, Azazi SA, Bedewi MA, Ghobrial GA (1976) Tin Tantalum deposits of Abu Dabbab. Ann Geol Survey Egypt 6:93–117

Sakran ShM, Hussein AA, Takla MA, Makhlouf AA (2001) Structural evolution of Um Radam area, south Eastern desert, Egypt. Ann Geol Survey Egypt XXIII(2):1–14

Shackleton RM (1986) Precambrian collision tectonics in Africa. Geol Soc Lond Spec Publ 19(1):329–349. https://doi.org/10.1144/gsl.sp.1986.019.01.19

Shackleton RM (1994) Review of late Proterozoic sutures, ophiolitic mélanges and tectonics of eastern Egypt and north Sudan. Geol Rundsch 83:537–546

Shalaby A (2010) The northern dome of Wadi Hafafit culmination, Eastern Desert, Egypt: structural setting in tectonic framework of a scissor-like wrench corridor. J Afr Earth Sci 57:227–241

Shalaby A, Stüwe K, Fritz H, Makroum F (2006) The El Mayah molasse basin in the Eastern Desert of Egypt. J Afr Earth Sci 45:1–15

Shalaby A, Stüwe K, Makroum F, Fritz H, Kebede T, Klotzli U (2005) The Wadi Mubarak belt, Eastern Desert of Egypt: a Neoproterozoic conjugate shear system in the Arabian-Nubian Shield. Precambr Res 136:27–50

Smith M, O'Connor E, Nasr BB (1999) Transpressional flower structures and escape tectonics: a new look at the Pan-African collision in the Eastern Desert, Egypt. In: De Wall H, Greiling RO (eds) Aspects of Pan-African Tectonics. International Cooperation, Bilateral Seminars Int Bureau, Germany, Forschungszentrum Jülich, pp 81–82

Stephens JR, Mair JL, Oliver NH, Hart CJ, Baker T (2004) Structural and mechanical controls on intrusion-related deposits of the Tombstone Gold Belt, Yukon, Canada, with comparisons to other vein-hosted ore-deposit types. J Struct Geol 26(6–7):1025–1041

Stern RJ (1985) The Najd fault system, Saudi Arabia and Egypt: a late Precambrian rift-related transform system. Tectonics 4:497–511

Stern RJ (1994) Arc assembly and continental collision in the Neoproterozoic East African Orogen: implications for the consolidation of Gondwanaland. Ann Rev Earth Planet Sci 22:319–351

Stern RJ, Hedge CE (1985a) Geochronologic and isotopic constraints on late Precambrian crustal evolution in the Eastern Desert of Egypt. Am J Sci 258:97–127

Stern RJ, Hedge CE (1985b) Geochronologic constraints on late Precambrian crustal evolution in the Eastern Desert of Egypt. Am J Sci 285:97–127

Stern RJ, Kröner A, Manton WI, Reischmann T, Mansour M, Hussein IM (1989) Geochronology of the late Precambrian Hamisana shear zone, Red Sea Hills, Sudan and Egypt. J Geol Soc Lond 146:1017–1030

Stern RJ, Nielsen KC, Best E, Sultan M, Arvidson RE, Kroner A (1990) Orientation of late Precambrian sutures in the Arabian-Nubian Shield. Geology 18:1103–1106

Stern RJ (2017) Neoproterozoic formation and evolution of Eastern Desert continental crust—the importance of the infrastructure-superstructure transition. J Afr Earth Sci 146:15–27

Stern RJ, Ali KA, Liegeois JP, Johnson PR, Kozdroj W, Kattan FH (2010) Distribution and significance of pre-Neoproterozoic zircons in juvenile Neoproterozoic igneous rocks of the Arabian-Nubian Shield. Am J Sci 310(9):791–811

Stern RJ, Kröner A, Rashwan AA (1991) A late Precambrian ($\sim$710 Ma) high volcanicity rift in the southern Eastern Desert of Egypt. Geol Rundsch 80:155–170

Stoeser DB, Camp VE (1985) Pan-African microplate accretion of the Arabian Shield. Geol Soc Am Bull 96:817–826

Sturchio NC, Sultan M, Batiza R (1983) Geology and origin of Meatiq Dome, Egypt: a Precambrian metamorphic core complex? Geology 11:72–76

Sultan M, Arvidson RE, Duncan IJ, Stern RJ, El Kalioubi B (1988) Extension of the Najd Shear System from Saudi Arabia to the central Eastern Desert of Egypt based on integrated field and Landsat observations. Tectonics 7:1291–1306

Takla MA, Hussein AA, Sakran ShM, Makhlouf AA (2002) Tectonometamorphic history of Um Radam area, south Eastern Desert, Egypt. Ann Geol Surv Egypt XXIV:41–61

Taylor WEG, El Hamad YA, El-Kazzaz YA, Rashwan AA (1993) An outline of the tectonic framework for the Pan-African orogeny in the vicinity of Wadi Um Relan, SE Desert, Egypt. In: Thorweihe U, Shandelmeier H (eds) Geoscientific research in NE Africa. Balkema, Rotterdam, pp 31–34

Teyssier Ch, Tikoff B (1999) Fabric stability in oblique convergence and divergence. J Struct Geol 21:969–974

Tirel C, Brun J-P, Burov E (2008) Dynamics and structural development of metamorphic core complexes. J Geophys Res 113:B04403

Unzog W, Kurz W (2000) Progressive development of lattice preferred orientations (LPOs) of naturally deformed quartz within a transpressional collision zone (Panafrican orogen in the Eastern Desert of Egypt). J Struct Geol 22:1827–1835

Vail JR (1985) Pan-African (late Precambrian) tectonic terrains and the reconstruction of the Arabian-Nubian Shield. Geology 13:839–842

Wallbrecher E, Fritz H, Khudeir AA, Farahad F (1993) Kinematics of Pan-african thrusting and extension in Egypt. In: Thorweih U, Shandelmeister H (eds) Geoscientific research in Northeast Africa. Balkema, Rotterdam, pp 27–30

Whitehouse MJ, Stoeser D, Stacey JS (2001) The Khida Terrane—geochronological and isotopic evidence for paleoproterozoic and Archean Crust in the Eastern Arabian Shield of Saudi Arabia. Gondwana Res 4:200–202

Zimmer M, Kröner A, Jochum KP, Reischmann T, Todt W (1995) The Gabal Gerf complex: a Precambrian N-MORB ophiolite in the Nubian Shield, NE Africa. Chem Geol 123:29–51

Zoheir B (2012) Lode-gold mineralization in convergent wrench structures: examples from South Eastern Desert, Egypt. J Geochem Explor 114:82–97

Zoheir B, Moritz R (2014) Fluid evolution in the El-Sid gold deposit, Eastern Desert, Egypt. In Garofalo PS, Ridley JR (eds) Gold-transporting hydrothermal fluids in the Earth's crust. Geological Society, London, Special Publications, 402. https://doi.org/10.1144/sp402.3

Zoheir B, Deshesh F, Broman C, Pitcairn I, El-Metwally A, Mashaal S (2017) Granitoid-associated gold mineralization in Egypt: a case study from the Atalla mine. Miner Deposita 53(5):701–720

Zoheir B, Feigenson M, Zi J-W, Turrin B, Deshesh F, El-Metwally A (2018) Ediacaran ($\sim$600 Ma) orogenic gold in Egypt: age of the Atalla gold mineralization and its geological significance. Int Geol Rev 1–16

Zoheir BA (2008) Characteristics and genesis of shear zone-related goldmineralization in Egypt: a case study from the Um El Tuyor mine, south Eastern Desert. Ore Geol Rev 34:445–470

Zoheir BA (2011) Transpressional zones in ophiolitic mélange terranes: potential exploration targets for gold in the South Eastern Desert, Egypt. J Geochem Explor 111:23–38

Zoheir BA (2012) Lode-gold mineralization in convergent wrench structures: Examples from South Eastern Desert, Egypt. J Geochem Explor 114:82–97. https://doi.org/10.1016/j.gexplo.2011.12.005

Zoheir BA, Creaser RA, Lehmann B (2015) Re-Os geochronology of gold mineralization in the Fawakhir area, Eastern Desert, Egypt. Int Geol Rev 57:1418–1432. https://doi.org/10.1080/00206814.2014.935964

Zoheir BA, Goldfarb RJ, Weihed P (2011) Granitoidassociated lode gold deposits in the central Eastern Desert of Egypt. In: Geological Society of America (GSA) annual meeting. Minneapolis, MN, 470 pp

Zoheir BA, Lehmann B (2011) Listvenite-lode association at the Barramiya gold mine, Eastern Desert, Egypt. Ore Geol Rev 39:101–115

Zoheir BA, Weihed P (2014) Greenstone-hosted lode-gold mineralization at Dungash mine, Eastern Desert, Egypt. J Afr Earth Sci 99(1):165–187